



Hydrogeology and Geochemistry of Aquifers Underlying the San Lorenzo and San Leandro Areas of the East Bay Plain, Alameda County, California



Water-Resources Investigations Report 02-4259

**U.S. DEPARTMENT OF THE INTERIOR
U.S. GEOLOGICAL SURVEY**

Prepared in cooperation with the **EAST BAY MUNICIPAL UTILITY DISTRICT**
and **ALAMEDA COUNTY FLOOD CONTROL AND WATER CONSERVATION DISTRICT**

Hydrogeology and Geochemistry of Aquifers Underlying the San Lorenzo and San Leandro Areas of the East Bay Plain, Alameda County, California

By John A Izbicki, James W. Borchers, David A. Leighton, Justin Kulongoski, Latoya Fields, Devin L. Galloway, *and* Robert L. Michel

U.S. GEOLOGICAL SURVEY

Water-Resources Investigations Report 02-4259

Prepared in cooperation with the

EAST BAY MUNICIPAL UTILITY DISTRICT and
**ALAMEDA COUNTY FLOOD CONTROL AND WATER
CONSERVATION DISTRICT**

3006-07

Sacramento, California
2003

U.S. DEPARTMENT OF THE INTERIOR

GALE A. NORTON, *Secretary*

U.S. GEOLOGICAL SURVEY

Charles G. Groat, *Director*

Any use of trade, product, or firm names in this publication is for descriptive purposes only and does not imply endorsement by the U.S. Government.

For additional information write to:

District Chief
U.S. Geological Survey
Placer Hall– Suite 2012
6000 J Street
Sacramento, CA 95819-6129
<http://ca.water.usgs.gov>

CONTENTS

Abstract	1
Introduction	2
Description of Study Area.....	2
Purpose and Scope	2
Acknowledgments.....	6
Hydrogeology.....	6
Geologic Framework.....	6
Aquifer Systems	7
Recharge and Discharge.....	7
Water Levels and Ground-Water Movement.....	8
Water Levels at the Oakport Injection/Recovery Site.....	8
Water Levels at the Bayside Injection/Recovery Site.....	14
Water-Level Response to Tidal Fluctuation.....	17
Background	17
Tidal Responses at the Oakport Injection/Recovery Site.....	18
Tidal Responses at the Bayside Injection/Recovery Site.....	18
Geophysical Logging of Selected Wells	21
Well Bore Logging Techniques	21
Well 2S/3W-22Q2.....	21
Well 2S/3W-19Q3.....	24
Well 3S/3W-14K2.....	26
Chemistry of Ground Water.....	27
Physical Properties and Chemical Characteristics of Water from Wells.....	27
Chemical Reactions Controlling Major-Ion Chemistry	30
Major-Ion Composition of Depth-Dependent Samples	32
Source of High-Chloride Water to Wells.....	33
Chloride-to-Bromide Ratios.....	34
Chloride-to-Iodide Ratios	36
Chloride-to-Barium Ratios.....	37
Chloride-to-Boron Ratios.....	37
Noble-Gas Concentrations	38
Background	38
Ground-Water Recharge Temperatures and Excess-Air Concentrations.....	39
Excess Nitrogen And Denitrification	42
Isotopic Composition of Ground Water	43
Oxygen-18 and Deuterium.....	43
Tritium and Helium-3	46
Background	46
Tritium and Helium-3 Ages	48
Carbon-14 and Carbon-13.....	50
Background	50
Carbon-14 Activity and Carbon-13 Composition of Dissolved Inorganic Carbon	50
Interpretation of Carbon-14 Data.....	51
Limitations on Carbon-14 Interpretations.....	56
Summary and Conclusions.....	56
References Cited	57
Appendixes.....	61

Figures

Figure 1.	Satellite image of the San Francisco Bay area, California, July 7, 1994.....	3
Figure 2.	Maps showing location of study area, selected wells, and hydrogeologic sections; and selected wells at the Oakport injection/recovery and Bayside injection/recovery sites, East Bay Plain, Alameda County, California.....	4
Figure 3.	Graphs showing generalized hydrogeologic sections A–A' and B–B', East Bay Plain, Alameda County, California.....	9
Figure 6.	Graph showing altitude of water in San Francisco Bay at Alameda Island and water levels in wells 2S/3W-17K1, 3, and 4 at the Oakport injection/recovery site, East Bay Plain, Alameda County, California, October 14, 1999, to September 14, 2000.....	13
Figure 7.	Graph showing water levels in selected wells at the Bayside injection/recovery site, East Bay Plain Alameda County, California, measured during injection tests and static periods, March 6 to November 15, 2000.....	15
Figure 8.	Graph showing water levels in selected wells at the Bayside injection/recovery site, East Bay Plain, Alameda County, California, November 25–29, 1998.....	16
Figure 9.	Graph showing frequency response of water levels in wells 2S/3W-17K1, 3, and 4 at the Oakport injection/recovery site to tides in San Francisco Bay, October 15, 1999, to May 15, 2000.....	19
Figure 10.	Graph showing altitude of water surface in San Francisco Bay at Alameda Island and water levels in wells 2S/3W-17K1, 3, and 4 at the Oakport injection/recovery site, November 23–27, 2000.....	20
Figure 11.	Graph showing well construction, geophysical logs, and depth-dependent water-chemistry and isotopic data for well 2S/3W-22Q2 under nonpumped and pumped conditions, East Bay Plain, Alameda County, California, December 6–7, 1999.....	22
Figure 12.	Graph showing well construction, geophysical logs, and depth-dependent water-chemistry and isotopic data for well 2S/3W-19Q3 under pumped conditions, East Bay Plain, Alameda County, California, December 8, 1999.....	25
Figure 13.	Graph showing well-construction data and geophysical logs and for well 2S/3W-14K2 under nonpumped conditions, East Bay Plain, Alameda County, California, August 9, 2000.....	26
Figure 14.	Box plots showing pH and selected major-ion, nutrient, and trace-element concentrations in water from sampled wells having less than 250 milligrams per liter chloride in the East Bay Plain, Alameda County, California, 1997–2000.....	29
Figure 15.	Graph showing major-ion composition of samples from selected wells and of depth-dependent samples from wells 2S/3W-22Q2 and 19Q3 in the East Bay Plain, Alameda County, California, 1997–2000.....	31
Figure 16.	Graph showing selected trace-element ratios as a function of chloride concentration in water from wells, East Bay Plain, Alameda County, California, 1997–2000.....	35
Figure 17.	Graph showing selected noble-gas concentrations in water from selected wells in the East Bay Plain, Alameda County, California, 1999–2000.....	41
Figure 18.	Graph showing delta oxygen-18 ($\delta^{18}\text{O}$) as a function of delta deuterium (dD) in water from wells, East Bay Plain, Alameda County, California, 1997–2000.....	44
Figure 19.	Graph showing volume-weighted tritium concentrations in p recipitation at Santa Maria, California, 1952–1997.....	46
Figure 20.	Graph showing ground-water ages (time since recharge) along hydrologic sections A–A' and B–B', East Bay Plain, Alameda County, California.....	49
Figure 21.	Graphs showing selected changes in chemical and isotopic composition of water from wells used to interpret carbon-14 data along sections A–A' and B–B', east Bay Plain, Alameda County, California, 1998–2000.....	52

Figure E1. Semi-quantitative mineral abundance in selected samples by x-ray diffraction, East Bay Plain, Alameda County, California	86
Figure E2. Scanning electron photomicrographs of selected core material, East Bay Plain, Alameda County, California.....	87

TABLES

Table 1.	Dissolved noble-gas and nitrogen-gas concentrations, recharge temperatures, excess air-concentrations, tritium values, and time since recharge for water from selected wells in the East Bay Plain, Alameda County, California, 1998–99.....	40
Table 2.	Carbon-13 and carbon-14 data and time since recharge for water from selected wells, East Bay Plain, Alameda County, California, 1997–2000	51
Table 3.	Chemical reactions used to interpret carbon-14 data	55
Table D1.	Analytical methods and reporting limits for water samples submitted to the U.S. Geological Survey National Water Quality Laboratory	79
Table D2.	Analytical methods and reporting limits for water samples submitted to the East Bay Municipal Utility District Laboratory	80
Table D3.	Analytical methods and reporting limits for water samples submitted to the California Department of Water Resources Laboratory	81
Table E1.	Samples of core material and cuttings analyzed by x-ray diffraction and scanning electron microscopy, East Bay Plain, Alameda County, California.....	83
Table E2.	Semi-quantitative mineral abundance in selected samples by x-ray diffraction, East Bay Plain, Alameda County, California	85

CONVERSION FACTORS, VERTICAL DATUM, ABBREVIATIONS, AND ACRONYMS

CONVERSION FACTORS

Multiply	By	To obtain
acre-foot (acre-ft)	1,233	cubic meter (m ³)
acre-foot per year (acre-ft/yr)	1,233	cubic meter per year (m ³ /yr)
inch (in.)	25.4	millimeter (mm)
foot (ft)	0.3048	meter (m)
foot per minute (ft/min)	0.3048	meter per minute (m/min)
foot per day (ft/d)	0.3048	meter per day (m/d)
gallon per minute (gal/min)	0.003785	cubic meter per minute (m ³ /min)
gallon per day (gal/d)	0.003785	cubic meter per day (m ³ /d)
mile (mi)	1.609	kilometer (km)
square mile (mi ²)	2.590	square kilometer (km ²)
pound (lb)	0.4536	kilogram (kg)

Temperature is given in degrees Celsius (°C), which can be converted to degrees Fahrenheit (°F) by the following equation:

$$^{\circ}\text{F} = 9/5 ^{\circ}\text{C} + 32.$$

VERTICAL DATUM

Sea Level: In this report, “sea level” refers to the National Geodetic Vertical Datum of 1929 (NGVD of 1929)—a geodetic datum derived from a general adjustment of the first-order level nets of both the United States and Canada, formerly called Sea Level Datum of 1929.

ABBREVIATIONS

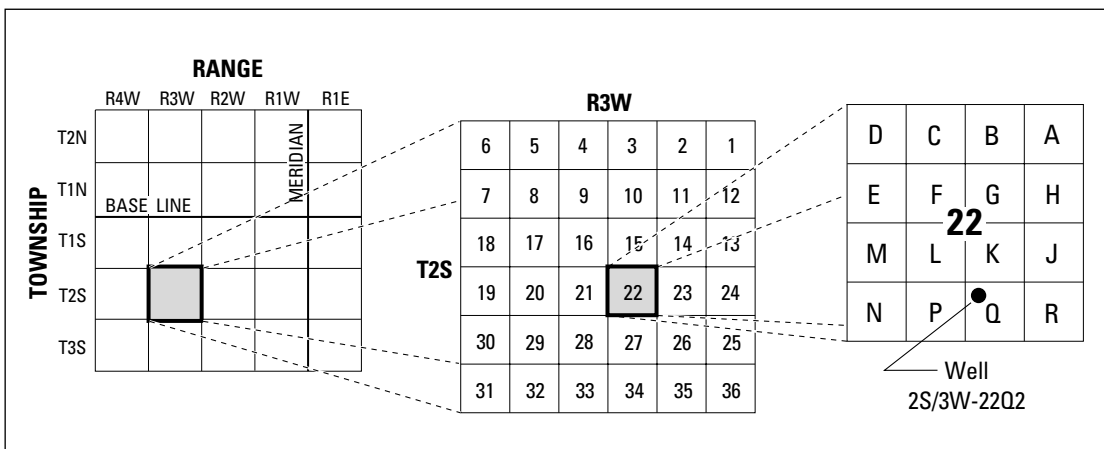
cm ³ /kg	cubic centimeter per kilogram
mcm ³ /kg	10 ⁻⁶ cubic centimeter per kilogram
cm ³ /L	cubic centimeter per liter
mg/L	milligram per liter
µg/L	microgram per liter
µm	micrometer
kg	kilogram
µS/cm	microseimen per centimeter at 25° Celsius
per mil	parts per thousand, as used with delta (d) notation
pCi/L	picocurie per liter
pcm ³ /kg	10 ⁻¹² centimeter cubed per kilogram
pmc	percent modern carbon
MCL	Maximum contaminant level
SMCL	Secondary maximum contaminant level
STP	Standard temperature and pressure
TU	Tritium unit
VSMOW	Vienna Standard Mean Ocean Water

ACRONYMS

CDWR	California Department of Water Resources
EBMUD	East Bay Municipal Utility District
USEPA	U. S. Environmental Protection Agency
USGS	U. S. Geological Survey

WELL-NUMBERING SYSTEM

Wells were assigned a State well number according to their location in the rectangular system for the subdivision of public lands. The identification consists of the township number, north or south; the range number, east or west; and the section number. Each section is further divided into sixteen 40-acre tracts lettered consecutively (except I and O), beginning with “A” in the northeast corner of the section and progressing in a sinusoidal manner to “R” in the southeast corner. Within the 40-acre tract, wells are sequentially numbered in the order they are inventoried. The final letter refers to the base line and meridian. In California, there are three base lines and meridians: Humboldt (H), Mount Diablo (M), and San Bernardino (S). All well numbers in the study area are referenced to the Mount Diablo meridian (M). Well numbers consist of 15 characters and follow the format 002S003W022Q02M. In this report, well numbers are abbreviated and written 2S/3W-22Q2. Wells in the same township and range are referred to by only their section designation, 22Q2. The following diagram shows how the number for well 2S/3W-22Q2 is derived.



Well-numbering diagram

Wells also were assigned a U.S. Geological Survey well number according to their location in the grid system of latitude and longitude. The number consists of 15 digits. The first six digits denote degrees, minutes, and seconds of latitude; the next seven digits denote degrees, minutes, and seconds of longitude; and the last two digits, assigned sequentially, identify individual wells. This station number once assigned has no locational significance. As a result, if an error was made in the field location of a well and that error resulted in an incorrect calculation of latitude and longitude, the identification number associated with that site will not be changed after the error is discovered. However, the latitude and longitude associated with that site will be corrected in the U.S. Geological Survey’s computerized National Water Information System (NWIS). A correlation between State well number, USGS well number, and local name is provided along with well-construction data in Appendix A

Hydrogeology and Geochemistry of Aquifers Underlying the San Lorenzo and San Leandro Areas of the East Bay Plain, Alameda County, California

By John A Izbicki, James W. Borchers, David A. Leighton, Justin Kulongoski, Latoya Fields, Devin L. Galloway, and Robert L. Michel

ABSTRACT

The East Bay Plain, on the densely populated eastern shore of San Francisco Bay, contains an upper aquifer system to depths of 250 feet below land surface and an underlying lower aquifer system to depths of more than 650 feet. Injection and recovery of imported water has been proposed for deep aquifers at two sites within the lower aquifer system. Successful operation requires that the injected water be isolated from surface sources of poor-quality water during storage and recovery. Hydraulic, geochemical, and isotopic data were used to evaluate the isolation of deeper aquifers.

Ground-water responses to tidal changes in the Bay suggest that thick clay layers present within these deposits effectively isolate the deeper aquifers in the northern part of the study area from overlying surficial deposits. These data also suggest that the areal extent of the shallow and deep aquifers beneath the Bay may be limited in the northern part of the study area. Despite its apparent hydraulic isolation, the lower aquifer system may be connected to the overlying upper aquifer system through the corroded and failed casings of abandoned wells. Water-level measurements in observation wells and downward flow measured in selected wells during nonpumped conditions suggest that water may flow through wells from the upper aquifer system into the lower aquifer system during nonpumped conditions.

The chemistry of water from wells in the East Bay Plain ranges from fresh to saline; salinity is greater than seawater in shallow estuarine

deposits near the Bay. Water from wells completed in the lower aquifer system has higher pH, higher sodium, chloride, and manganese concentrations, and lower calcium concentrations and alkalinity than does water from wells completed in the overlying upper aquifer system. Ground-water recharge temperatures derived from noble-gas data indicate that highly focused recharge processes from infiltration of winter streamflow and more diffuse recharge processes from infiltration of precipitation occur within the study area. However, recharge of imported water from leaking water-supply pipes, believed by previous investigators to be a large source of ground-water recharge, was not supported on the basis of oxygen-18 and deuterium data collected as part of this study.

Based on tritium/helium-3 ages, most water in the upper aquifer system is relatively young and was recharged after 1952; however, water in the lower aquifer system is older and does not contain detectable tritium. Carbon-14 ages interpreted for water from wells in the lower aquifer system and underlying partly consolidated rocks range from 500 to more than 20,000 years before present. The greatest ages were in water from wells completed in the partly consolidated deposits that underlie the northern part of the study area. Ground water from wells in the lower aquifer system near the proposed Bayside injection/recovery site was recharged about 9,400 years before present and appears to be isolated from surface sources of recharge and ground-water contamination.

INTRODUCTION

The East Bay Plain consists of about 120 mi² of tidal marshes and alluvial lowlands near Oakland, Calif., on the east side of San Francisco Bay. In 1999, the East Bay Plain had a population of more than 900,000 (San Francisco Bay Regional Water Quality Control Board, 1999) and was a highly urbanized area with multiple land uses (fig. 1).

The study area is that part of the East Bay Plain composed of the alluvial fans of San Leandro and San Lorenzo Creeks (fig. 2), which are underlain by a complex series of aquifers more than 650 ft thick (Brown and Caldwell, Inc., 1986; CH₂M-Hill, Inc., 2000). The East Bay Municipal Utility District (EBMUD) is considering using deeper aquifers as a source of public supply. Water from this source may be used directly to help meet short-term needs arising from drought, seismic, and other water-supply emergencies—or imported water from the Sierra Nevada may be injected, stored, and later recovered for public supply. For injection and recovery of imported water to be successful, the deeper aquifer systems must be capable of accepting large quantities of imported water; and, while in storage and during recovery, that water must remain isolated from surface sources of contamination and naturally occurring poor-quality water. There is concern that water in shallow aquifers that has been degraded by seawater intrusion, industrial contamination, and residential land uses such as septic disposal (San Francisco Regional Water Quality Control Board, 1999) may contaminate deeper aquifers. In addition, deeper aquifers may be susceptible to contamination from naturally occurring poor-quality water in surrounding and underlying deposits.

The EBMUD has done a series of studies to evaluate the geologic and hydraulic properties of deep aquifers. The purpose of these studies was to determine the yield of wells in these aquifers and assess their suitability for injection and recovery of imported water. Most of this work has been site specific and related to the installation and performance of injection and recovery wells (Fugro West, Inc., 1998, 1999b), although a regional assessment of subsurface geohydrologic conditions has been completed (CH₂M-Hill Inc., 2000). Additional data and a more comprehensive understanding of the geohydrology and geochemistry of the aquifer system, especially the

hydraulic connection between different aquifers, are needed to assist water-resources managers in the planning and implementation of large-scale injection and recovery operations in aquifers underlying the East Bay Plain.

Description of Study Area

The study area is on the east side of San Francisco Bay in the San Lorenzo and San Leandro areas of the East Bay Plain (fig. 1). The area has a mediterranean climate with mild, wet winters and warm, dry summers. The average annual temperature is 13.2 °C; average winter temperatures (December–February) are about 9° C and average summer (June–August) temperatures are about 15° C. Most precipitation falls as rain between November and March, and precipitation averages 23 in. annually (Muir, 1997). The area is densely populated and highly urbanized and is characterized by industrial, commercial, and residential land uses. Although agriculture was important in the past, there is little agricultural land use in the study area at the present time.

San Leandro and San Lorenzo Creeks are the principal streams in the study area. These streams originate in the Diablo Range and flow westward into San Francisco Bay. The upland area drained by these streams (43 and 44 mi², respectively) contains two large reservoirs but, with the exception of the Castro Valley area, the drainage basins are not extensively developed.

Purpose and Scope

The purpose of this report is to evaluate hydrogeologic, and geochemical conditions in aquifers underlying the East Bay Plain in Alameda County, California. Specific issues addressed include (1) sources of recharge to different hydrogeologic units; (2) integrity of confining layers and isolation of hydrologic units; and (3) water quality in the different hydrogeologic units. This information will be used by EBMUD and other agencies to evaluate the suitability of aquifers underlying the East Bay Plain for water-supply development, including the injection and recovery of imported water from the Sierra Nevada.

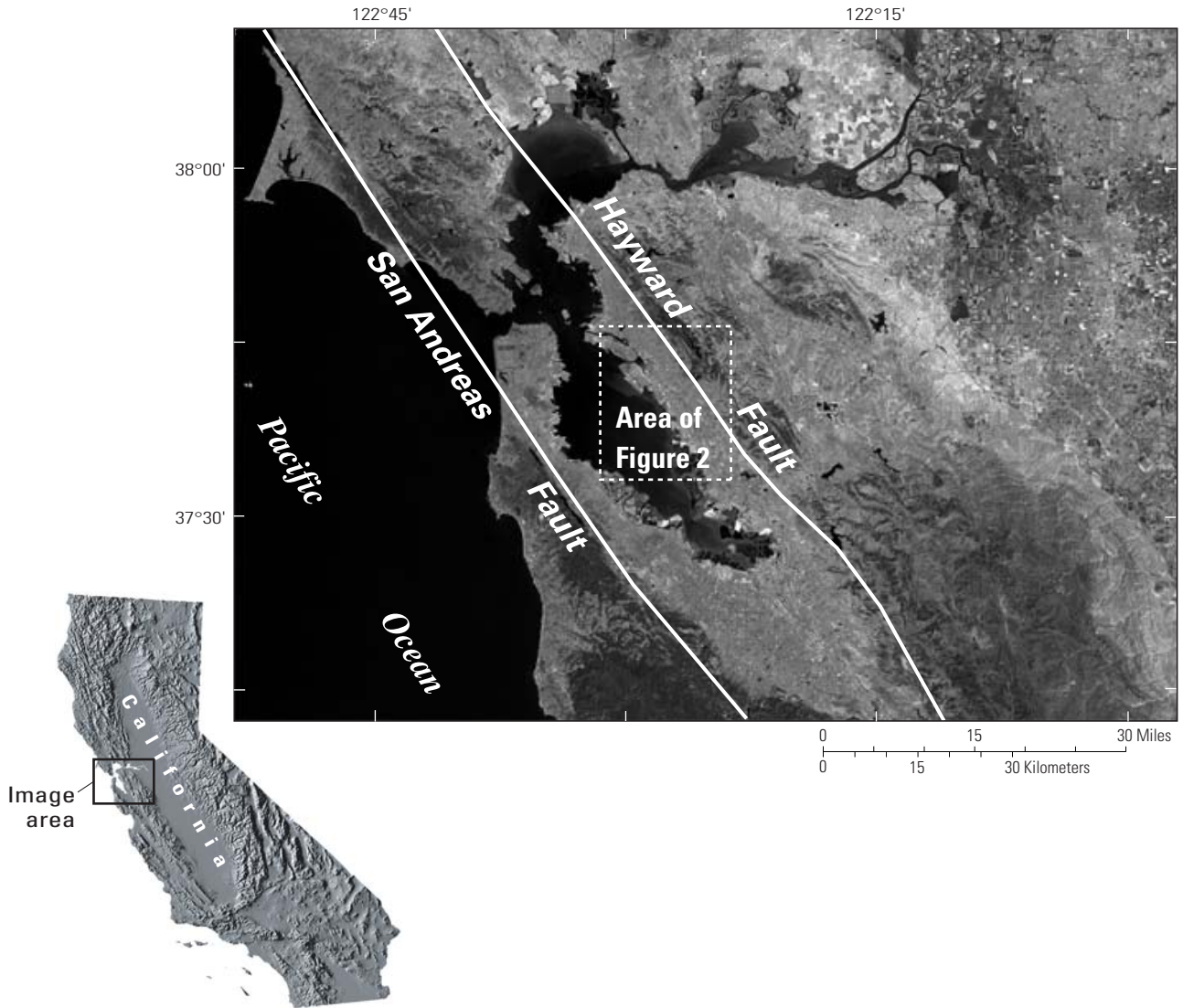


Figure 1. Satellite image of the San Francisco Bay area, California, July 7, 1994.

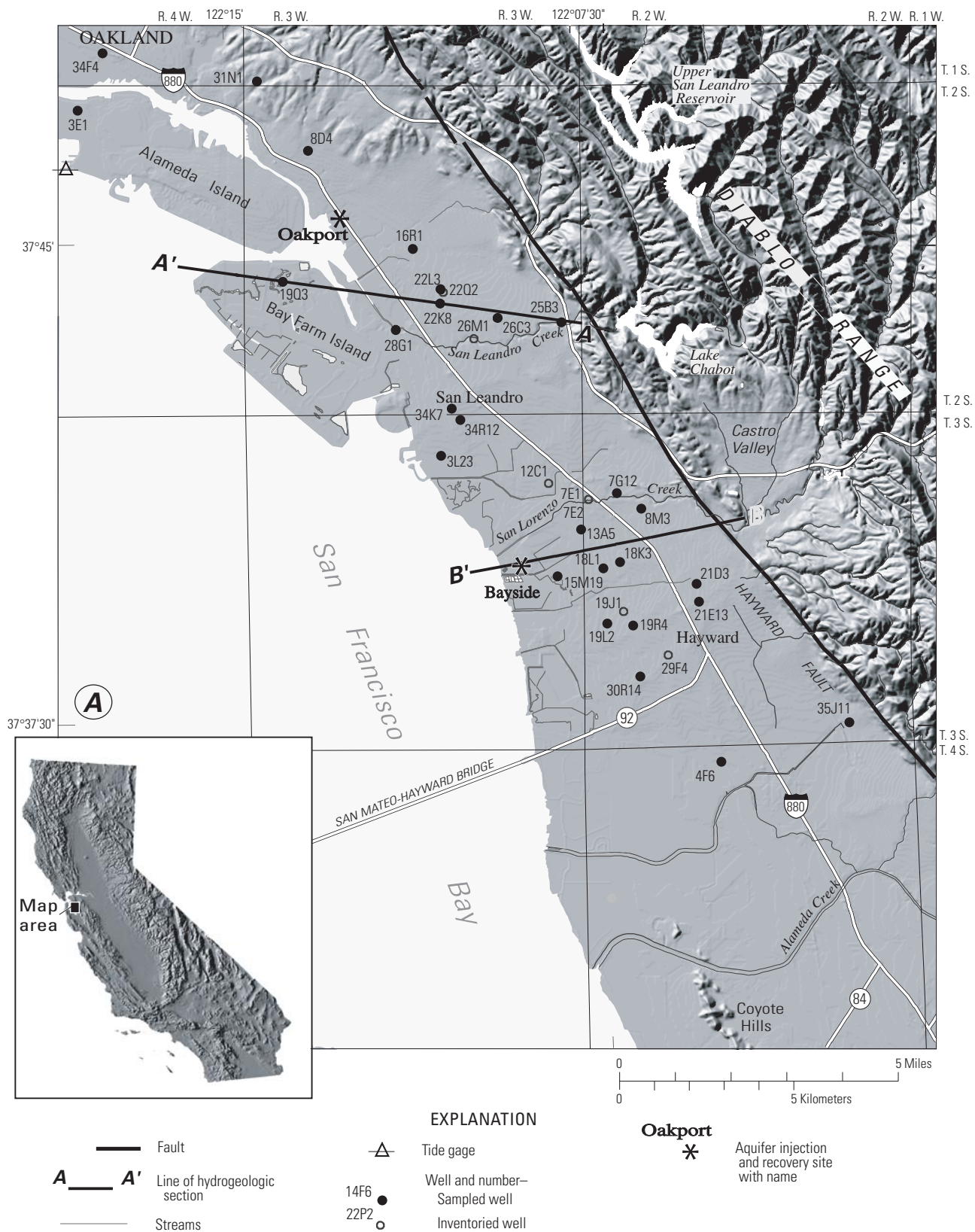


Figure 2. Location of study area, selected wells, and hydrogeologic sections; and selected wells at the Oakport injection/recovery and Bayside injection/recovery sites, East Bay Plain, Alameda County, California.

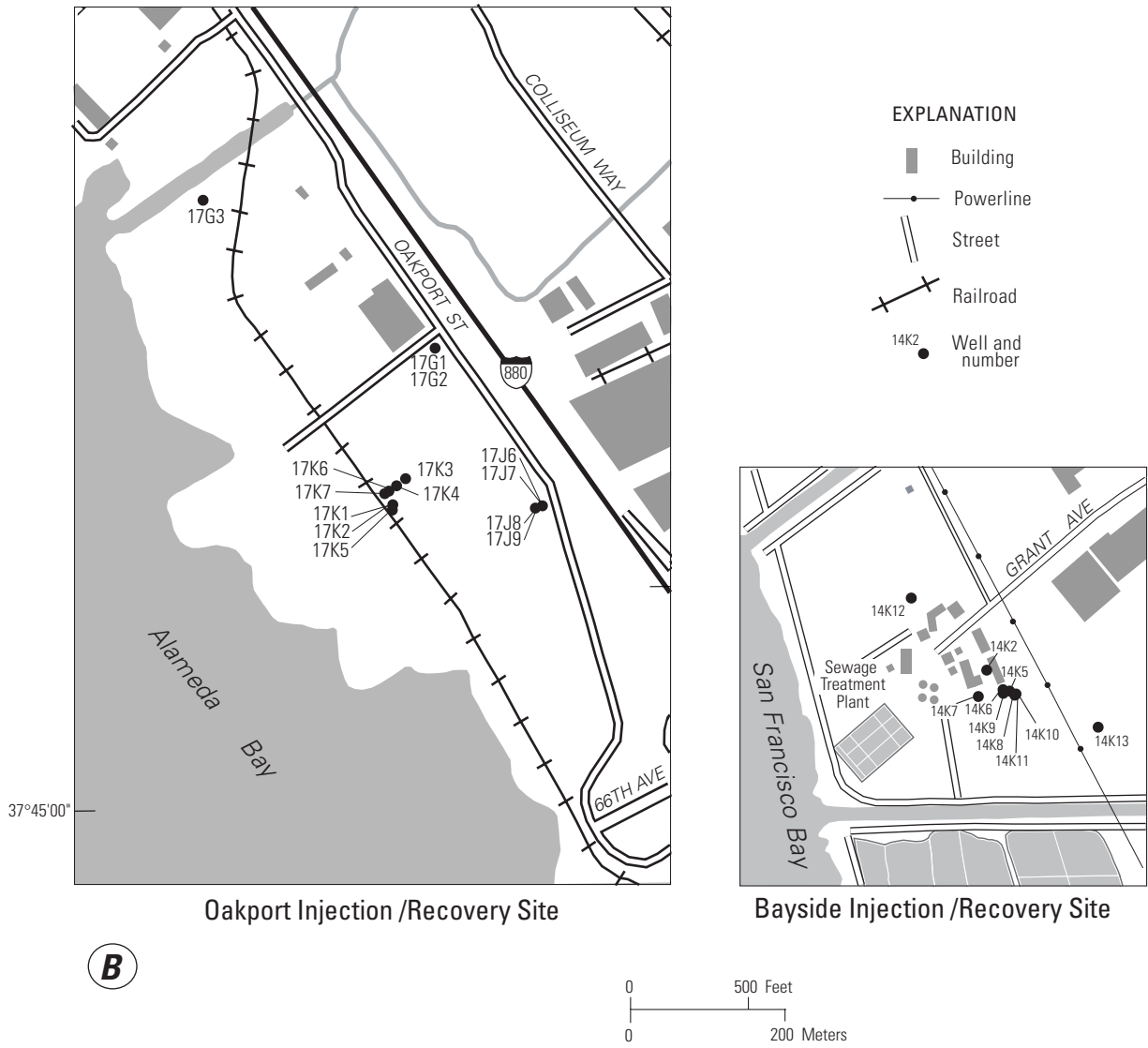


Figure 2.—Continued.

The scope of the study included (1) assembling, reviewing, and interpreting existing geophysical logs; (2) collecting water-level data from existing wells; (3) collecting borehole geophysical logs and depth-dependent water-quality data from existing wells; and (4) collecting chemical and isotopic data from existing wells. Most data were collected along two ground-water flow paths that extend from recharge areas near streams in the local mountains to discharge areas along San Francisco Bay.

Acknowledgments

This study was completed by the U.S. Geological Survey in cooperation with the East Bay Municipal Utility District and Alameda County Flood Control and Water Conservation District. The authors of this report acknowledge the contributions of Jennifer Hyman of East Bay Municipal Utility District and Andreas Godfery and James Yoo of Alameda County Public Works Agency for their technical assistance and field support. The authors also acknowledge David Gardner and Michael Burke of Fugro West, Inc., and Dan Wendell and Lucius Taylor of CH₂M-Hill, who provided access to wells, test-drilling data, and water-level data collected at aquifer-injection and extraction facilities in support of this study.

HYDROGEOLOGY

Geologic Framework

The study area is located in a structural depression underlying San Francisco Bay that is bounded by the San Andreas Fault to the west and the Hayward Fault to the east (Trask and Rolston, 1951; Marlow and others, 1999; Sedlock, 1995). The thickest deposits in the study area are located near San Leandro along the margin of San Francisco Bay (Rogers and Figuers, 1991; Marlow and others, 1999), and deposits thin to the north. Deeper deposits within this structural depression have been compressed and folded as a result of movement along the faults (Marlow and others, 1999). During at least the last 130,000 years, the areal extent of the Bay has been controlled by sea-level changes, geologic movement along faults, and sedimentation from upland streams. For example,

during periods of low sea level, coinciding with glacial maximums, the Bay was a broad valley incised by streams (Atwater and others, 1981).

The study area is underlain by a complex sequence of unconsolidated marine and continental deposits. The marine deposits consist primarily of estuarine mud and salt-marsh deposits that include the Young Bay Mud, the Old Bay Mud [also known as the Yerba Buena Mud (Sloan, 1992)], and several other units (Trask and Rolston, 1951; Ross, 1977; Atwater and others, 1981; Rogers and Figuers, 1991; Sloan, 1992; CH₂M-Hill Inc., 2000). In some studies, these units and interbedded alluvial deposits are collectively referred to as the Alameda Formation (Figuers, 1998). Continental deposits consist of coarse-grained stream-channel deposits and finer grained flood-plain deposits (Sloan, 1992; Koltermann and Gorelick, 1992), which compose the coalescing alluvial fans of San Leandro and San Lorenzo Creeks and other drainages along the east side of San Francisco Bay.

Variations in climate—coupled with rising and falling sea levels, and tectonic activity—produced a complex sequence of coarse-grained aquifers and fine-grained confining layers (Koltermann and Gorelick, 1992). Marine and continental deposits underlying the study area interfinger in a broad transition zone. Predominantly marine or estuarine sections may contain sporadic gravel and sand deposits from buried stream channels, and predominantly alluvial deposits may contain isolated estuarine mud or salt-marsh deposits (Sloan, 1992) depending on specific climatic and geologic conditions at the time of deposition.

During the Holocene, sea-level altitude and the rate of sea-level rise relative to sediment deposition from encroaching alluvial fans controlled the bayward extent of sand and gravel deposits that compose present-day aquifers. The same factors controlled the landward extent of fine-grained estuarine deposits that, along with fine-grained alluvial deposits, compose confining units between aquifers (Atwater and others, 1977). For example, about 10,000 to 8,000 years before present, sea level was 160 ft lower than at present. At that time, sea-level rise exceeded sedimentation rates. Wetter climatic conditions and high-energy gradients along streams resulting from the lower sea level allowed the transport of sand and gravel farther from the mountain front than under present-day conditions (Koltermann and Gorelick, 1992). As a result, alluvial deposits extended farther into the present-day bay, and mudflats and salt marshes were limited in areal extent.

Beginning about 8,000 years before present, sea-level rise slowed and continued deposition allowed the development of areally extensive mudflats and salt marshes (Atwater and others, 1977). Rising sea levels decreased the energy gradients along streams, and coarse-grained materials were not transported as far from the mountain front.

As a result of sea-level changes and tectonic activity during the Holocene, San Leandro and San Lorenzo Creeks eroded and dissected deposits inland from the margin of the Bay; subsequently, these incisions were backfilled and buried by later deposition. Some buried channels underlying the study area are as much as 150 ft thick (Figuers, 1998). In most previous studies, it was reported that it is difficult to correlate coarse-grained stream-channel deposits over great distances between wells. Deeper deposits have been transported northward as a result of movement along the Hayward Fault, and the coarse-grained alluvial deposits at depth may have been originally deposited by streams farther to the south (Maslonkowski, 1988; Koltermann and Gorelick, 1992).

Aquifer Systems

The four primary aquifers in the study area consist of aeolian sand, alluvial sand, and gravel deposits separated by estuarine mud or fine-grained alluvial flood-plain deposits. In many areas, the aquifers are discontinuous and it is difficult to correlate sand and gravel layers over great distances between wells. In the study area, the aquifers are named (from shallowest to deepest) the Newark, Centerville, Freemont, and Deep aquifers. The names are derived from aquifer names defined in the alluvial fans of Alameda Creek, commonly known as the Niles Cone basin, farther to the south and were originally extended into the study area by Brown and Caldwell (1986) and Maslonkowski (1988). In the study area, the aquifers identified by these names are believed to be “time-equivalent” units, and it is not known if they are hydraulically connected to aquifers in the Niles Cone basin.

The Newark aquifer is present throughout the study area to a depth of 30 to 130 ft below land surface (CH₂M-Hill Inc., 2000). Water in the Newark aquifer is generally confined except near recharge areas along the mountain front. The underlying Centerville aquifer is

about 100 ft thick and extends to depths of about 220 ft (Maslonkowski, 1984). In the Niles Cone basin the Freemont aquifer is a generic name for discontinuous sand and gravel deposits between 240 and 400 ft below land surface. In the study area the name has been applied to sand and gravel deposits as deep as 500 ft by CH₂M-Hill, Inc. (2000). The Deep aquifer is between 500 and 650 ft below land surface and in some areas it is as much as 100 ft thick. The Deep aquifer is thickest and most continuous south of San Leandro (Maslonkowski, 1988) and thins, eventually disappearing, to the north (CH₂M-Hill, Inc., 2000). In this area, aquifers are underlain by partly consolidated deposits (Marlow and others, 1999) having low porosity and low permeability.

For the purposes of this report, the aquifers have been divided into upper and lower aquifer systems having similar properties (fig. 3). This division approximates the shallow-zone aquifers and deep-zone aquifers described by Muir (1997) in his study of the East Bay Plain. The upper aquifer system contains the Newark and Centerville aquifers and is present to depths of 200 to 250 ft below land surface. For the purposes of this report, the lower aquifer system contains units designated as the Freemont aquifer by CH₂M-Hill, Inc. (2000) and the underlying Deep aquifer.

Recharge and Discharge

Under predevelopment conditions, recharge to the aquifers occurred primarily as infiltration of streamflow from San Leandro and San Lorenzo Creeks. Smaller amounts of recharge are believed to have occurred as infiltration of precipitation. Muir (1996a) estimated that annual recharge from infiltration of streamflow and direct infiltration of precipitation in the San Leandro and San Lorenzo areas was about 3,500 and 800 acre-ft, respectively. Some recharge may have occurred to deeper aquifers as ground-water movement from the Niles Cone basin to the south. The Hayward Fault is a barrier to ground-water flow, and under predevelopment conditions ground-water discharge along the fault maintained flow in springs (Figuers, 1998). To the west of the Hayward Fault ground water flowed toward San Francisco Bay where it discharged to tidal wetlands or continued to flow west under the Bay (Muir, 1996b).

As a result of agricultural and urban development beginning in the late 1800s, ground-water pumping became an important source of discharge from the study area. More than 15,000 wells were drilled in the study area between 1886 and 1950 (Figuers, 1998). Most of these wells were less than 100 ft deep, although some wells were more than 400 ft deep and a few were drilled to depths greater than 1,000 ft (Fig. 4). Ground-water pumping in excess of recharge caused water-level declines and seawater intrusion in the upper aquifer system. Figuers (1998) attributed increasing chloride in the lower aquifer system to flow from overlying intruded aquifers through leaking and abandoned wells into underlying aquifers. Recharge from ground-water movement into the basin from the Niles Cone basin to the south of the study area may have increased as a result of pumping and subsequent water-level declines in the lower aquifer system.

As a result of urbanization, additional recharge is believed to have occurred as leakage from underground water-supply and sewer pipes. Muir (1996a) estimated that total recharge from leaking pipes was about 3,100 acre-ft/yr in the San Leandro and San Lorenzo areas—one of the largest single sources of recharge in the study area. However, data presented in this report suggest that recharge from leaking pipes may be less important than reported by Muir (1996a) or may not be uniformly distributed across the study area. Most of this water would originate outside the basin as imported water from the Sierra Nevada. At the same time that recharge from leaking water-supply and sewer pipes increased, natural recharge may have decreased as a result of urbanization because streams were channelized and lined with concrete and permeable soil surfaces were paved.

Water Levels and Ground-Water Movement

A map of the water-table altitude between 1998 and 2000 made using water-level measurements in shallow wells and shallow-cone penetrometer data (Tom Holzer, USGS, written commun., 2000) indicates that ground water in the upper aquifer system generally flows west from the mountain front to discharge areas near San Francisco Bay (fig. 5). The water-level contours indicate movement of ground water from San Leandro and San Lorenzo Creeks into the underlying aquifer systems. Muir (1993) identified these streams

as the primary recharge areas for aquifers underlying the East Bay Plain. However, Muir also suggested that direct infiltration of precipitation, return from lawn watering, and leaking pipes also contribute to ground-water recharge in these areas.

Under predevelopment conditions, the direction of ground-water flow in the lower aquifer was probably similar to that of the upper aquifer system. Water-level maps constructed by CH₂M-Hill, Inc. (2000) using average water-level altitudes collected from wells during 1990–98 indicate that ground-water levels have been affected by pumping in the northern part of the study area; and these maps suggest that there may be a small component of flow in the Deep aquifer within the lower aquifer system from the south (CH₂M-Hill, Inc., 2000). Based on earlier water-level data, Muir (1993) also believed that ground water moved from the south within the Deep aquifer.

Water Levels at the Oakport Injection/Recovery Site

Water levels in selected wells completed at different depths at the Oakport injection/recovery site were measured at 15-minute intervals using pressure transducers over an annual cycle from October 1999 to September 2000. Based on these data, water levels in aquifers at the Oakport injection/recovery site are above mean sea level (fig. 6).

The highest water levels at the Oakport injection/recovery site are in well 2S/3W-17K1, which is completed in the upper aquifer system 140 to 180 ft below land surface. Water levels are as much as 2 ft lower in well 2S/3W-17K3, which is completed in the lower aquifer system about 260 to 350 ft below land surface (fig. 6), and the vertical hydraulic gradient between the upper and lower aquifer systems at this site is downward. Downward gradients may be related to current pumping or to historical pumping that lowered the ground-water levels in the lower aquifer system. Ground water at the site would tend to move downward in response to the hydraulic gradient. The rate of movement will be determined by the vertical hydraulic conductivity and by the areal extensiveness of the intervening deposits. If the vertical hydraulic conductivity is low and the confining units are continuous, the quantity of water moving from the upper aquifer system into lower aquifer system will be small.

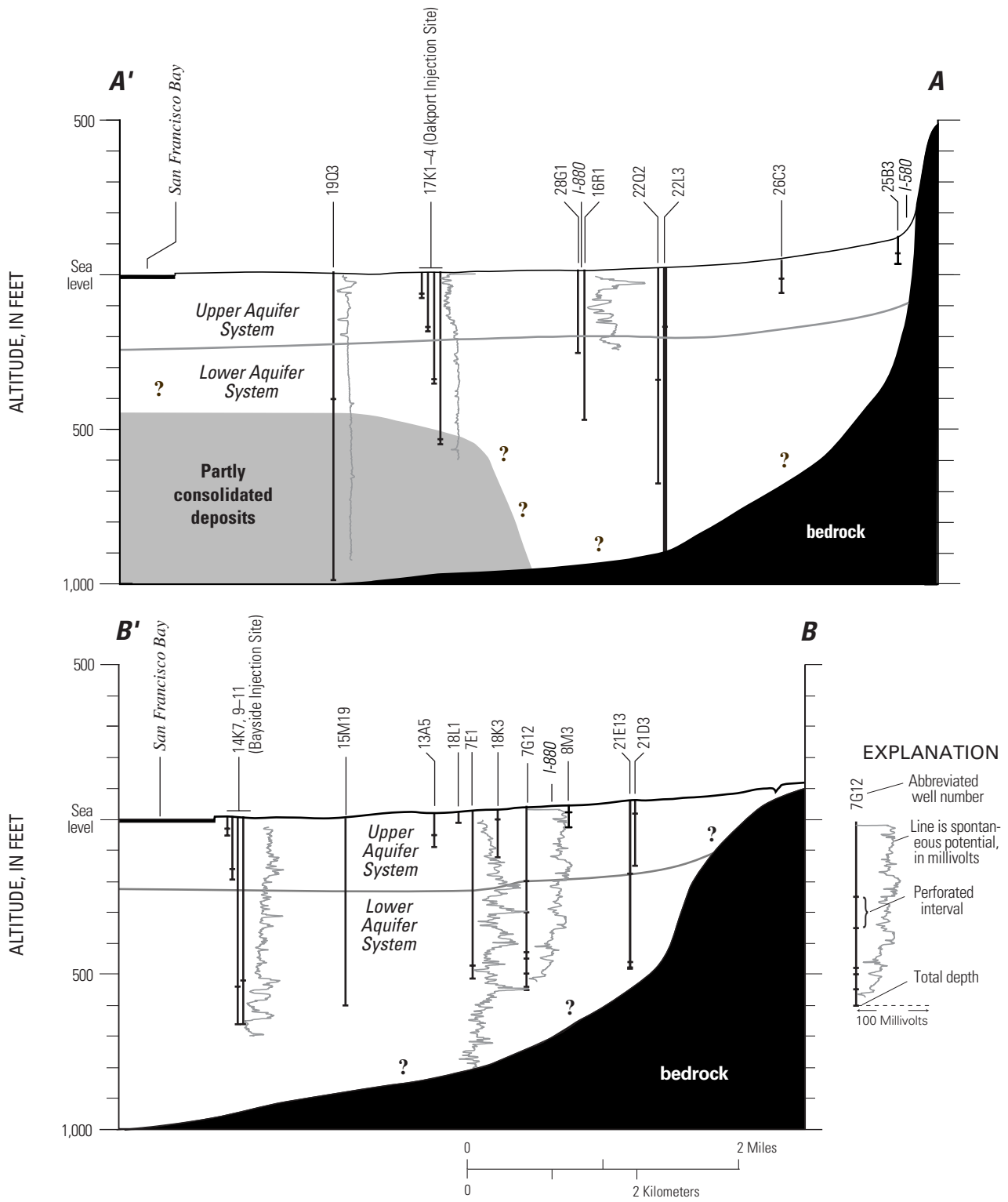


Figure 3. Generalized hydrogeologic sections A-A' and B-B', East Bay Plain, Alameda County, California.

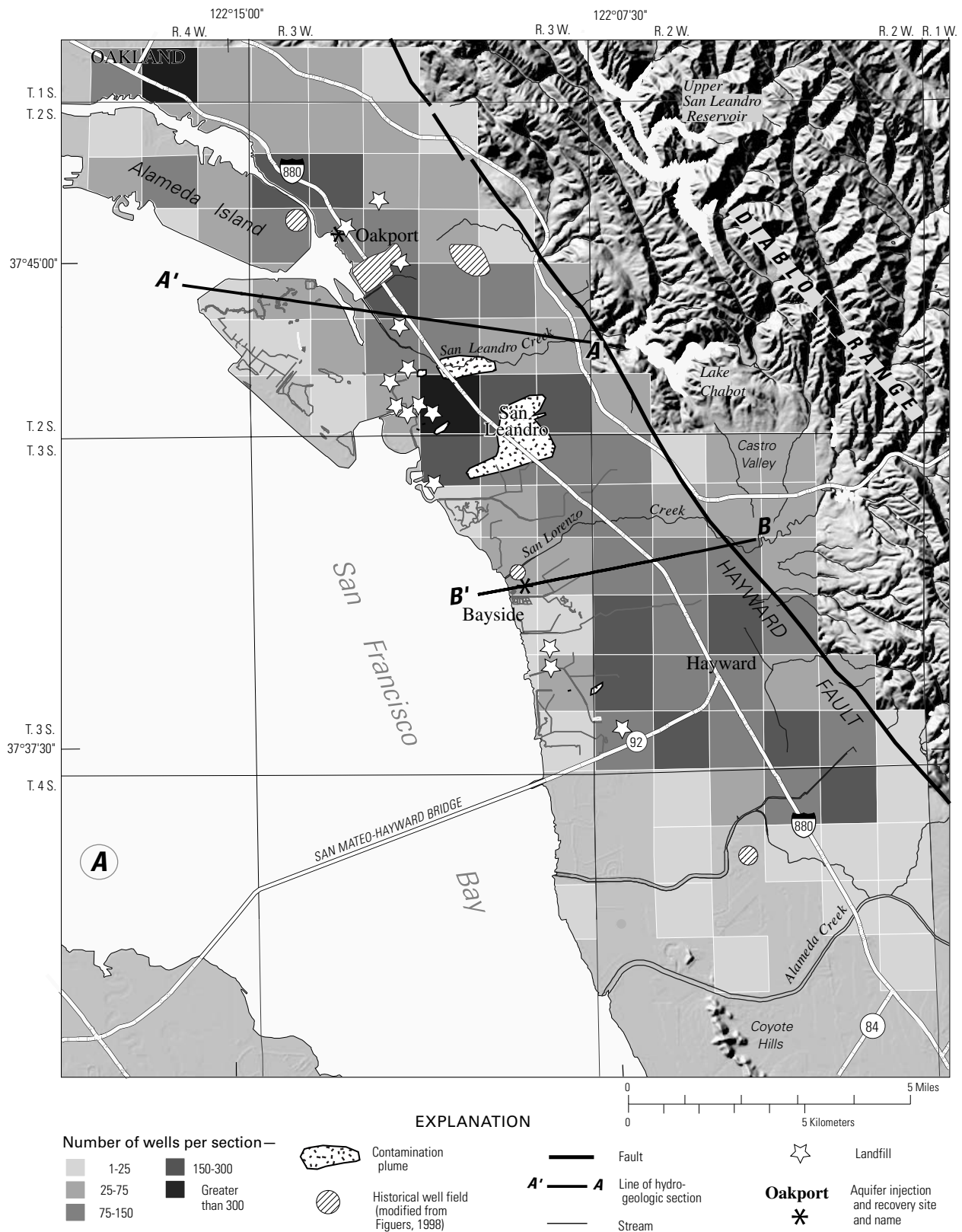


Figure 4. Number of wells per section (**A**), and number of wells per section greater than 400 feet deep (**B**) in the East Bay Plain, Alameda County, California. Data from Alameda County Regional Flood Control and Water Conservation District well data base, 1999, and San Francisco Regional Water Quality Control Board, 1999.

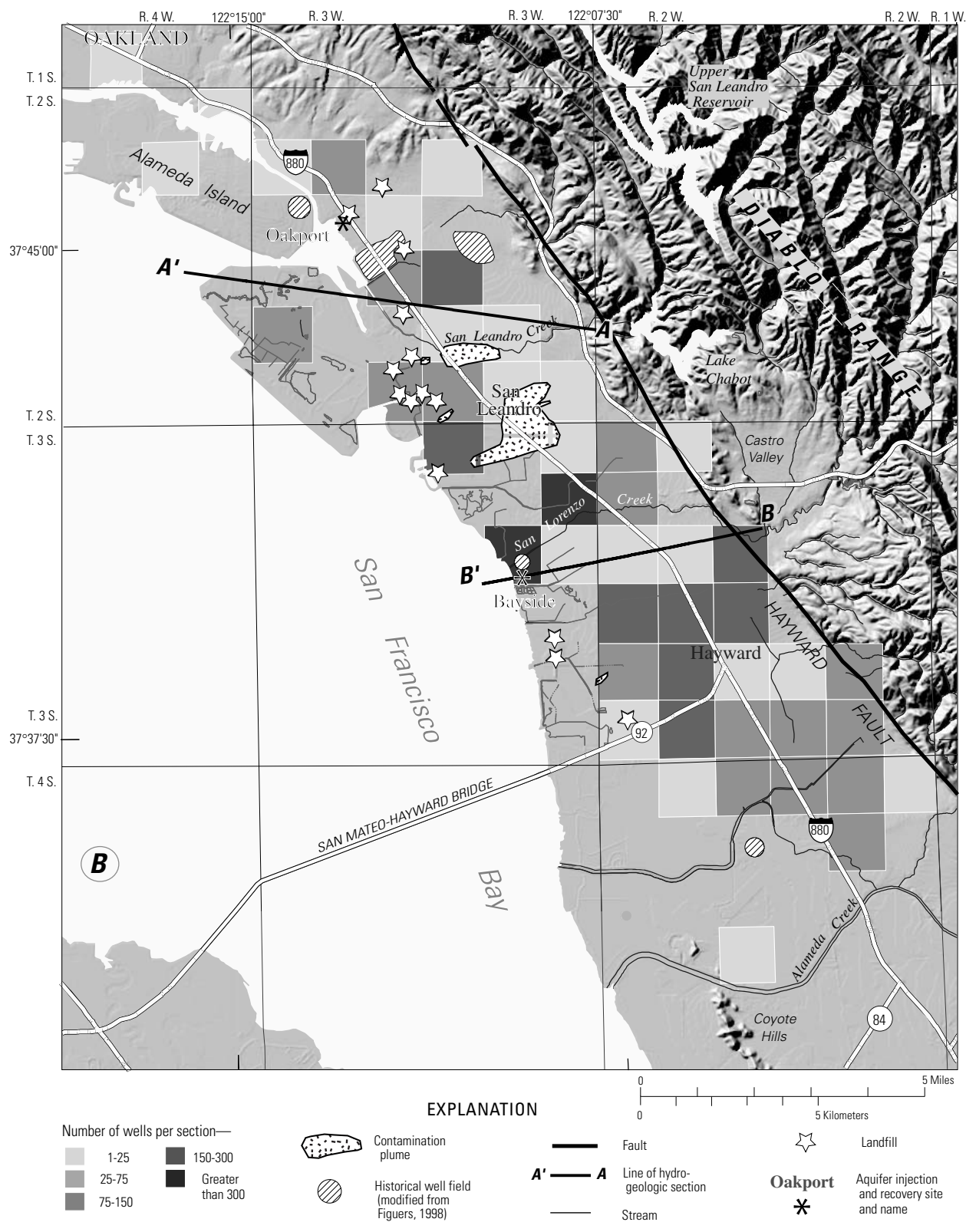
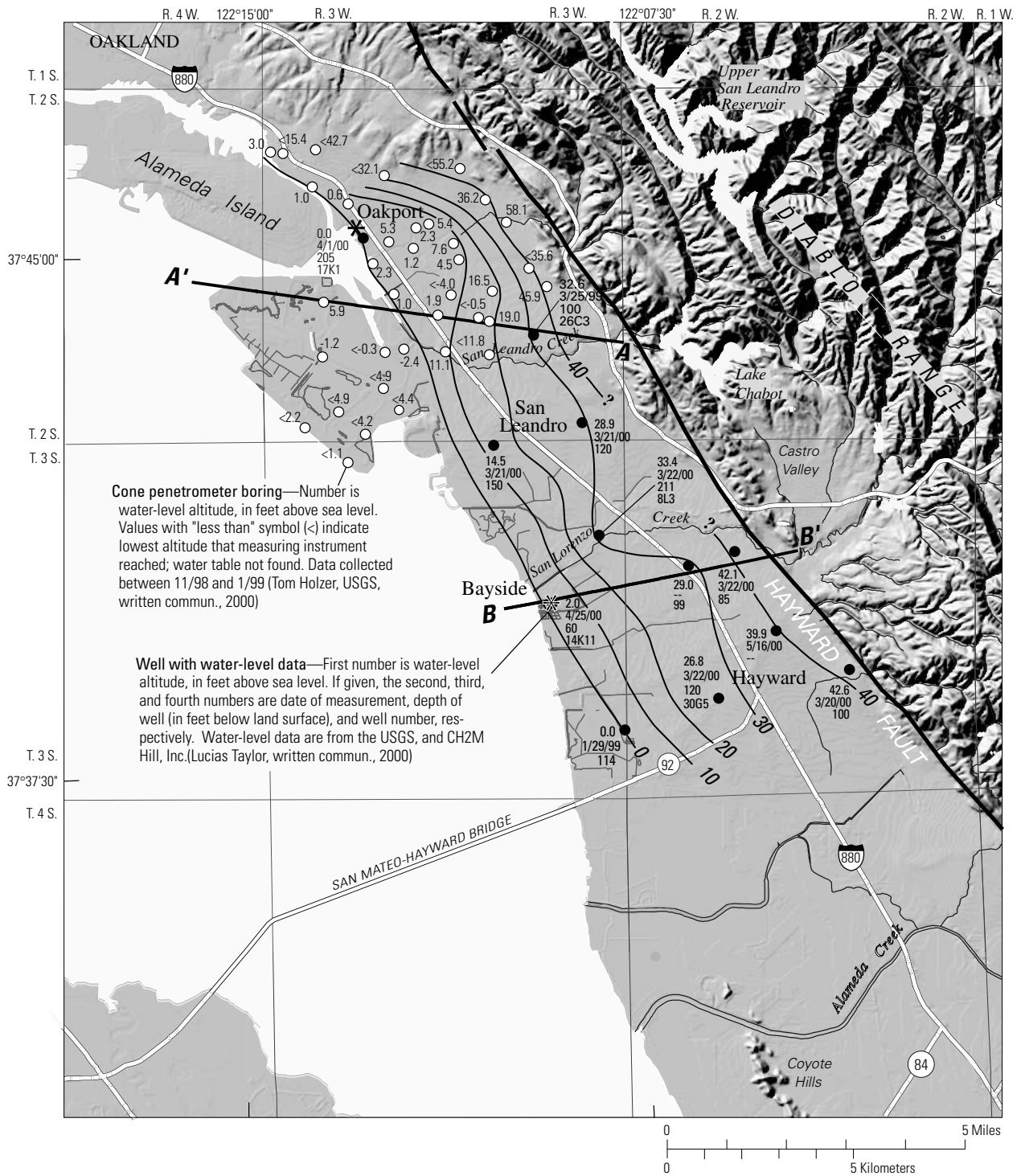


Figure 4.—Continued



- EXPLANATION**
- Fault
 - 40— Water-level contour—Altitude of water level, in feet. Datum is sea level. Queried where uncertain
 - Cone penetrometer boring
 - A'—A Line of hydrogeologic section
 - Well
 - Stream
 - Oakport** * Aquifer injection and recovery site and name

Figure 5. Winter-spring water levels in shallow wells and borings, East Bay Plain, Alameda County, California, 1999–2000.

(Water-level altitudes not corrected for density variations caused by shallow saline water in nearshore areas.)

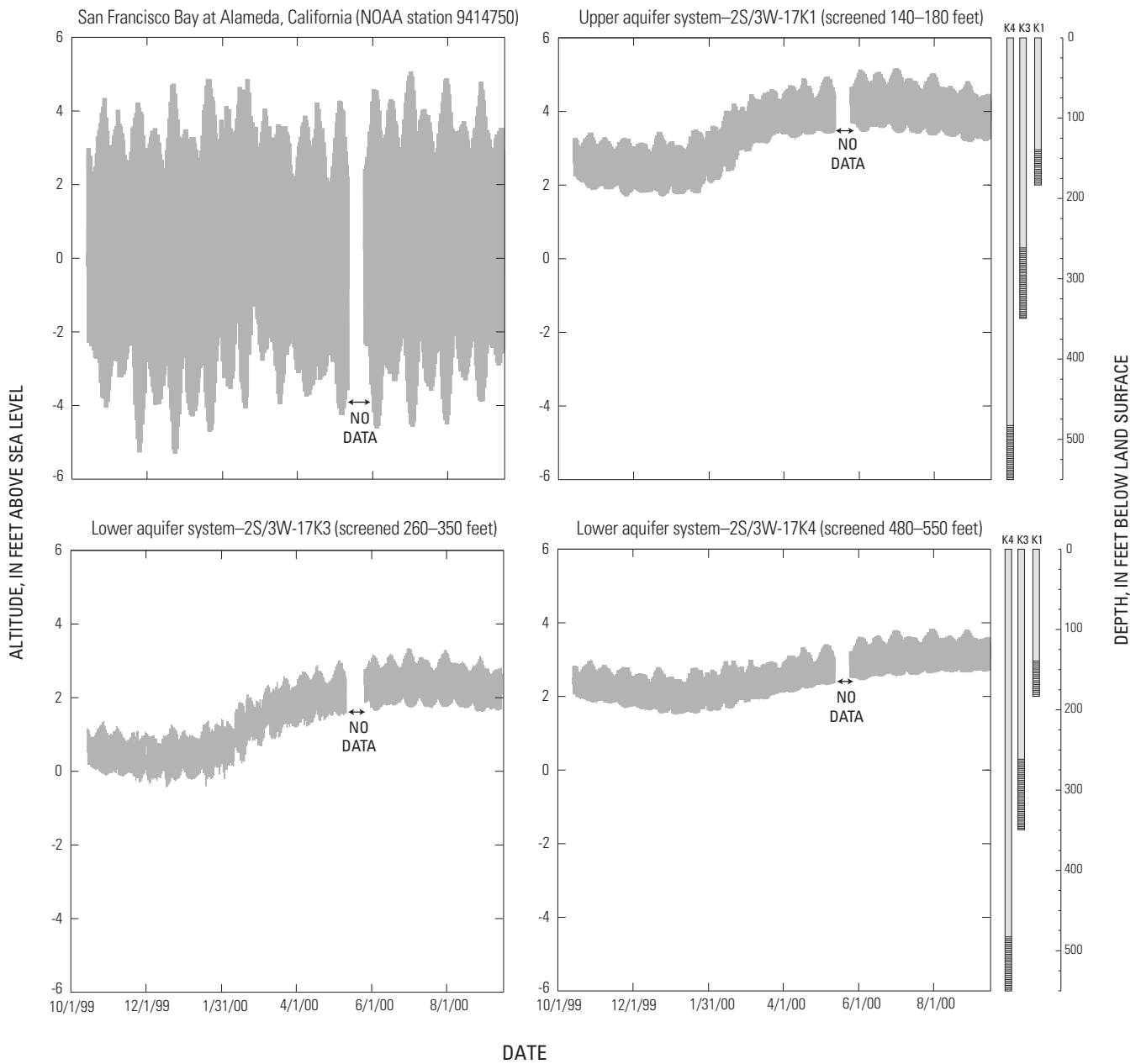


Figure 6. Altitude of water in San Francisco Bay at Alameda Island and water levels in wells 2S/3W-17K1, 3, and 4 at the Oakport injection/recovery site, East Bay Plain, Alameda County, California, October 14, 1999, to September 14, 2000.

At greater depths, water levels in well 17K4, screened from 480 to 550 ft below land surface in the partly consolidated rocks that underlie the lower aquifer system, are higher than water levels in the lower aquifer system and the vertical hydraulic gradient is upward. Under these conditions, water in partly consolidated deposits will tend to move upward into overlying deposits.

Water levels in wells 17K1 and 17K3 completed in the upper and lower aquifer systems, respectively, change 1 to 2 ft in response to seasonal distribution of pumping and ground-water recharge; the response is less in well 17K4 (fig. 6). These water-level data suggest that water in the underlying partly consolidated deposits is more isolated from pumping and surface sources of recharge than is water in the upper and lower aquifer systems.

Water levels in all three wells at the Oakport injection/recovery site show short-term, cyclical responses to tides in San Francisco Bay. These short-term water-level responses can be used to estimate the areal extent of the aquifer deposits beneath the Bay and to evaluate the properties of the confining layers separating the aquifer systems.

Water Levels at the Bayside Injection/Recovery Site

Water levels in selected wells at the Bayside injection/recovery site were measured by Fugro West, Inc. (1999a,b) during injection/recovery tests done between November 1998 and April 1999 using pressure transducers. Additional water-level measurements were made intermittently in selected wells from March 2000 through November 2000 (Michael Burke, Fugro West, Inc., oral commun., 2000). Based on these data, water levels at this site are above sea level only in the shallow well screened between 40 and 60 ft below land surface in the upper aquifer system. Water levels were near or slightly below sea level in deeper parts of the upper aquifer system (well 14K10 screened between 160 and 190 ft below land surface) and several feet below sea level in three wells screened in the Deep aquifer within the lower aquifer system.

The downward hydraulic gradient at the Bayside injection/recovery site may be related to current pumping from the lower aquifer system or to historical pumping that lowered ground-water levels in this part

of the lower aquifer system to more than 70 ft below land surface during the 1970s (James Yoo, Alameda County Public Works Agency, written commun., 2000).

Injection and extraction testing in the lower aquifer system since November 1998 has caused water levels to range between 27 ft above to more than 170 ft below land surface in injection-test well 3S/3W-14K5 (Fugro West, Inc., 1999a,b). During periods of injection, water levels in wells 14K 6–8 completed at the injection depth in the lower aquifer system rose above sea level (fig. 7). Water levels in well 14K10 completed in the upper aquifer system also responded to the hydraulic pressure created in the lower aquifer system by injection of imported water. [Well 14K10 also responded during periods of extraction in the lower aquifer system (Michael Burke, Fugro West, Inc., written commun., 2000)]. Water levels in well 14K11 completed between 40 and 60 ft below land surface in the upper aquifer system were apparently unaffected by injection. During injection the hydraulic gradient at the site was reversed and water would tend to move upward from the lower aquifer system into the overlying upper aquifer system. As previously discussed, the rate of movement would be determined by the vertical hydraulic conductivity and areal extent of the confining layers at the site.

Water levels in a long-screened production well, 3S/3W-14K2, present at the site reflect water levels in the lower aquifer system even though the well is perforated from 150 to 813 ft below land surface and completed in both the upper and lower aquifer systems. It is possible that under some circumstances water may move between the upper and lower aquifer systems through this well. The direction of movement would be determined by the water levels and resulting hydraulic gradient between the aquifer systems.

The available data do not allow for an evaluation of water-level responses to seasonal pumping and recharge in the same manner as data collected at the Oakport injection/recovery site.

Short-term cyclical changes in water levels from tides in San Francisco Bay are present in water levels in well in the Deep aquifer at the Bayside injection/recovery site (fig. 8). Unlike the Oakport site, water-level changes from tides are small in the upper aquifer system.

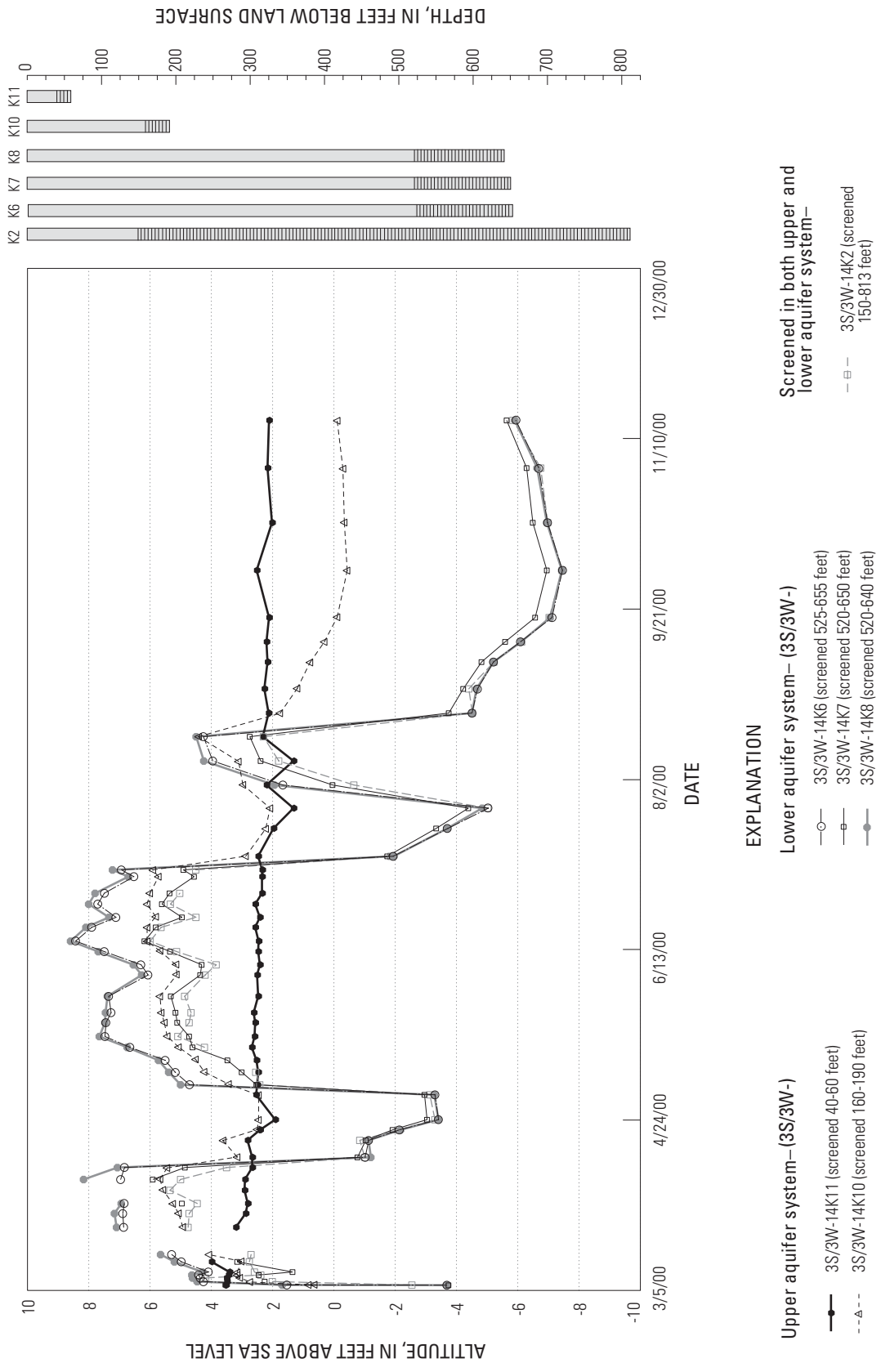
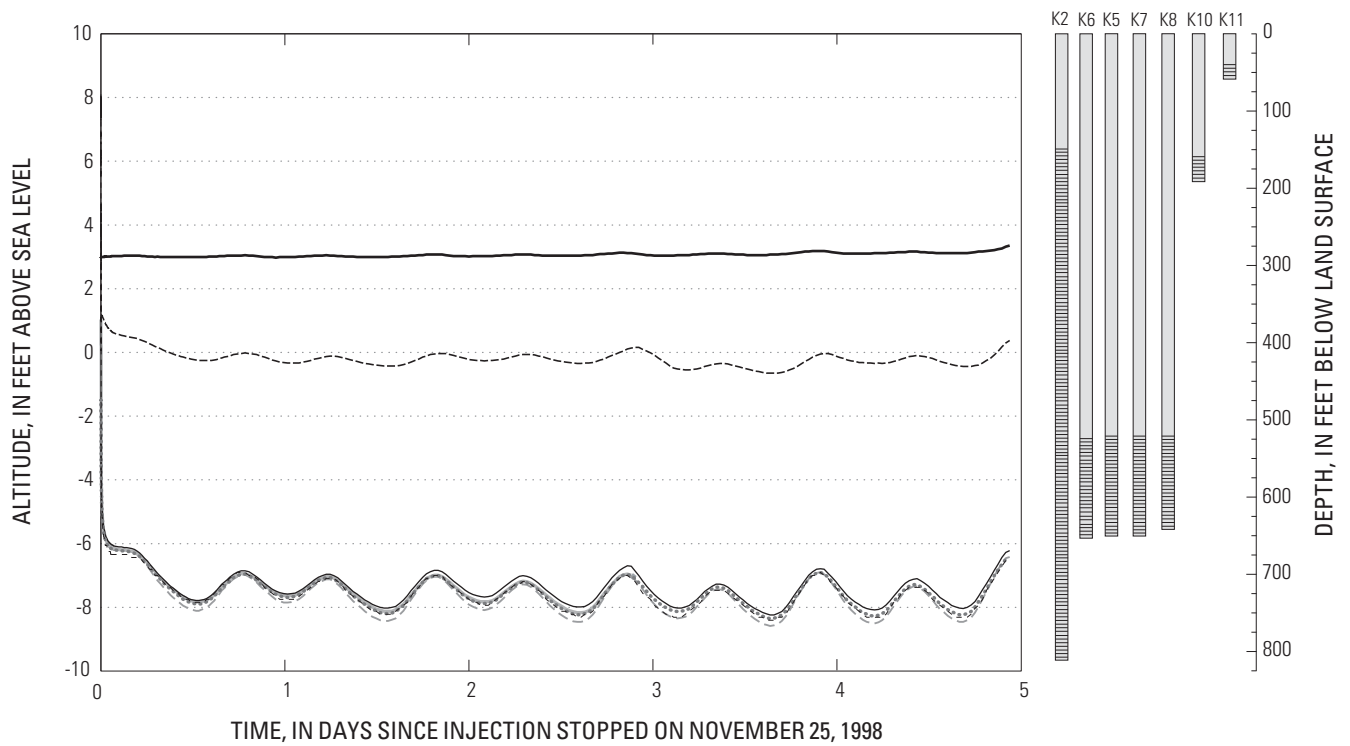


Figure 7. Water levels in selected wells at the Bayside injection/recovery site, East Bay Plain Alameda County, California, measured during injection tests and static periods, March 6 to November 15, 2000.



EXPLANATION

Upper aquifer system— (3S/3W-)	Lower aquifer system—(3S/3W-)	Screened in both upper and lower aquifer system—
— 3S/3W-14K11 (screened 40–60 feet)	--- 14K5 (screened 520–650 feet)	— 3S/3W-14K2 (screened 150–813 feet)
- - - - 3S/3W-14K10 (screened 160–190 feet) 3S/3W-14K6 (screened 525–655 feet)	
	- · - · - 3S/3W-14K7 (screened 520–650 feet)	
	— 3S/3W-14K8 (screened 520–640 feet)	

Figure 8. Water levels in selected wells at the Bayside injection/recovery site, East Bay Plain, Alameda County, California, November 25–29, 1998.

WATER-LEVEL RESPONSE TO TIDAL FLUCTUATION

Short-term, cyclic water-level changes in observation wells at the Oakport and Bayside injection/recovery sites are a pressure response to tides in San Francisco Bay. The correlation between water levels and tides in San Francisco Bay can be used to evaluate the areal extent of aquifers beneath the bay and the hydraulic properties of confining layers. A water-level response to tidal changes does not indicate that saline Bay water moves into or out of the aquifer. Thick estuarine clay beds separate the saline water in the Bay from the intervals monitored by the observation wells. In this report, the correlation between Bay tides and water levels in the aquifer zones is related only to tidal loading as described in the following.

Background

During a rising tide, the stage and volume of water filling the Bay increases. The increased load compresses sedimentary deposits beneath the Bay, elastically reducing their pore volume, increasing pore-fluid pressure and, thereby, causing water-level rises in wells. A confined aquifer system responds to changing overburden load, which is uniformly applied over the aquifer system over a large areal extent, according to the compressibility of the saturated sediment (Van der Kamp, 1972). In general, shallow unlithified sediments are more compressible than are sediments that are partly cemented with secondary mineral precipitates, or sediments that have been deeply buried, and fine-grained sediments are generally more compressible than are coarse-grained sediments. When the load is applied over only part of the aquifer system, as with tidal loading from San Francisco Bay, other unloaded areas of the aquifer system respond by fluid-pressure diffusion. For a well monitoring an aquifer directly beneath the applied load, the expected water-level response would be instantaneous, with a magnitude that is some fixed proportion of the applied load. This response is defined as the loading efficiency of the aquifer. For a well at some distance from where the load is applied, the expected water-level response would be an increase in water level that lags the rising tide. This is defined as the loading response. The

loading response is expressed as the change in water level in the well divided by the tidal change in the bay, and it is less than or equal to the loading efficiency. For a well at some distance from the applied load, the water-level response to the tidal load also varies with the frequency of the tide. The response to higher frequency (shorter period) tides is attenuated with respect to the response to low-frequency tides of the same magnitude. As a result, the loading response of each aquifer underlying the East Bay Plain decreases as the frequency of the tide increases.

Analytical models (Van der Kamp, 1972) that use the timelag between the tidal source function and the water-level response in wells to estimate aquifer properties require that the distance between an observation well and the location of the source function (the tide change) be known and unchanging. Quantitative analysis of the phase shift in the tidal signal is complicated by the bathymetry of Alameda and San Francisco Bays. As the tide recedes most of the bottom of Alameda Bay and much of the bottom of San Francisco Bay between Alameda and Bay Farm Islands ([fig. 2](#)) are exposed as mud flats. Because the distance between observation wells and the location of the source function varies with tidal stage, analytical models typically used to interpret water-level response to tidal fluctuations are not appropriate for this setting, and the analysis presented in this report is largely qualitative. The geometry of the aquifer zones beneath the Bay also may affect the water-level response. For example, if an aquifer is thin or absent beneath the Bay, the loading efficiency will be small.

The tides used for this analyses include the familiar lunar tides that occur twice a day and smaller, less frequent (low frequency) tides caused by the sun or planets and local shallow-water interference tides that occur in San Francisco Bay. Tidal fluctuations in San Francisco Bay were measured by a tide gage (National Oceanic and Atmospheric Administration site 9414750) located 5 mi west of Oakport, on Alameda Island ([fig. 2](#)). The average delay in the arrival of the tidal signal to observation wells at the Oakport injection/recovery site is about the same as the estimated travel time of the tide from the tide gage to the east shore of Alameda Bay adjacent to monitoring wells at the Oakport injection recovery site; about 0.5 hour. No tide gages are located near the Bayside injection/extraction site

Tidal Responses at the Oakport Injection/Recovery Site

The response and timing (phase shift) of water levels to tidal fluctuations in water from wells 2S/3W-17K1, 3, and 4 during October 1999 to May 2000 is illustrated as a function of tidal frequency in [figure 9](#). A continuous period of record is needed to calculate these parameters, and missing data from May 11 to 25, 2000, precluded using the entire period of record shown in [figure 6](#).

The loading response of water levels in well 17K4 ([fig. 9](#)) ranges from about 0.17 to 0.32 and is less than the response in well 17K1, which ranges from about 0.22 to 0.37. This indicates that hydraulic diffusivity (transmissivity/storage coefficient), the hydraulic property of the sedimentary deposits controlling fluid pressure transmission, is lower in the deeper deposits (17K4) than in the shallow deposits (17K1). This difference may result from partial cementation, lower porosity, and greater overburden compression of the deeper, partly consolidated deposits penetrated by well 17K4. The loading response curves at low frequencies for wells 17K1 and 17K4 ([fig. 9](#)) indicate that fluid pressures imposed by low-frequency tides do not dissipate by drainage through confining units. This implies that vertical hydraulic conductivity of clayey beds that confine both the upper aquifer and underlying partly consolidated rocks is very low. If the aquifer zones were not tightly confined, fluid pressures resulting from low-frequency loads would dissipate with time, and the loading response curves ([fig. 9](#)) would decline at low frequencies (Galloway and Rojstaczer, 1988).

In contrast, water levels in well 17K3 are not correlated with the Bay tides between October 1999 and May 2000 ([fig. 9](#)). The reasons for this are uncertain, but could be due to undefined response to barometric pressure change, or to the effects of pumping in wells that produce ground water from this depth. Because wells 17K1 and 17K4 are adjacent to well 17K3, it is unlikely that the lack of correlation results from barometric pressure differences at the wells or differences in the response of well 17K3 to barometric pressure change. It is more likely that ground-water pumping is partly responsible both for the lack of correlation ([fig. 9](#)), and for the vertical distribution of hydraulic head discussed previously ([fig. 6](#)).

The extent of the upper and lower aquifers beneath San Francisco Bay at Oakport also affects the response of the wells to tidal fluctuations. The shape of water-level hydrographs in wells 17K1, 3, and 4 varies depending on the altitude of the Bay tide ([fig. 10](#)). The well hydrographs are smoothly peaked during high tides and smoothly troughed during low tides when the altitude of the bay remains above about -2 ft. However, the troughs of the hydrographs are truncated when the altitude of the water surface in the bay decreases to below -3 ft. The lack of response to reduced load during very low tides may be related to limited lateral extent of the aquifer beneath the Bay. If aquifer zones do not extend great distances to the west beneath the Bay, they would not experience loading or unloading during very low tides because tidal fluctuations would occur when the shoreline is positioned to the west of the aquifer-zone boundaries. Because hydrograph truncation reduces the amplitude of the aquifer hydraulic-head response at very low tides, the loading responses calculated for each aquifer zone ([fig. 9](#)) were lower than expected.

Tidal Responses at the Bayside Injection/Recovery Site

The response of aquifer hydraulic head to Bay tides is shown for November 25–29, 1998, in [figure 6](#). Water-level altitudes in observation wells under static conditions between injection cycles varied cyclically ([fig. 8](#)) at frequencies that correspond to Bay tidal frequencies (Fugro West, Inc., 1999b). Hydraulic-head response to tidal loading was greatest in wells screened in the lower aquifer, between about 520 and 650 ft below land surface (3S/3W-14K2, and 5–8), smaller in well 17K10, screened between 160 and 190 ft below land surface, and barely perceptible in well 14K11, screened between 40 and 60 ft below land surface ([fig. 8](#)).

Continuous water-level measurements were not collected for a sufficiently long period at the Bayside injection/recovery site to allow a thorough analysis of loading response and phase shift changes with tidal frequency similar to the analysis done at the Oakport site. However, the relative magnitude of the tidal response and the general shape of the hydrographs indicate that the lower aquifer has a higher diffusivity or perhaps a greater lateral extent beneath San Francisco Bay than does the overlying upper aquifer system.

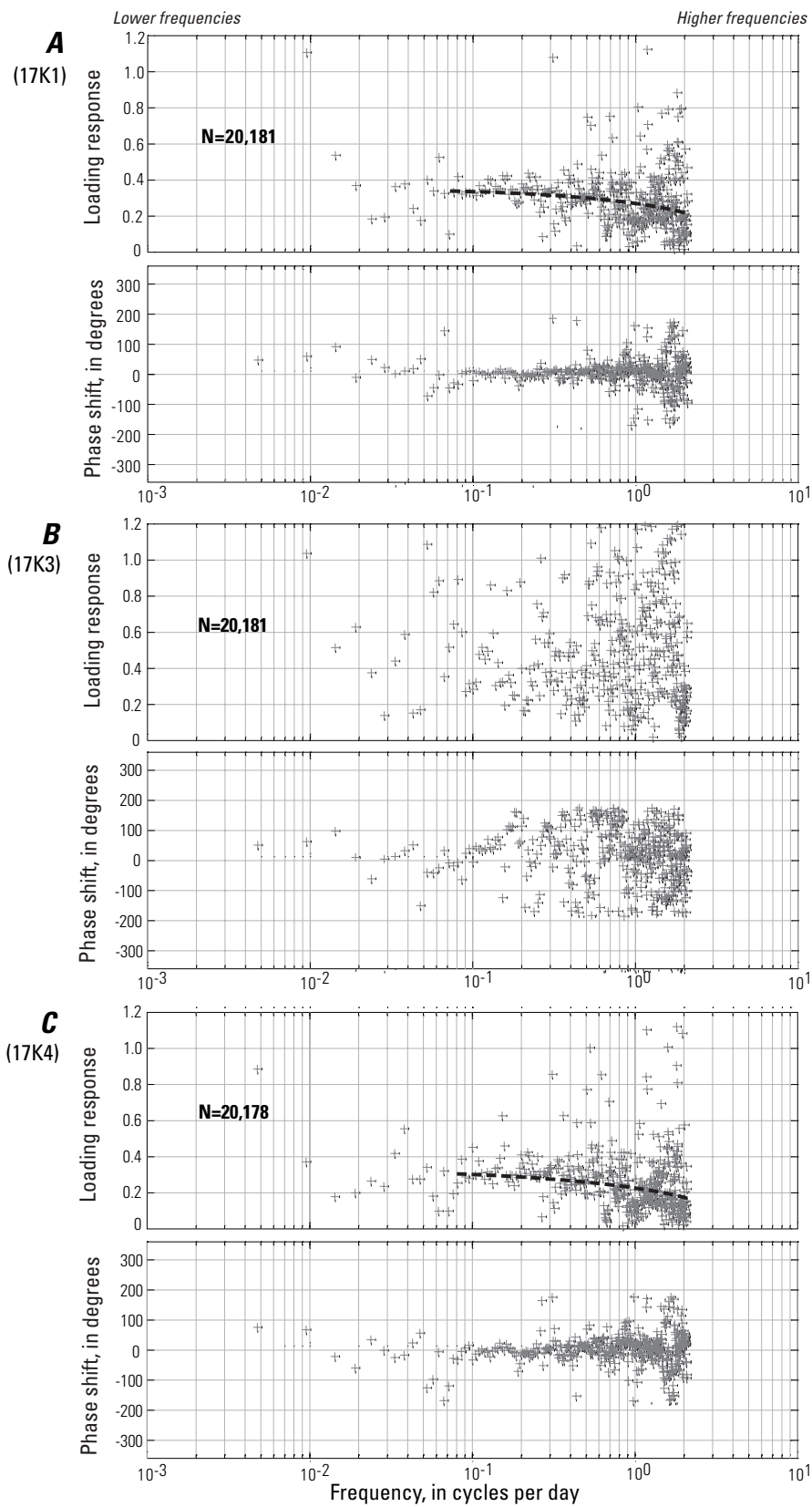
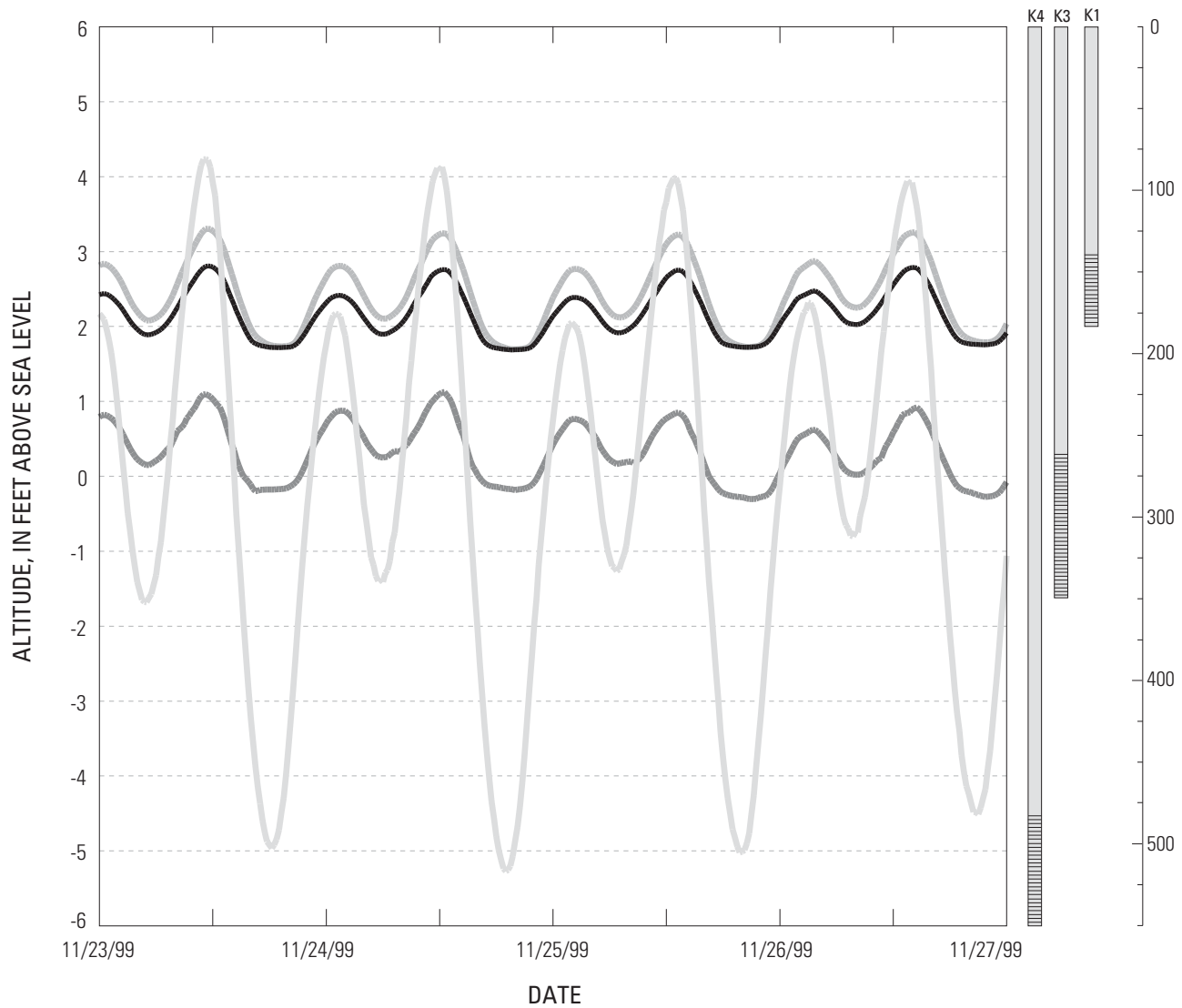


Figure 9. Frequency response of water levels in wells 2S/3W-17K1, 3, and 4 at the Oakport injection/recovery site to tides in San Francisco Bay, October 15, 1999, to May 15, 2000.



- EXPLANATION**
- 2S/3W-17K4 (screened 480-550 feet)
 - 2S/3W-17K3 (screened 260-350 feet)
 - 2S/3W-17K1 (screened 140-180 feet)
 - San Francisco Bay at Alameda, California (NOAA Station 9414750)

Figure 10. Altitude of water surface in San Francisco Bay at Alameda Island and water levels in wells 2S/3W-17K1, 3, and 4 at the Oakport injection/recovery site, November 23–27, 2000.

GEOPHYSICAL LOGGING OF SELECTED WELLS

Water-level data from observation wells completed in different aquifers and the correlation of cyclic changes in water levels with tides in San Francisco Bay suggest that aquifers underlying the Oakport and Bayside injection/recovery sites are separated by thick, areally extensive confining layers that limit the vertical movement of water between different aquifers. Well drilling has modified the natural system, and some wells may serve as conduits for flow between aquifers. Geophysical logs were collected to test hypotheses about flow between aquifers through wells under pumped and nonpumped conditions.

Well Bore Logging Techniques

Geophysical logs collected from the bores of existing wells as part of this study include natural gamma, well-bore velocity, fluid resistivity, and temperature logs.

Natural gamma logs measure the intensity of gamma-ray emissions from the natural decay of certain radioactive elements, primarily potassium-40 and the daughter products of uranium and thorium decay series (Driscoll, 1986). Natural gamma logs are used to identify clay layers within the aquifer deposits; however, high gamma intensities also may be associated with potassium-feldspar-rich layers, such as sand and gravel.

Well-bore velocity logs are a direct measure of vertical flow within the well. Depending on the expected flow rate and construction characteristics of the well, these logs were collected using either a vertical-axis current meter (spinner tool), a heat-pulse flow-meter, or an electromagnetic flow-meter. The spinner tool measures uphole velocities as low as 2 feet per minute as counts (revolutions) per second; flow in gallons per minute can be calculated if the well diameter is known. The heat-pulse flow-meter measures either uphole or downhole velocity as the time required for water to travel from a heating element to sensors a known distance from the heating element. The heat-pulse flow-meter measure velocities as low as 0.2 feet per minute and was used for the low velocities encountered during unpumped conditions in well 22Q2. The electromagnetic flow-meter measures either

uphole or downhole velocity according to Faraday's Law as the response of an induced magnetic field to the movement of charged ions within water flowing past the tool. The electromagnetic flow-meter measures velocities as low as 0.5 feet per minute and was used for the great depths and low velocities encountered during pumping of well 19Q3. The sensitivity of all three instruments may be increased by using a device to constrict flow in the well and increase velocity near the meter. This device was used under nonpumped conditions in well 22Q2.

The effect of vertical flow through the well bore on water quality, under pumped and nonpumped conditions, was evaluated using fluid-resistivity and temperature logs. Fluid-resistivity logs provide a measure of the quality of water in a well. The resistance of water to the flow of an electric current is inversely related to the quantity of dissolved ionic salts in the water. The less dissolved salts the greater the resistivity; the more dissolved salts the lower the resistivity. Fluid-resistivity is the inverse of fluid conductivity, which is related to the specific conductance of the water. Specific conductance is a field parameter measured on water samples collected as part of this study. Temperature is a physical property of water. In ground water, temperature can be affected by the depth of an aquifer and its proximity to recharge sources (among other factors) and ground water in different aquifers may have different temperatures. Movement of water through a well under pumped or nonpumped conditions will alter the fluid-resistivity and temperature profile of water in the well.

Well-bore logs are related to depth-dependent water-quality samples collected from the well bore under pumped and nonpumped conditions later in this report.

Well 2S/3W-22Q2

Well 2S/3W-22Q2 is an unused well located about 150 ft from the nearby pumped well 22L3. Well 22Q2 is perforated between 320 and 682 ft below land surface (fig. 11). It is possible that well 22Q2 may be a conduit for water movement between the upper and lower aquifer systems due to a failed casing. This casing failure was identified using video logs contracted by the owner of the well that indicate the casing has separated about 264 ft below land surface.

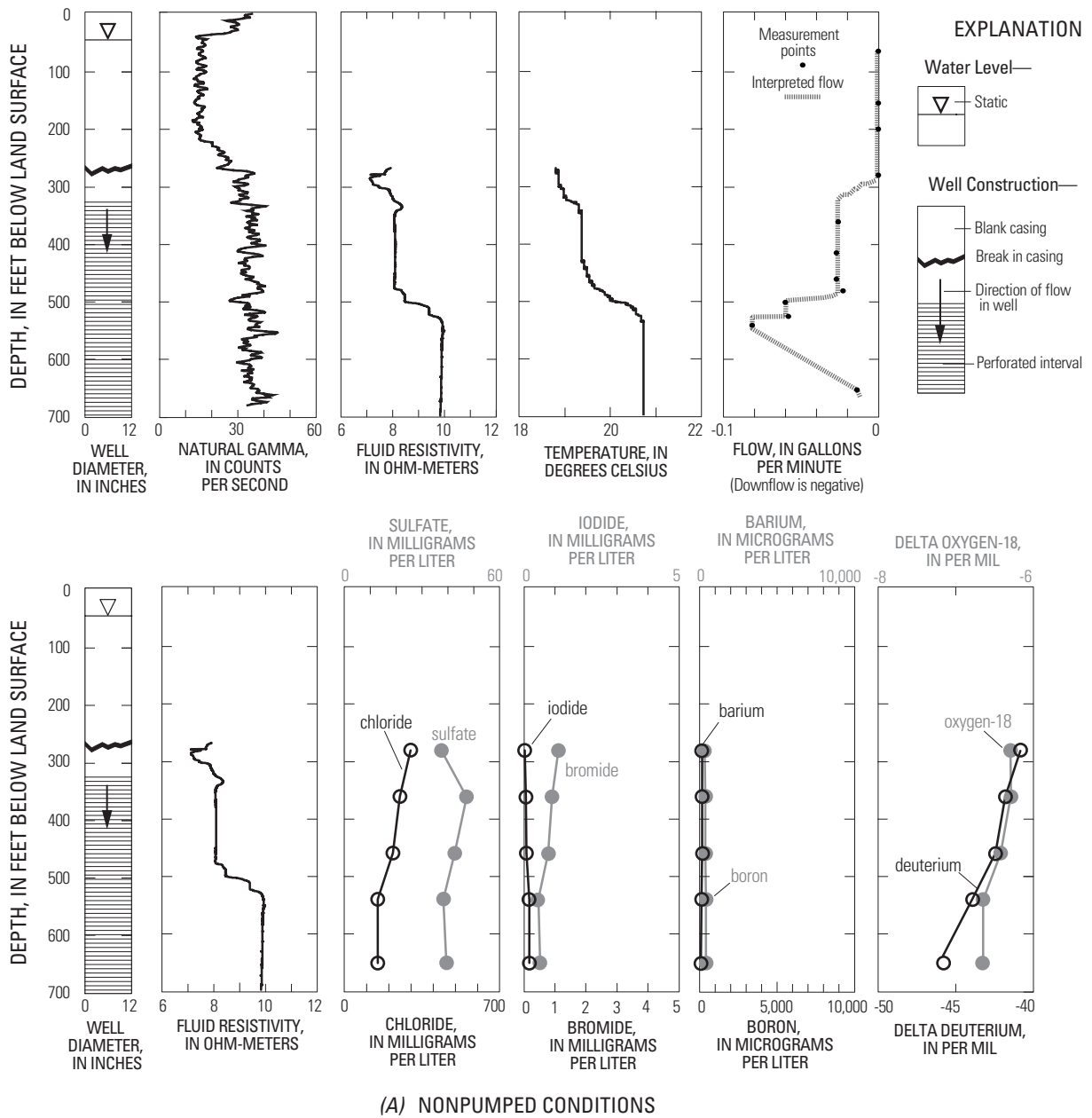
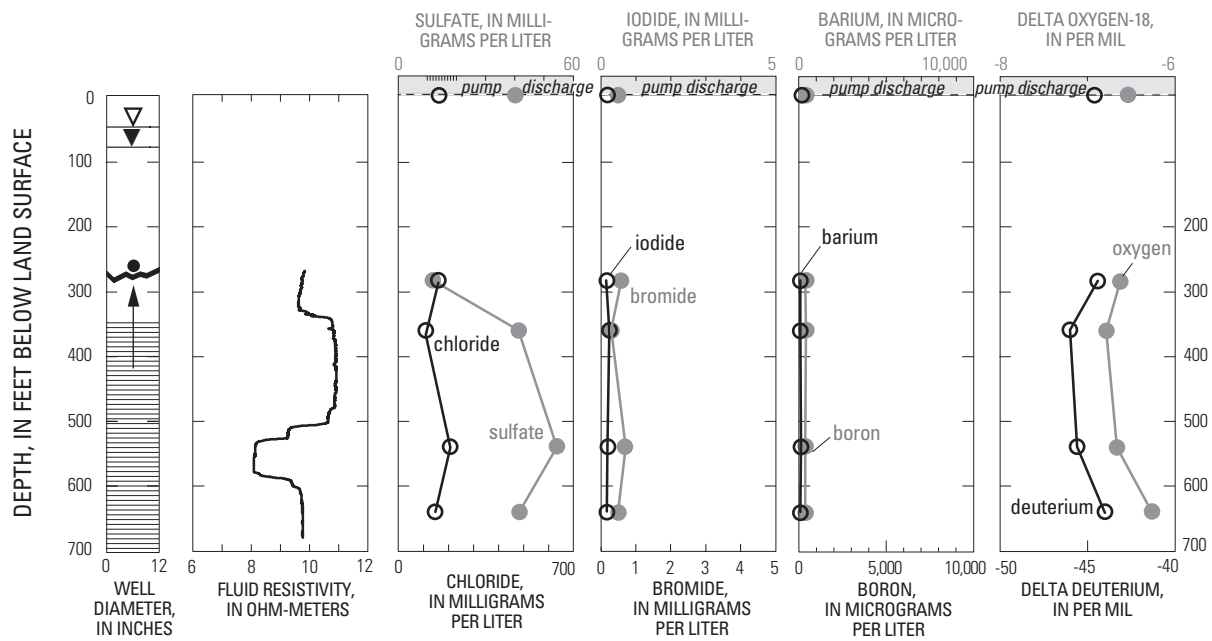
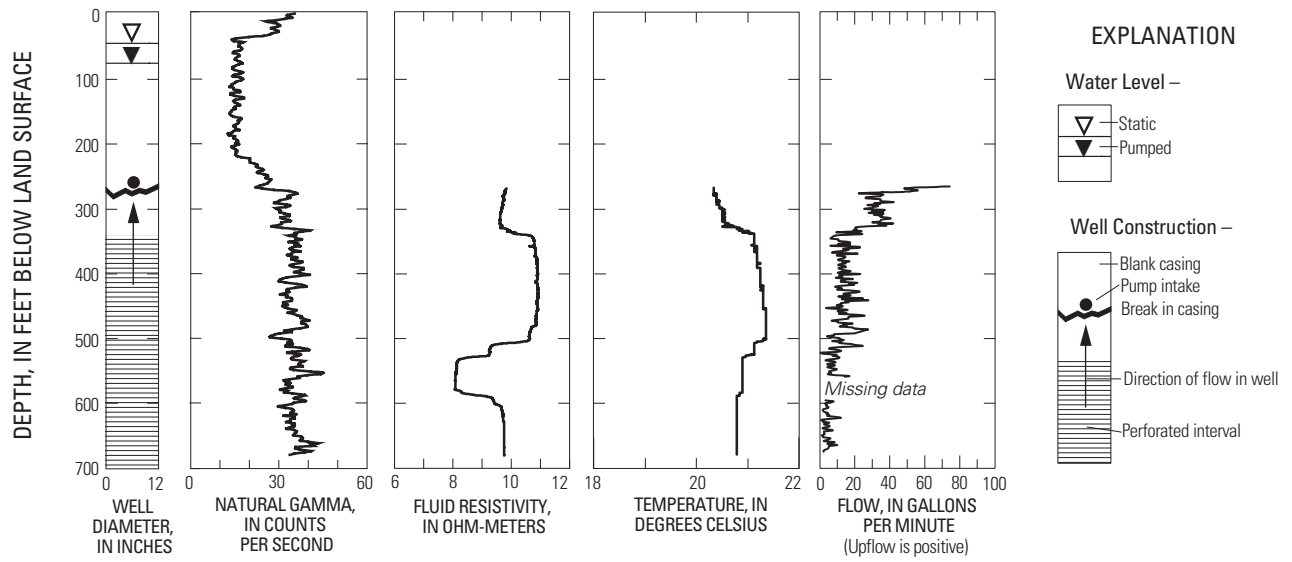


Figure 11. Well construction, geophysical logs, and depth-dependent water-chemistry and isotopic data for well 2S/3W-2202 under nonpumped (A) and pumped (B) conditions, East Bay Plain, Alameda County, California, December 6–7, 1999.



(B) PUMPED CONDITIONS, 77 GALLONS PER MINUTE

Figure 11.—Continued.

Based on the natural gamma counts (and driller's data), the contact between the upper and lower aquifer systems is between 230 and 270 ft below land surface. Within the lower aquifer system, an increase in gamma counts occurs at 340 ft and a peak in the gamma counts is present near 560 ft.

Under nonpumped conditions, flow is downward through the entire perforated interval, reaching a maximum of about 0.08 gal/min near 540 ft. This corresponds to a flow of about 115 gal/d or about 0.13 acre-ft/yr. As a result of downward flow, the fluid resistivity log shows that less-resistive (higher conductance), poorer quality water from the upper aquifer system is present in the well from the failed casing at 264 ft to about 480 ft; presumably, this water reenters the aquifer below 540 ft as downward flow decreases. A similar distribution is shown by the temperature log.

Under pumped conditions, flow through well 22Q2 is upward toward the pump intake. Due to pumping, the fluid-resistivity and temperature logs are greatly different from logs collected under nonpumped conditions. Less-resistive water, similar to water measured in the well under nonpumped conditions, enters the well between 530 and 580 ft; however, based on the velocity log data, this water accounts for only a small proportion of the total yield of the well. More-resistive, higher quality water is present throughout most of the perforated interval of the well, but about half of the yield from the well is less-resistive, poor-quality water that enters the well near the top of the perforated interval. Based on these data, water from well 22Q2 reflects the chemistry of water near the upper part of the perforated interval despite its comparatively great depth. In addition, water flowing through this well under nonpumped conditions may alter the chemistry of water in the deeper aquifer and water from the nearby pumped well 22L3.

Downhole chemistry and isotopic data collected from well 22Q2 are discussed along with chemistry and isotopic data from other wells later in this report.

Well 2S/3W-19Q3

Well 2S/3W-19Q3 is 980 ft deep and is screened in selected zones between 410 and 980 ft below land surface ([fig. 12](#)). The well penetrates partly consolidated deposits that underlie the freshwater aquifers about 450 ft below land surface. Geologic changes within these partly consolidated deposits are indicated by changes in the gamma counts with depth. In some areas, these partly consolidated deposits contain poor-quality water that may discharge to overlying freshwater aquifers. The contact between the upper and lower aquifer systems is about 230 ft below land surface, well above the perforated interval of the well. Although equipped with a pump, the well is not used because of low yields and poor-quality water.

The pump is set in the well at about 460 ft below land surface. Under pumped conditions flow from the upper part of the screened interval is downward toward the pump; flow from the lower part of the screened interval is upward to the pump. Resistive (presumably lower dissolved-solids concentration) water is present in the well above the pump intake, and less resistive (presumably higher dissolved-solids concentration) water is present in the well below the pump intake. The least resistive water is present at depths near the bottom of the well.

The temperature of water within well 19Q3 is much greater than in well 22Q2, and approaches 30° C at the bottom of the well. Large changes in fluid resistivity and temperature are present within the well near the pump intake and at geologic changes indicated on the gamma log. As with data from well 22Q2, downhole chemistry and isotopic data collected from well 19Q3 under pumped conditions are discussed with chemistry and isotopic data from other wells later in this report.

Downhole chemistry and isotopic data were not collected from well 19Q3 under nonpumped conditions, and geophysical logs collected under nonpumped conditions are not shown in [figure 12](#). As with well 22Q2, downhole chemistry and isotopic data collected from well 19Q3 under pumped conditions are discussed along with chemistry and isotopic data from other wells later in this report.

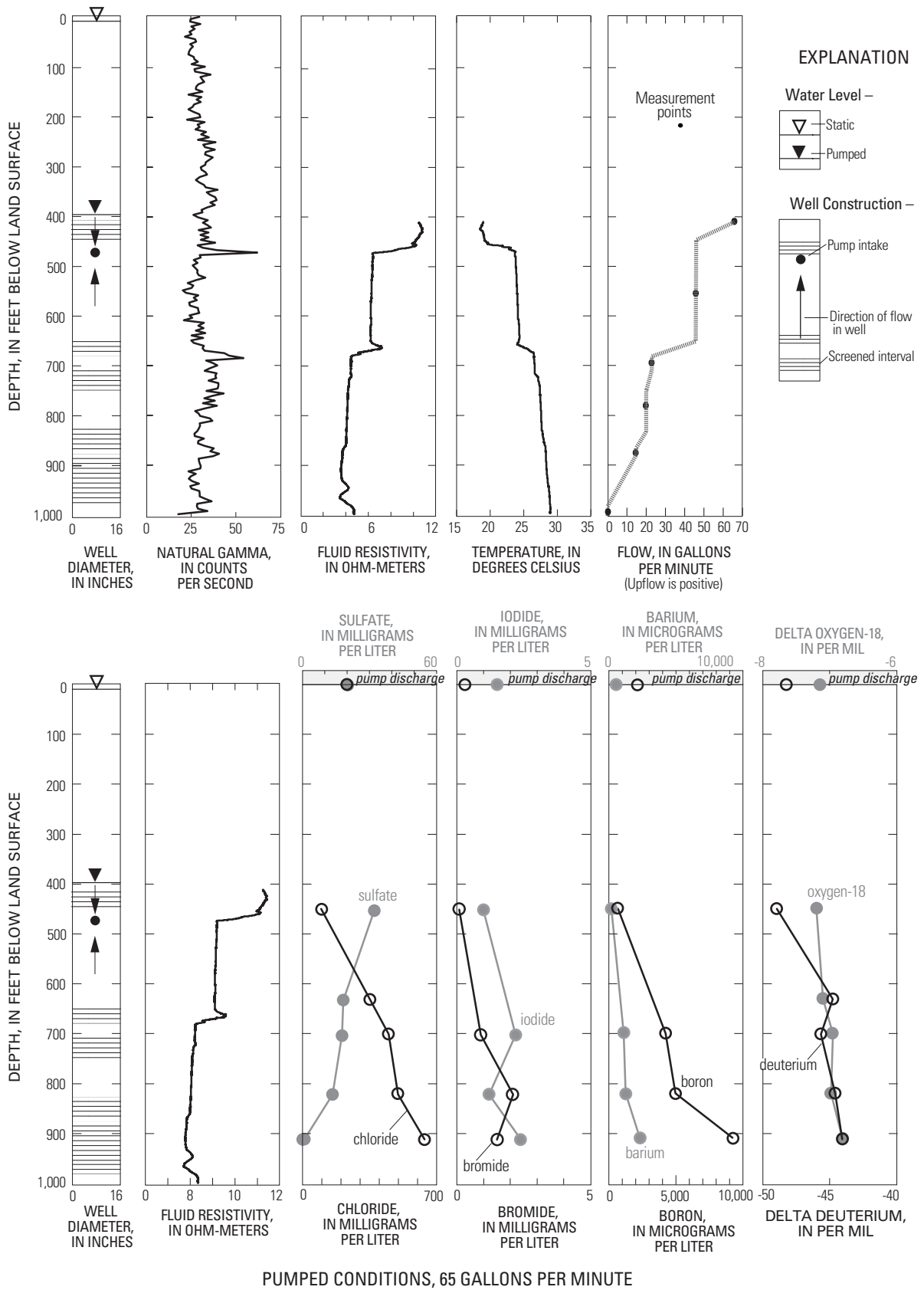


Figure 12. Well construction, geophysical logs, and depth-dependent water-chemistry and isotopic data for well 2S/3W-19Q3 under pumped conditions, East Bay Plain, Alameda County, California, December 8, 1999.

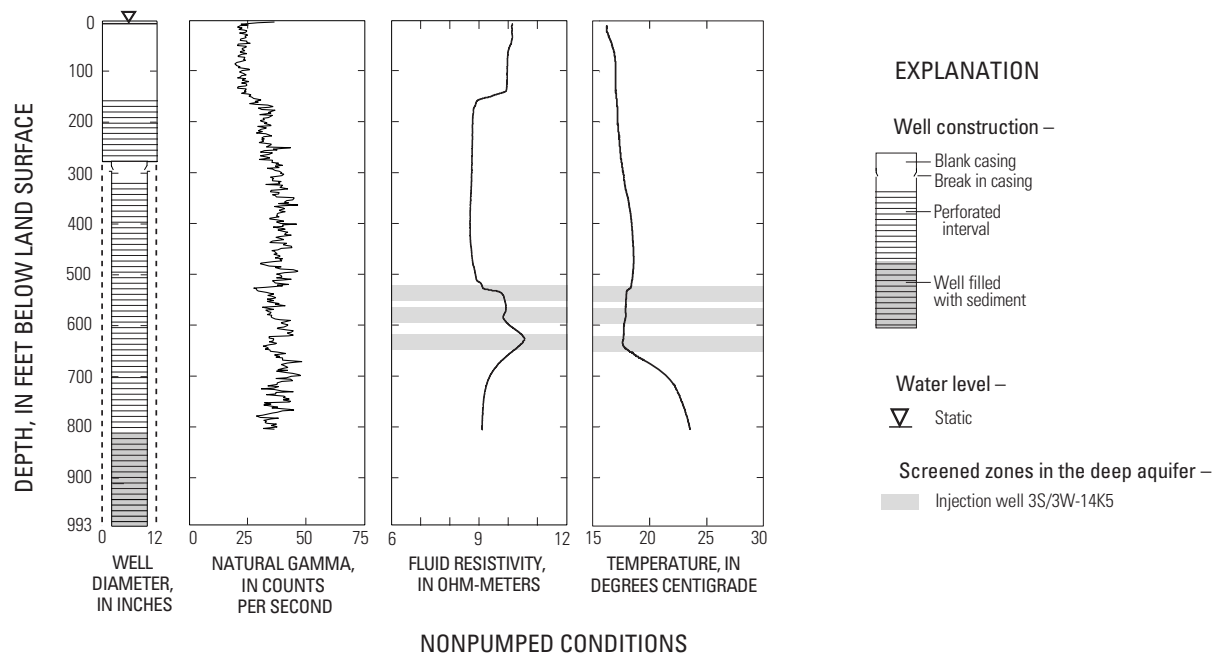


Figure 13. Well-construction data and geophysical logs and for well 2S/3W-14K2 under nonpumped conditions, East Bay Plain, Alameda County, California, August 9, 2000.

Well 3S/3W-14K2

Well 3S/3W-14K2 is an unused well located about 180 ft north of the Bayside injection well (fig. 2B). The well is perforated between 162 and 993 ft below land surface but has been back-filled to a depth of 811 ft (fig. 13). It is not known if the well was deliberately backfilled or material entered through a failed casing. It is possible that well 14K2 is a conduit for water movement between the upper and lower aquifer systems and that mixing of water flowing downward through the well from the upper aquifer system could alter the chemistry of injected water prior to its recovery from the aquifer.

Based on the gamma log (and geologic and geophysical logs collected from nearby observation wells), the contact between the upper and lower aquifer systems is about 180 ft below land surface, which is below the top of the perforated interval. Data from nearby observation wells show that highly saline water is present in shallow overlying deposits, but water in well 14K2 at this depth is fresh.

Fluid resistivity and temperature logs shown in figure 13 were collected under nonpumped conditions while imported water was being injected into the Deep aquifer within the lower aquifer system at nearby well 3S/3W-14K5 (fig. 2B). The injected water is apparent as resistive water between 520 and 650 ft below land surface (fig. 13). There also are corresponding changes in the temperature log at these depths.

The upward water-level gradient at the Bayside injection/recovery site measured during injection suggests that downward flow of water from the upper aquifer system into the Deep aquifer would not occur during injection. However, water-level data show that the gradient at the site is downward when injection is not occurring, and water may move from the upper aquifer system into the injection zone within the Deep aquifer during those times. The Bayside injection/recovery site is near the abandoned Robert's Landing well field which may contain other abandoned deep wells similar in construction to well 14K2. The combined effect of these wells on water quality within the deep aquifer is not known.

CHEMISTRY OF GROUND WATER

The chemistry of water in aquifers underlying the East Bay Plain is controlled by several factors, including the chemistry of the natural recharge water and the geochemical reactions that occur within the aquifer system. Intruding seawater, mixing with water from surrounding and underlying deposits, or mixing with water from estuarine deposits near San Francisco Bay, also may alter ground-water chemistry, increase chloride concentrations, and degrade the quality of ground water. Seawater intrusion in aquifers underlying the East Bay Plain has been a problem since the late 1800s and was extensively studied in the early 1960s by the California Department of Water Resources (1960, 1963). Surface sources of contamination, such as industrial discharges and leaking sewer pipes or septic systems, have made much of the shallow ground water unsuitable for many beneficial uses due to the presence of trace organic compounds, trace elements, or high nitrate concentrations (Hickenbottom and others, 1988; Muir, 1997, San Francisco Bay Regional Water Quality Control Board, 1999). Flow from shallow contaminated aquifers into deeper aquifers through the failed and leaking casings of abandoned wells has been identified as a potential source of water-quality contamination to the lower aquifer system (San Francisco Bay Regional Water Quality Control Board, 1999).

In this study, ground-water chemistry was evaluated on the basis of major-ion and selected trace-element data to determine native ground-water quality, the sources of high-chloride water to wells, and the geochemical reactions that occur within aquifers underlying the East Bay Plain. The distribution of surface sources of industrial chemicals, such as volatile organic carbon compounds or trace elements, was not evaluated as part of this study.

Most samples collected as part of this study were from domestic or industrial well discharges. These samples integrate, usually in unknown proportions, water that entered the well throughout the entire screened interval into a single sample. As a result, it is difficult to interpret samples collected from long-screened wells completed in more than one aquifer.

Samples were collected from monitoring wells completed at different depths at the Oakport and Bayside injection/recovery sites to provide information on changes in ground-water chemistry with depth, but depth-dependent monitoring wells were not available at most other locations in the study area. To overcome this limitation, depth-dependent data were collected from long-screened production wells that penetrate different aquifers using down-hole water-quality data-collection techniques (U.S. Patent Numbers 6,131,451 and 6,164,127, Izbicki and others, 1999) at two wells 2S/3W-22Q2 and 19Q3 along section A-A' ([fig. 2](#)).

Results of chemical analysis of 58 samples collected by the U.S. Geological Survey (USGS) and 28 samples collected by East Bay Municipal Utility District (EBMUD) and the California Department of Water Resources (CDWR) are given in Appendixes B and C, respectively, at the back of this report. Sample collection, preservation, and analytical methods are given in Appendix D at the back of this report. Both the EBMUD and CDWR participate in the U.S. Geological Survey Standard Reference Water program (Farrar, 2000).

Physical Properties and Chemical Characteristics of Water from Wells

The physical properties, and the chemical characteristics of water from wells perforated in the upper aquifer system are different from those of water from wells perforated in the lower aquifer system. In addition, water from numerous wells in both the upper and lower aquifer systems have been affected by seawater intrusion or mixing with poor-quality, high-chloride water from fine-grained estuarine deposits near San Francisco Bay. For the purpose of this report, statistically significant differences were evaluated on the basis of the median test (Neter and Wasserman, 1974) at a confidence criterion of $\alpha=0.05$. Water from wells having chloride concentrations greater than 250 mg/L that were believed to result from seawater intrusion or mixture with other sources of high-chloride water were excluded from statistical comparisons presented in this report.

The pH (field) of water from wells in the study area ranged from 6.2 to 8.4, and the median pH of all wells sampled was 7.7. The lowest pH was in water from well 2S/3W-26C3 in the upper aquifer system near the mountain front. The highest pH was in water from well 2S/3W-19Q3, which penetrates the lower aquifer system and is completed in underlying partly consolidated deposits. The median pH was significantly higher in water from wells in the lower aquifer system than in water from wells in the upper aquifer system (fig. 14).

Dissolved-solids concentrations (residue on evaporation) ranged from 358 to 77,300 mg/L. The median dissolved-solids concentration of all wells sampled was 590 mg/L. The highest dissolved-solids concentration was in water from well 3S/3W-14K11, which is 60 ft deep and is completed in estuarine deposits near San Francisco Bay at the Bayside injection/recovery site. The median dissolved-solids concentration was significantly higher in water from wells in the lower aquifer system (fig. 14) than in water from wells in the upper aquifer system. In both the upper and lower aquifer systems, high dissolved-solids concentrations were associated with high chloride concentrations.

Chloride concentrations ranged from 16 to 42,000 mg/L. Excluding wells believed to be intruded by seawater or containing water mixed with other sources of high-chloride water (greater than 250 mg/L), the median chloride concentration of water from wells in the upper aquifer system was 48 mg/L. The median chloride concentration of water from wells in the lower aquifer system was 71 mg/L. Chloride concentrations in water from well 3S/3W-14K11 at the Bayside injection/extraction site completed between 40 and 60 ft below land surface were as high as 42,000 mg/L; for comparison, the chloride concentration of seawater is about 19,000 mg/L. Chloride concentrations greater than seawater are not unusual in shallow ground water along the California coast (Piper, Garret, and others, 1953; Izbicki, 1991). These high chloride concentrations result from evaporative concentration of seawater in shallow estuaries prior to deposition or from the dissolution of chloride salts remaining after the evaporation of seawater or discharging ground water. Most sampled wells having chloride concentrations greater than the U.S. Environmental Protection Agency MCL (maximum contaminant level)

of 250 mg/L were located in the San Leandro area along section A–A' and are believed to result from seawater intrusion. Water from some wells having high chloride concentrations may also result from mixing with high-chloride water from underlying partly consolidated deposits or from mixing with high-chloride water from estuarine deposits.

Nitrate concentrations in water from wells ranged from less than the detection limit of 0.05 to 25 mg/L as N and water from two wells, 3S/2W-8M3 and 18K3, exceeded the U.S. Environmental Protection Agency MCL for nitrate of 10 mg/L as N (Appendix C). Both wells are completed in the upper aquifer system and are located in the southern part of the study area along section B–B'. Nitrate concentrations in water from some shallow wells in other parts of the basin also approach the MCL for nitrate. The median nitrate concentration in water was 8.9 mg/L as N from samples collected from wells completed in the upper aquifer system and 0.15 mg/L as N from samples collected from wells completed in the lower aquifer system (fig. 14).

Iron and manganese concentrations in water from wells in the East Bay Plain ranged from 5.2 to 340 µg/L and 0.62 to 39,000 µg/L, respectively. Water from 6 percent of the wells sampled exceeded the U.S. Environmental Protection Agency SMCL (secondary maximum contaminant level) for iron of 300 µg/L, and water from 72 percent of the wells sampled exceeded the U.S. Environmental Protection Agency SMCL for manganese of 50 µg/L. Based on the median test with a confidence criterion of $\alpha=0.05$, median manganese concentrations were significantly greater for water in the lower aquifer system than for water from wells perforated in the upper aquifer system. Although low concentrations of dissolved oxygen are present, these data indicate that slightly reducing conditions are present in the lower aquifer, even though the amount of sulfate reduction that occurs is small. Iron and manganese concentrations were greatest for wells having high-chloride concentrations (greater than 250 mg/L) in areas believed to be intruded by seawater. This is consistent with strongly reducing zones present near the leading edge of the seawater intrusion front as seawater intrudes freshwater aquifers (Appelo and Willemsen, 1987), or with the mobilization of water from estuarine deposits near San Francisco Bay.

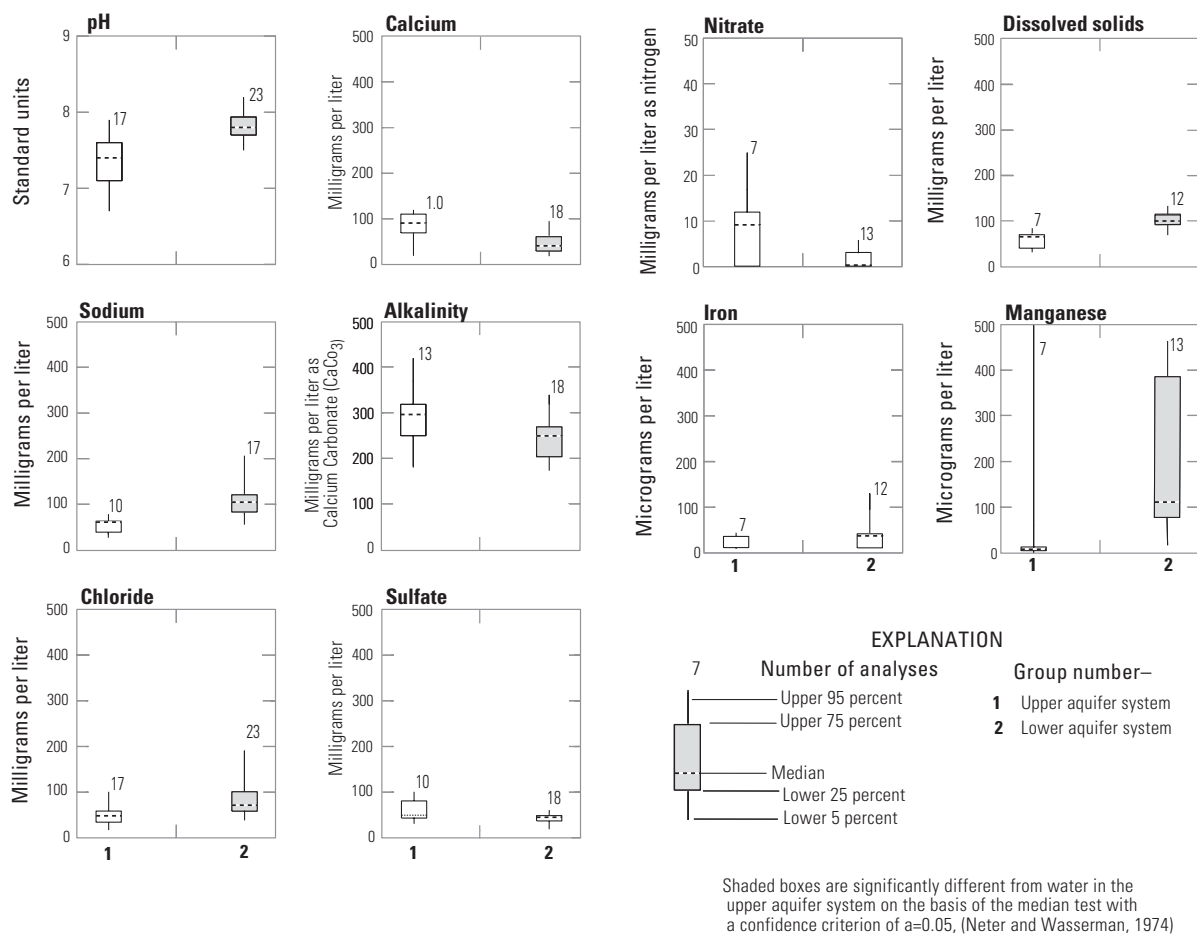


Figure 14. pH and selected major-ion, nutrient, and trace-element concentrations in water from sampled wells having less than 250 milligrams per liter chloride in the East Bay Plain, Alameda County, California, 1997–2000.

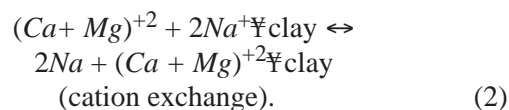
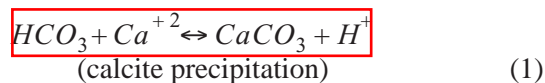
Arsenic concentrations in water from wells sampled by the U.S. Geological Survey ranged from less than the detection limit of 2 to 37 µg/L. Water from two wells, 2S/3W-19Q3 and 2S/3W-17K4, completed in partly consolidated deposits along geologic section A–A', exceeded the U.S. Environmental Protection Agency MCL for arsenic of 10 µg/L.

Chemical Reactions Controlling Major-Ion Chemistry

The major-ion composition of water from sampled wells was evaluated using a Piper (trilinear) diagram. A Piper diagram (Piper, 1945) shows the relative contribution of major cations and anions, on a charge-equivalent basis, to the total ionic content of the water. Percentage scales along the sides of the diagram indicate the relative concentration, in milliequivalents per liter, of each major ion. Cations are shown in the left triangle and anions are shown in the right triangle. The central diamond integrates the data.

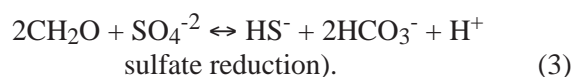
Water from shallow wells near recharge areas along the front of the mountains has a mixed chemical composition and plots within the shaded circle shown in the central diamond within the Piper diagram in [figure 15A](#). The major-ion composition of water from these wells is similar to that of water from most wells sampled in the upper aquifer system by Muir (1997).

Water from some wells in the lower aquifer system, such as 3S/2W-7G12 and 21E13 along section B–B', that are near recharge areas near the mountain front also plot within the shaded circle shown in [figure 15A](#). However, most water from wells in the lower aquifer system plot to the right and below the shaded circle, due to an increase in sodium (plus potassium relative to calcium plus magnesium) as water flows through the aquifers. Similar changes in coastal aquifers in California have been attributed to precipitation of calcite and (or) exchange of calcium and magnesium for sodium on clay within aquifer deposits (Izbicki and others, 1992) according to the following equations:



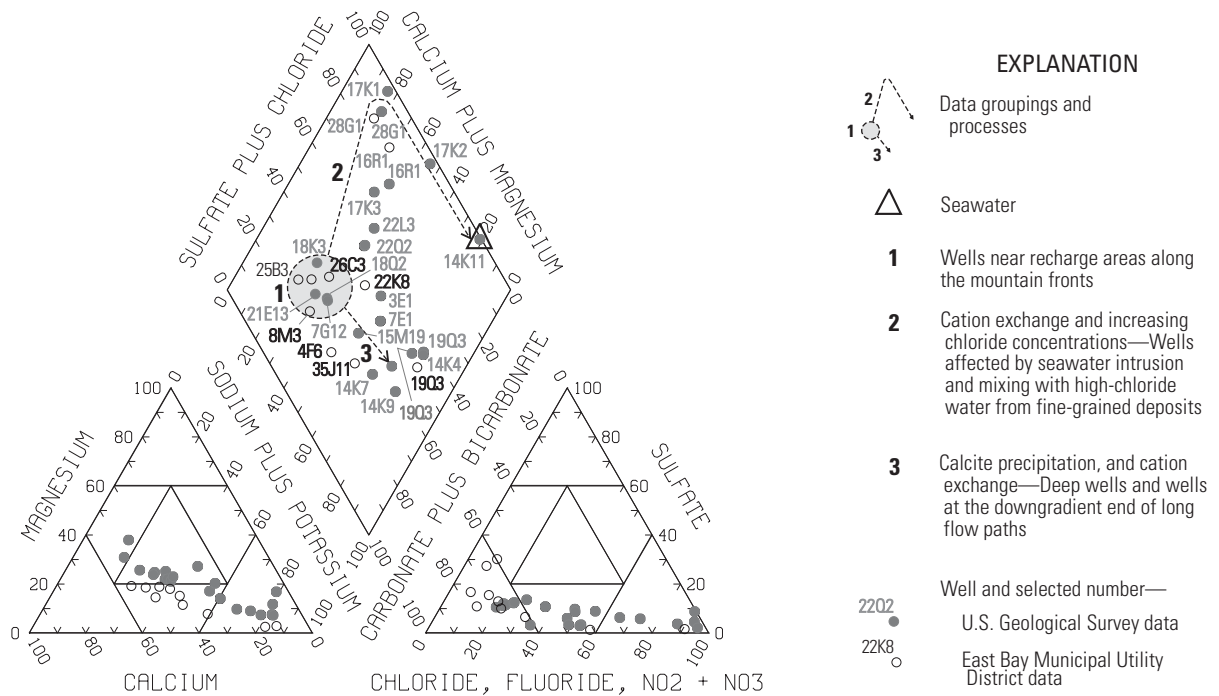
Precipitation of calcite may, in part, explain the lower alkalinity observed in the deeper aquifers ([fig. 14](#)). However, this reaction cannot explain the increase in pH and increase in dissolved-solids concentration observed in the lower aquifer system.

Statistically significant increases in bicarbonate and decreases in sulfate resulting from sulfate reduction that have been observed in many coastal aquifers in California (Piper, Garrett, and others, 1953; Izbicki, 1991) were not observed in water from wells in the East Bay Plain ([fig. 15](#)). Sulfate reduction is a microbially mediated reaction that occurs in the absence of oxygen according to the following equation:



Although oxygen concentrations are low, the presence of small amounts of oxygen and the absence of hydrogen sulfide in water from most wells show that reducing conditions necessary for sulfate reduction are not generally present in aquifers underlying the study area. However, sulfate reduction, and even methane production, may occur within fine-grained, organic-rich estuarine deposits that contain abundant organic material in deeper parts of the lower aquifers system, as well as in the partly consolidated rocks that underlie the lower aquifer system. Methane was present in water from well 2S/3W-19Q3 at a concentration of 8 mg/L (Robert Poreda, University of Rochester, written commun., 1999), suggesting that water from deep wells near downgradient ends of long flow paths through the lower aquifer system and water from wells that penetrate partly consolidated deposits that surround and underlie the basin may be highly reducing. High dissolved-oxygen concentrations in water from well 19Q3 at the time of sample collection (Appendix B) probably result from aeration during pumping when the water level was drawn below the well screen. This aeration may have interfered with the collection and analysis of samples for noble gases discussed later in this report.

A. Water from selected wells (U.S. Geological Survey and East Bay Municipal Utility District data)



B. Depth-dependent samples (U.S. Geological Survey data)

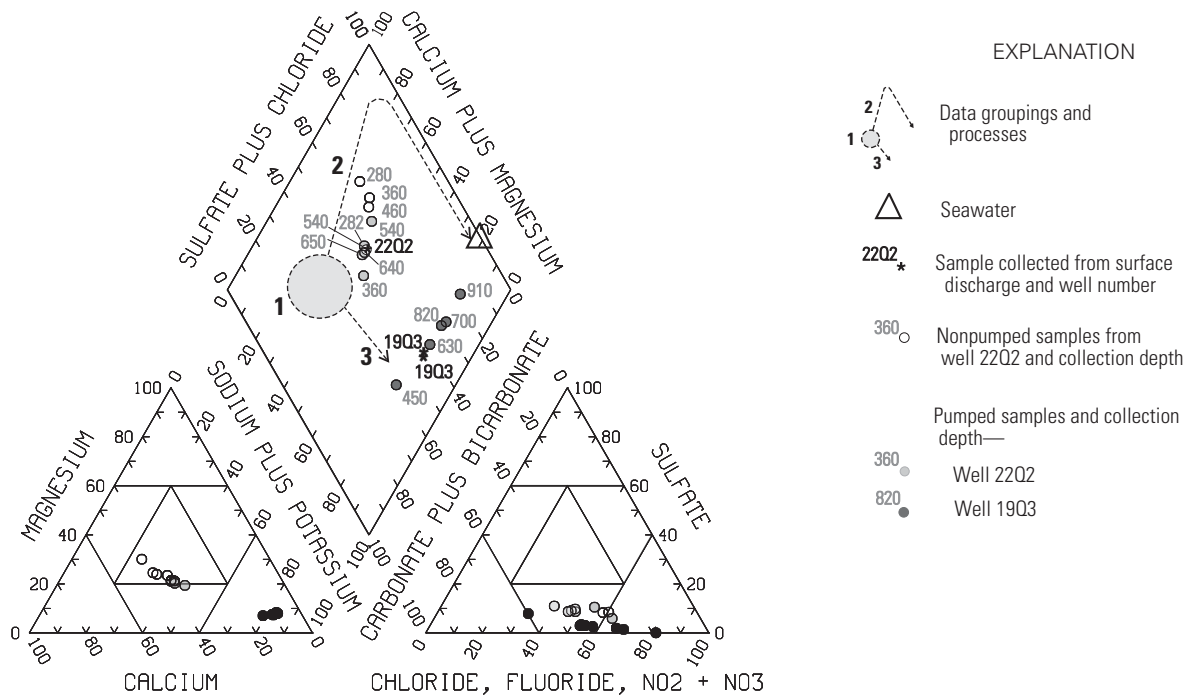


Figure 15. Major-ion composition of samples from selected wells (**A**) and of depth-dependent samples from wells 2S/3W-2202 and 1903 (**B**) in the East Bay Plain, Alameda County, California, 1997–2000.

Water from wells in the upper aquifer system having high chloride concentrations plot along a line above and to the right of the shaded circle in [figure 15A](#) in a pattern characteristic of seawater-intruded ground water in California (Piper, Garrett, and others, 1953). Water having this characteristic composition also was observed in the East Bay Plain by Muir (1997). This characteristic pattern is the result of the exchange of sodium for calcium and magnesium on clay in aquifer materials. In contrast, high-chloride water from deep wells, such as 2S/3W-19Q3, that completely penetrate the lower aquifer system and yield water from the underlying partly consolidated deposits has a much different chemical composition than that of water affected by seawater intrusion ([fig. 15A](#)).

Major-Ion Composition of Depth-Dependent Samples

Changes in chloride and sulfate concentrations in depth-dependent samples collected from wells 2S/3W-22Q2 and 2S/3W-19Q3 are shown in [figures 11](#) and [12](#), respectively; and changes in the major-ion composition with depth of water from these wells are shown in a Piper diagram in [figure 15B](#). Although both wells have elevated dissolved-solids and chloride concentrations, the sources and distribution of high-chloride water in each well are different.

Under nonpumped conditions, flow in well 2S/3W-22Q2 was downward ([fig. 11A](#)), possibly due to vertical hydraulic gradients created by nearby pumping in well 22L3. The highest chloride concentration in the well was 300 mg/L at 280 ft below land surface near where the casing is believed to have failed. This sample is representative of water in the aquifer at that depth. Water samples collected below 280 ft under nonpumped conditions were a mixture of the high-chloride water collected at 280 ft and water that entered the well below that depth. With increasing depth, the data plot along a mixing line between the shallowest

(280 ft) and deepest sample (650 ft) ([fig. 15B](#)). High-chloride water moving downward through well 22Q2 may have contributed to the increased chloride concentrations and changes in major-ion chemistry observed by local agencies in the nearby pumped well 2S/3W-22L3, which is screened in the lower aquifer system. Although industrial contaminants, such as volatile organic compounds or trace elements, were not measured as part of this study, small amounts of contaminated water from overlying aquifers could contaminate deeper aquifers through this process.

Under pumped conditions, flow in well 2S/3W-22Q2 was upward toward the pump intake above the perforated interval about 260 ft below land surface ([fig. 11B](#)). The depth-dependent water sample collected near the bottom of the perforated interval, at 640 ft below land surface, is representative of water in the aquifer at that depth, and samples collected above 640 ft are a mixture of all water that entered the well below that sample depth. The relative proportion of water in the well from different depths can be evaluated on the basis of the flow log shown in [figure 11B](#). Water at the pump discharge had a chloride concentration of 160 mg/L. This is less than the maximum chloride concentration of 300 mg/L measured 280 ft below land surface under nonpumped conditions because of mixing within the well. Most samples plot as a group on a Piper diagram ([fig. 15B](#)) near the composition of water from the pump discharge. However, water collected 360 ft below land surface has different major ion-chemistry and is similar to the composition of water from wells near recharge areas ([fig. 15A](#)). Water collected 540 ft below land surface has high chloride concentrations and a major-ion composition approaching that of the high-chloride water collected near the top of the perforated interval. This water may have entered the aquifer during nonpumped conditions when flow in the well was downward and was recovered during pumping.

Under pumped conditions, flow in well 2S/3W-19Q3 was toward the pump intake within the screened interval about 460 ft below land surface (fig. 12). Unlike previously collected samples from this well, this sample was collected without drawing the water level below the screened interval and aerating the water prior to sample collection. The highest chloride concentration, 640 mg/L, was 910 ft below land surface near the bottom of the perforated interval. This sample is representative of water from partly consolidated deposits at this depth. Water samples collected above 910 ft were a mixture of the high-chloride water collected at 910 ft and water that entered the well above that depth—except the sample collected above the pump intake at 450 ft below land surface, which is representative of the water from the lower aquifer system at that depth. At the pump discharge, water from well 19Q3 had a chloride concentration of 250 mg/L, reflecting mixing of water from above and below the pump. The samples plot on a mixing line between the deepest and shallowest sample (fig. 15B), and the high-chloride samples plot near the major-ion composition of seawater and show no evidence of chemical alteration from cation exchange as water moved through aquifer materials to the well. Depending on the direction of flow through the well under nonpumped conditions, high-chloride water from partly consolidated deposits at depth could contaminate overlying freshwater aquifers. Where these partly consolidated deposits are adjacent to freshwater aquifers, high-chloride water from partly consolidated deposits could move laterally into freshwater aquifers due to pumping.

Sulfate concentrations in water from well 19Q3 decreased with depth and were as low as 14 mg/L at 910 ft below land surface (fig. 12). Low sulfate concentrations may result from reducing conditions and sulfate reduction at depth within the partly consolidated deposits that underlie freshwater aquifers in the study area. As previously discussed, methane, indicative of highly reducing conditions, was present in water from this well.

Source of High-Chloride Water to Wells

Piper, Garrett, and others (1953) demonstrated that certain trace elements could be used to determine the source of high-chloride water to wells in the Long Beach and Santa Ana areas of southern California. Since that time, the application of trace elements to the study of the source and movement of seawater and other brines in aquifers has become widespread (Jones and others, 1999). In California, the approach was refined for use in coastal aquifer systems having multiple sources of chloride to distinguish mixtures of native (fresh) water and seawater from mixtures of native water and high-chloride water from surrounding and underlying partly consolidated deposits (Izbicki, 1991). In this paper, bromide, iodide, barium, and boron were used to determine the source of high-chloride water to wells and to evaluate the geochemical evolution of water as it flows through unconsolidated deposits underlying the East Bay Plain. The use of several trace elements, each of which has slightly different chemistry, allows increased constraint on the interpretation of the source of high-chloride water and of ground-water movement to wells.

Changes in selected trace-element concentrations were evaluated as ratios relative to changes in chloride concentrations. Chloride is highly soluble and not readily sorbed on mineral surfaces or organic material. In addition, with the exception of evaporite salts, chloride does not occur at high concentrations in most rock-forming minerals or aquifer materials (Feth, 1981; Davis and others, 1998). Ratios are especially sensitive to mixing, and the addition of a small volume of water having different chloride and trace-element compositions may produce a large change in the trace element-to-chloride ratio of water from a well. In this report, ratios are presented on a millimole per millimole basis, rather than on a mass per mass basis; therefore, ratios calculated from different trace elements, each having different atomic masses, are comparable.

To establish ranges in chloride and trace-element compositions, trace-element ratios for water from wells in the East Bay Plain are compared with ratios in water from deep wells completed in partly consolidated marine rocks in the Ventura (Izbicki and others, 1995) and Los Angeles (Piper, Garrett, and others, 1953) Basins of southern California. The approach has been effectively demonstrated in each of these areas even though these basins have different geologic settings and the geochemical processes that have created high-chloride brines may be different.

Chloride-to-Bromide Ratios

Bromide is similar in chemical behavior to chloride, but it is less abundant (Hem, 1970; Davis and others, 1998). In this study, both chloride and bromide are presumed to be non-reactive (conservative) in ground-water systems. Seawater has a bromide concentration of 65 mg/L (Hem, 1970). Bromide concentrations greater than seawater are common in estuarine deposits along the California coast (Izbicki and others, 1995; Land and Crawford, in press). High-chloride water from partly consolidated deposits that surround and underlie coastal aquifers in California have bromide concentrations as high as 12 mg/L (Izbicki and others, 1995), and bromide concentrations in highly concentrated brines from deep wells can be as high as 3,480 mg/L (Hem, 1970).

Bromide concentrations in water from wells in the East Bay Plain ranged from less than 0.01 to 130 mg/L. The highest bromide concentrations were in water from well 3S/3W-14K11, which also had the highest chloride concentrations and was completed between 40 and 60 ft below land surface in estuarine deposits near San Francisco Bay. Excluding estuarine deposits and areas intruded by seawater, bromide concentrations increased with depth and were as high as 2.1 mg/L in depth-dependent samples collected 820 ft below land surface in well 2S/3W-19Q3 (fig. 12).

Water from wells screened in the upper aquifer system near recharge areas along the mountain front has low chloride concentrations, and the chloride-to-

bromide ratio is less than the ratio in seawater (fig. 16A). The chloride-to-bromide ratio gradually increases as water flows through the aquifer, and the chloride-to-bromide ratio in water from wells at the downgradient end of long flow paths through the lower aquifer system exceeds the chloride-to-bromide ratio in seawater.

Water from wells 3S/2W-7G12 and 21E13 screened in the upper and lower aquifer systems that was indistinguishable from water from shallower wells in the upper aquifer system on the basis of major-ion data has chloride to bromide ratios similar to those of water from other lower aquifer system wells. These data suggest that the water from these wells is primarily from the lower aquifer system.

High-chloride water from wells believed to be intruded by seawater, or wells completed in estuarine deposits near San Francisco Bay, have chloride-to-bromide ratios of about 660, which is near the ratio of seawater.

The chloride-to-bromide ratios in depth-dependent water samples collected from well 2S/3W-22Q2 are similar to the ratio in seawater. This is consistent with the interpretation that high-chloride water from overlying intruded aquifers is flowing through the well into deeper aquifers.

The chloride-to-bromide ratios in depth-dependent water samples collected below the pump intake from well 2S/3W-19Q3 are higher than the ratio in seawater and different from the ratios in water from other sampled wells. Well 19Q3 is the deepest well sampled in the study area, and the well is completed in partly consolidated deposits that underlie freshwater aquifers in this part of the basin.

The highest chloride-to-bromide ratio for the sampled wells was in water from well 2S/3W-17K4. This well also is completed 550 ft below land surface in low-yielding, partly consolidated deposits that underlie the lower aquifer system along section A-A' (fig. 3).

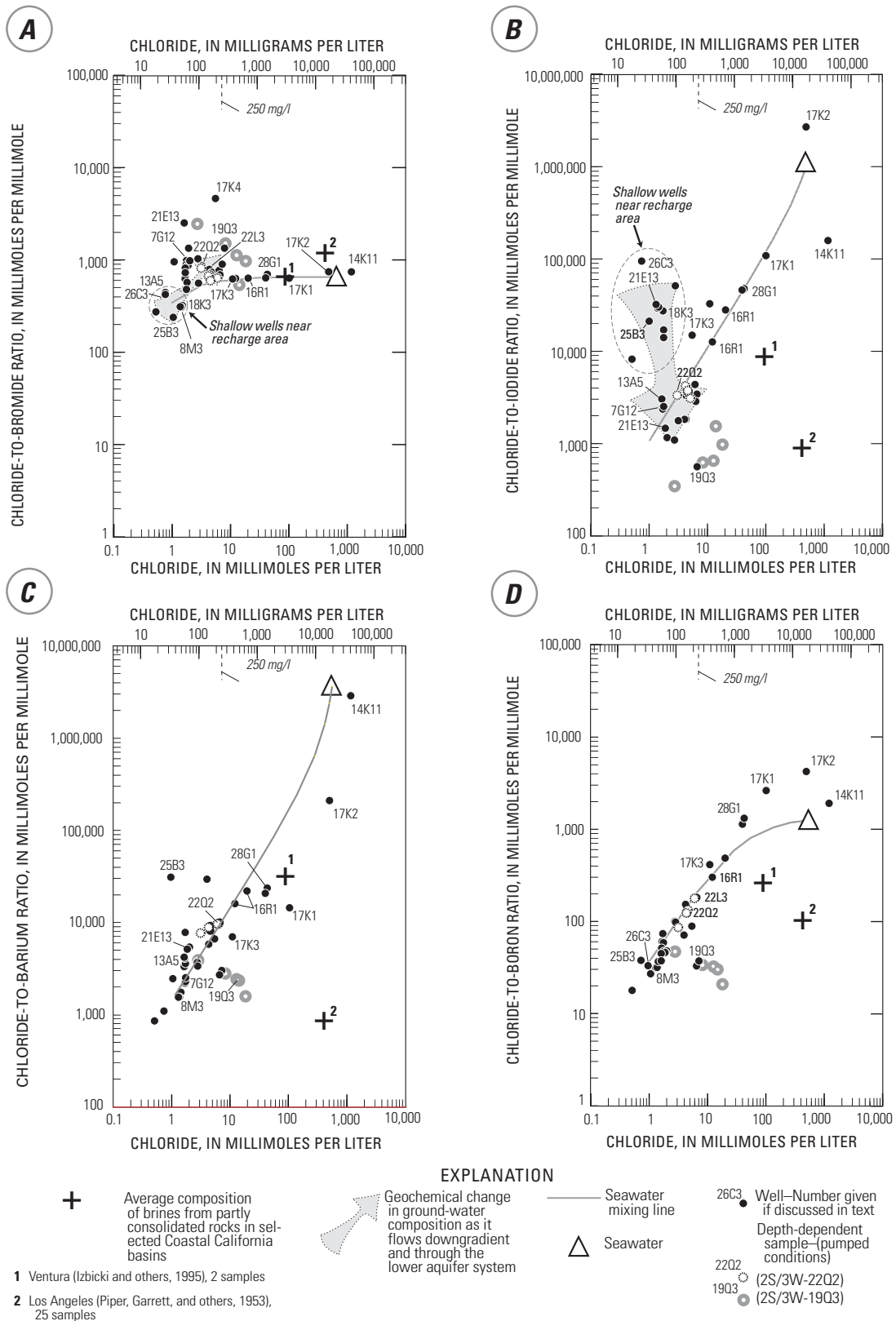


Figure 16. Selected trace-element ratios as a function of chloride concentration in water from wells, East Bay Plain, Alameda County, California, 1997–2000.

The chloride-to-bromide ratios of water from wells 19Q3 and 17K4 are similar to the ratios in water from deep wells completed in partly consolidated deposits underlying the Ventura and Los Angeles areas.

Chloride-to-Iodide Ratios

Iodide (IO_3^-) is different in chemical behavior from either chloride or bromide; it is biologically and redox active and is reactive in ground-water systems. Although iodide concentrations in seawater are low, about 0.06 mg/L, nearshore marine vegetation, especially kelp, concentrates iodide from seawater (Hem, 1970). As a result, iodide concentrations in marine rocks and unconsolidated material deposited in marine environments are elevated relative to seawater and nonmarine materials. This makes iodide an excellent indicator of the geologic material that water has encountered as it flows through aquifers. Iodide is concentrated in some brines (Hem, 1970), and previously reported iodide concentrations in high-chloride water from marine rocks that surround and underlie coastal aquifers in California are as high as 1.4 mg/L (Izbicki and others, 1995). Iodide concentrations in highly concentrated brines from some deep wells can be as high as 46 mg/L (Hem, 1970). Changes in chloride-to-iodide ratios are larger and easier to interpret than are changes in chloride-to-bromide ratios.

Iodide concentrations in water from wells underlying the East Bay Plain ranged from 0.001 to 2.4 mg/L. The highest iodide concentration was in the depth-dependent water sample collected from 910 feet below land surface in well 2S/3W-19Q3.

In water from shallow wells near recharge areas along the mountain front, the chloride-to-iodide ratios are high, with most values between 10,000 and 100,000 (fig. 16B). These values are typical of ratios measured in water from granitic terrain or in alluvial material weathered from nonmarine rocks (Izbicki, 1991). Imported water from the Sierra Nevada also has chloride-to-iodide ratios in this range; however,

isotopic data presented later in this report will show that this is not the result of recharge of imported water from leaking pipes. Chloride-to-iodide ratios decrease to about 2,000 in water from deeper wells and wells farther downgradient from recharge areas due to mobilization of iodide from aquifer materials. This ratio is typical of water from unconsolidated marine deposits or alluvial deposits weathered from marine rocks (Piper, Garrett, and others, 1953; Izbicki, 1991; Land and Crawford, in press). As with chloride-to-bromide ratios, water from wells, such as 7G12 and 21E13, that was indistinguishable from water from shallower wells on the basis of major-ion data, has chloride-to-iodide ratios similar to those of water from most other lower aquifer system wells. As previously discussed, these wells probably yield most of their water from the lower aquifer system.

High-chloride water from wells believed to be intruded by seawater or from wells completed in estuarine deposits near San Francisco Bay plot along, or slightly below, a mixing line between native (fresh) water and seawater (fig. 16). Because iodide is reactive, some chloride-to-iodide ratios (such as that for well 14K11, screened between 40 and 60 ft below land surface), do not necessarily plot along the mixing line between freshwater and seawater and are slightly lower than ratios expected due to simple mixing with native water and seawater.

The chloride-to-iodide ratios in water from well 2S/3W-22Q2 plot along a mixing line with fresh (native) water at one end and seawater at the other. High-chloride concentrations in water from this well probably result from seawater intrusion or movement of water from fine-grained estuarine deposits in overlying aquifers. In contrast, the chloride-to-iodide ratios in depth-dependent samples collected from well 2S/3W-19Q3 plot to the right of most values from deeper aquifers and are similar in composition to high-chloride brines from partly consolidated deposits that surround and underlie coastal aquifers in the Ventura and Los Angeles areas of southern California (fig. 16).

Chloride-to-Barium Ratios

Unlike the other trace elements included in this study, barium has significant limits on its solubility, especially in the presence of sulfate, and it is strongly sorbed by iron, manganese, and other metal oxides (Rai and Zachara, 1984). In coastal California, deeper aquifers and the surrounding partly consolidated deposits are depleted in oxygen and are often highly reducing. Under these conditions, sulfate reduction may occur. As sulfate concentrations decrease, barium concentrations can increase. As a result of these geochemical reactions, barium is an indicator of water from deeper aquifers that are occasionally highly reducing. These aquifers frequently contain high-chloride water and may be a source of contamination to overlying freshwater aquifers. Seawater has a barium concentration of 30 $\mu\text{g/L}$ (Hem, 1970).

Barium concentrations in water from wells underlying the East Bay Plain range from 6.2 to 2,300 $\mu\text{g/L}$. Barium concentrations were highest in depth-dependent samples collected 910 ft below land surface from well 19Q3. This is one the highest reported barium concentrations in a California coastal aquifer.

Barium concentrations are controlled primarily by its solubility in the presence of sulfate and sorption on iron and manganese oxides (Piper, Garrett, and others, 1953; Rai and Zachara, 1984). As a result, chloride-to-barium ratios do not change in the same manner as do chloride-to-bromide or chloride-to-iodide, and data are distributed along a mixing line between native ground water and seawater (fig. 16).

Depth-dependent samples collected from well 2S/3W-19Q3 are different from samples collected from most wells sampled and have low chloride-to-barium ratios relative to their chloride concentration. Low ratios are due to increasing barium concentrations as sulfate concentrations decrease owing to sulfate reduction with increasing depth in the partly consolidated deposits underlying freshwater aquifers. At higher chloride concentrations, samples plot increasingly below the seawater mixing line owing to reducing conditions near the seawater front, resulting in lower sulfate concentrations, dissolution of iron and manganese oxides, and consequently more barium in solution. Chloride-to-barium ratios in water from well 19Q3 are similar to ratios in water from deep wells in the Los Angeles Basin but are different from deep wells completed in partly consolidated deposits underlying freshwater aquifers in the Ventura Basin. The deposits

underlying the Ventura Basin are highly reducing and contain high concentrations of methane. Barium concentrations in ground water also are indirectly affected by changing redox conditions through their sorption on iron and manganese oxides. In more reducing environments where more iron and manganese are in solution, more barium also will be in solution.

Chloride-to-Boron Ratios

Boron has the most poorly understood chemistry of the trace elements used as tracers in this study (Rai and Zachara, 1984). However, at the relatively low concentrations typical of most freshwater aquifers, boron is highly soluble and relatively non-reactive. Boron concentration in sea water is 4,600 $\mu\text{g/L}$ (Hem, 1970). Boron concentrations as high as 10,500 $\mu\text{g/L}$ have been reported in California coastal aquifers near seawater intrusion zones (Land and Crawford, in press), and concentrations as high as 660,000 $\mu\text{g/L}$ have been reported in thermal spring water (Hem, 1970).

Boron concentrations in water from wells underlying the East Bay Plain ranged from 280 to 9,300 $\mu\text{g/L}$. The highest boron concentrations were from depth-dependent samples collected 910 ft below land surface in well 19Q3.

As chloride concentrations increase, chloride-to-boron ratios change along a mixing line between native water and seawater (fig. 16). At very high chloride concentrations, water from wells plot above the seawater mixing line, suggesting that boron may be removed from ground water by chemical precipitation, adsorption (Rai and Zachara, 1984), or some other mechanism. In contrast, depth-dependent samples collected from well 2S/3W-19Q3 are different from samples from most wells and plot below the seawater mixing line in the same manner as chloride-to-iodide and chloride-to-barium data. The ratios for water from wells in the Ventura and Los Angeles areas also plot below the seawater mixing line but do not closely resemble ratios in water from well 19Q3. Boron solubility, like barium solubility, is partly affected by changes in redox conditions though the changing solubility of iron and manganese oxides. This may partly explain differences in the chloride-to-boron ratios between East Bay Plain and the Ventura and Los Angeles Basins.

NOBLE-GAS CONCENTRATIONS

Noble gases include helium, neon, argon, krypton, xenon, and radon. Under most natural conditions these gases do not react chemically in the environment. As a result, noble-gas concentrations in ground water are controlled primarily by their atmospheric concentrations and by solubility at the water table, which is a function of temperature, pressure, and salinity. For certain noble gases, such as helium, *in-situ* production from the decay of radioactive elements, and fluxes from the Earth's mantle, also are important in determining concentrations in ground water. In combination with other chemical and isotopic data, noble-gas concentrations in ground water can be used to evaluate recharge processes and ground-water age (time since recharge).

Background

Solubility of noble gases at the water table can be estimated using Henry's Law, which states that for an ideal gas there is a linear relation between the activity of a volatile species in the liquid phase and its activity in the gas phase (Stumm and Morgan, 1996). For practical applications in which it is necessary to define the physical state of the system at the water table and incorporate non-ideal gas behavior (fugacity), Henry's Law can be written as:

$$C_s = \beta(T,S)P_x/P_o \quad (4)$$

where

- C_s is the concentration of the gas in water.
- β is the Bunsen coefficient which is a function of the temperature (T) and salinity (S) of ground water at the water table at the time of recharge.
- P_x is the partial pressure of the gas in the soil atmosphere. The partial pressure of the gas (P_x) is a function of the recharge altitude and the atmospheric composition in the unsaturated zone (Stute and Schlosser, 2000). The soil atmospheric composition is a function of the water-vapor concentrations; in most cases, the relative humidity of the unsaturated zone near the water table is constant and near 100 percent.
- P_o is the standard sea-level atmospheric pressure at a temperature of 0 °C.

The Bunsen coefficient is experimentally derived and accounts for non-ideal gas behavior by incorporating the effects of gas compressibility (Z_o) into the Henry's Law coefficient (k) for the gas according to the following:

$$k = \frac{(C\rho Z_o Z_e)}{(\beta)} \quad (5)$$

where

- C is a constant, Z_e is the gas compressibility under the experimental conditions, and
- ρ is the density of water under the experimental conditions (Benson and Krause, 1976).

In addition to the gas solubility predicted using Henry's Law, noble-gas concentrations in ground water may be affected by excess air. Excess air is the gas concentration in excess of the concentration expected, given the temperature and salinity of the ground water, at the point of recharge (Stute and Schlosser, 2000). Excess air enters ground water as infiltrating water traps bubbles of air that later dissolve as ground water moves to greater depth in the aquifer. Not all ground water contains excess air, but excess air may be present where a large quantity of water infiltrates rapidly through the subsurface (such as areas of highly focused recharge near streams, rivers, or artificial-recharge sites) or in areas where the water-table altitude changes rapidly. Calculations presented in this report assume complete dissolution of excess air and do not account for partial dissolution of entrapped air or partial reequilibrium of ground water with the atmosphere after entrapped air has dissolved. In some settings these processes may be important.

If the temperature and excess air in ground water at the time of recharge can be estimated, it may be possible to determine the timing of ground-water recharge (summer versus winter or, in some cases, present-day versus paleo-recharge) and the source of ground-water recharge (areal recharge from infiltrating precipitation versus highly focused recharge sources from infiltration of winter stormflows). In addition, both the temperature of ground-water recharge and the excess-air component are needed for tritium-helium ages (time since recharge) presented later in this report. The contributions from non-atmospheric sources such as radioactive decay and mantle degassing may increase the concentrations of certain noble gases, such as helium, as ground water flows through aquifers. This may help confirm the ages of older ground water

estimated from carbon-14 data presented later in this report. Finally, comparison of noble-gas concentrations with nitrogen-gas concentrations may allow a quantitative estimate of nitrate removal through denitrification in ground-water systems.

Ground-Water Recharge Temperatures and Excess-Air Concentrations

In this study, ground-water recharge temperatures were estimated from helium, neon, and argon data. The use of three noble gases provides additional constraint on the estimation of recharge temperature in comparison with methods that use only two noble gases. This is especially important because the solubility of heavier noble gases, such as argon, is more sensitive to temperature changes than that of lighter noble gases such as helium or neon. Higher-molecular-weight noble gases, such as krypton and xenon, which are even more sensitive to temperature, were not measured. To estimate ground-water recharge temperature, the equilibrium neon and argon concentration at a given temperature was calculated using Henry's Law and a Bunsen coefficient (β) derived from solubility data published by Weiss (1970, 1971) and a Henry's Law coefficient (k) published by Benson and Krause (1976). Non-atmospheric contributions of neon are rarely present (Lehmann and others, 1993), and non-atmospheric contributions of argon from potassium-40 decay to argon-40 were assumed small relative to its atmospheric abundance.

The following steps were used to estimate recharge temperatures and excess air concentrations. First, an initial estimate of the recharge temperature was calculated from the measured helium, neon, and argon concentrations using Henry's Law. The calculations accounted for the salinity of the water. In

most cases, the calculated recharge temperatures for each gas were different. To resolve these differences, the measured concentrations of each dissolved gas were then decreased by a small increment in proportion to their atmospheric concentration, and the recharge temperatures were recalculated. The process was repeated until the difference between recharge temperatures calculated from the helium, neon, and argon data was minimized. This value is the recharge temperature presented in [table 1](#). The excess-air concentration in [table 1](#) was calculated using the difference between the neon and argon in equilibrium with the atmosphere at the calculated recharge temperature and the measured concentrations.

A graphical approximation of the technique is shown for neon and argon in [figure 17](#). The water-air equilibrium line represents the expected neon and argon concentrations in pure water across a range of temperatures in a soil atmosphere having 100-percent relative humidity. Lines parallel to the axis to the right of the water-air equilibrium line represent the expected change in neon and argon concentrations if excess air is present in the sample. Using these axes, the recharge temperature of the sample water and the excess air concentrations for fresh ground water can be read directly from their respective lines shown in [figure 17](#). The graphical approach shown in [figure 17](#) does not account for salinity differences and results are slightly different from calculated results presented in [table 1](#). [Figure 17](#) is included in this paper to help the reader understand the chemical processes.

Noble-gas concentrations, calculated recharge temperatures, and calculated excess-air values are very sensitive to sample-collection errors. For example, entrapped air bubbles introduced due to improper sample collection or aeration of the sample can produce unreasonable results.

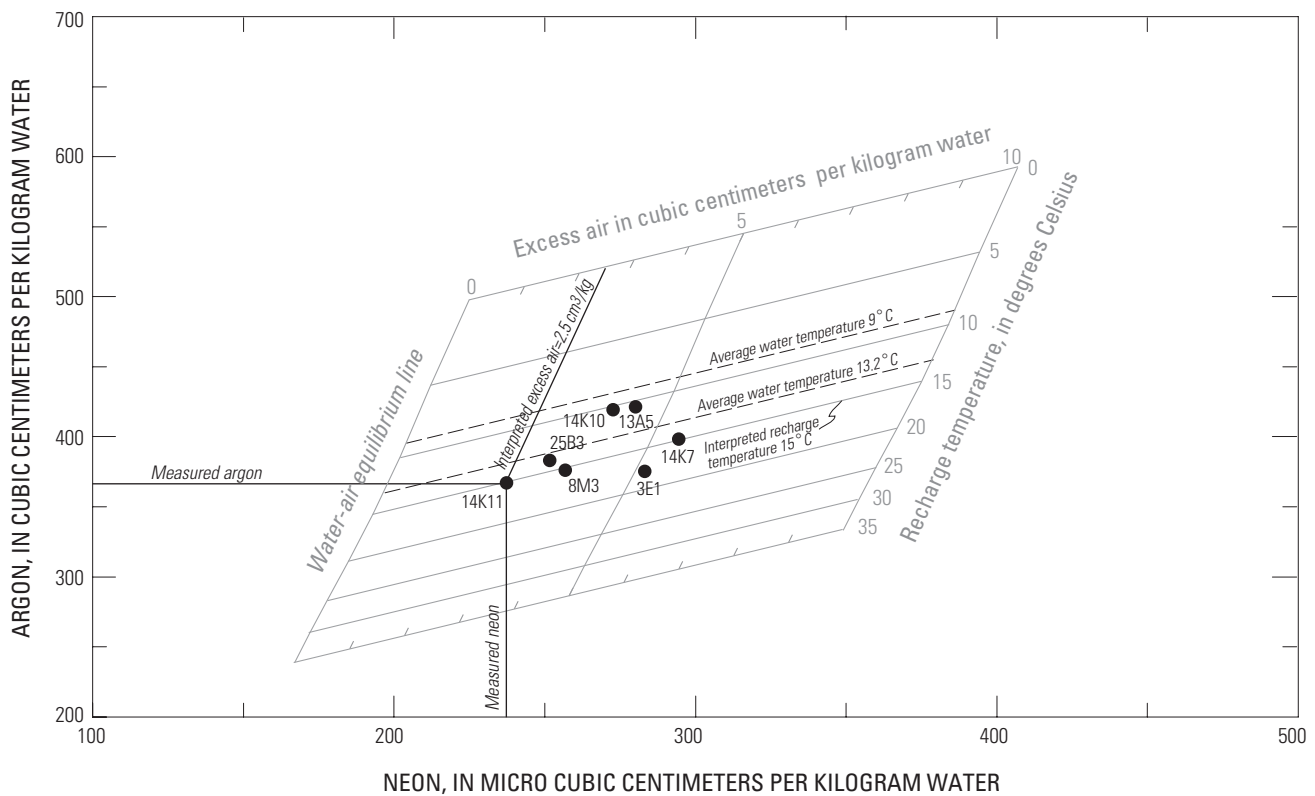
Table 1. Dissolved noble-gas and nitrogen-gas concentrations, recharge temperatures, excess air-concentrations, tritium values, and time since recharge for water from selected wells in the East Bay Plain, Alameda County, California, 1998–99

[Data analyzed by Robert Poreda, University of Rochester; all gas concentrations at standard temperature and pressure, which is 0°C (273.15 degrees Kelvin) and 1 atmosphere; °C, degrees Celsius; shaded rows are samples effected by seawater intrusion or mixing with water from other sources of high-chloride water; ft, foot, cm³/kg, cubic centimeter per kilogram; μcm³/kg, 10⁻⁶ cubic centimeter per kilogram; TU, tritium unit; –, no data.]

State well No.	Date	Temperature (°C)	Dissolved chloride (mg/L)	Depth (ft)	Dissolved helium-4 (μcm ³ /kg)	Delta helium-3 (percent)	Dissolved neon (μcm ³ /kg)	Dissolved argon (cm ³ /kg)	Dissolved nitrogen gas (cm ³ /kg)
2S/3W-16R1	12/11/98	18.9	700	495	338.9	17.0	354.0	0.374	17.0
2S/3W-17K1	12/08/98	18.0	420	205	152.3	-14.1	278.6	.347	15.8
2S/3W-17K2	12/08/98	17.9	17,000	80	118.0	-10.8	252.6	.367	16.7
2S/3W-19Q3	12/08/98	23.0	250	1,000	369.0	-33.9	348.8	.408	18.0
2S/3W-25B3	12/10/98	16.1	34	88	72.7	40.3	251.7	.383	16.4
2S/3W-28G1	08/25/99	18.2	1,400	250	178.6	51.2	293.2	.378	18.0
2S/4W-3E1	08/26/99	21.3	210	353	853.7	10.6	283.3	.375	18.1
3S/2W-8M3	12/09/98	18.1	48	85	64.7	15.9	256.8	.376	21.7
3S/3W-14K71	12/07/98	19.4	61	660	1,285	218.	294.6	.398	16.5
3S/3W-14K10	12/07/98	17.9	140	200	91.4	11.8	272.7	.419	18.3
3S/3W-14K11	12/07/98	18.6	42,000	60	63.1	-4.7	237.4	.367	16.4
3S/3W-13A5	12/09/98	17.3	58	85	72.2	2.3	280.2	.421	20.6

State well No.	Date	Recharge temperature (°C)	Excess air (cm ³ /kg)	Excess nitrogen gas (cm ³ /kg)	Tritium (TU)	Tritium error count + 1 s (TU)	Tritiogenic helium-3 (TU)	Age (in years before present)	Year isolated from the atmosphere
2S/3W-16R1	12/11/98	26.2	9.3	—	0.33	0.1	7.0	56	1942
2S/3W-17K1	12/08/98	23.6	5.1	—	.05	.1	2.0	—	pre-1952
2S/3W-17K2	12/08/98	16.9	.3	—	.21	.1	1.8	42	1956
2S/3W-19Q3	12/08/98	18.4	8.6	—	-.04	.09	2.4	—	pre-1952
2S/3W-25B3	12/10/98	14.4	2.9	0.3	5.0	.19	2.2	16	1982
2S/3W-28G1	08/25/99	18.8	5.5	—	.75	.12	5.2	39	1960
2S/4W-3E1	08/26/99	18.3	4.9	3.2	-.04	.1	.14	—	pre-1952
3S/2W-8M3	12/09/98	15.7	3.3	5.7	6.5	.23	1.6	14	1984
3S/3W-14K7 ¹	12/07/98	—	—	—	1.6	.12	—	—	—
3S/3W-14K10	12/07/98	10.6	3.7	.7	.23	.09	2.0	42	1956
3S/3W-14K11	12/07/98	15.6	2.2	—	.03	.1	1.2	—	pre-1952
3S/3W-13A5	12/09/98	11.0	3.9	2.6	.14	.09	1.5	46	1952

¹Sample affected by mixing of native water and water injected from a nearby well.



EXPLANATION

25B3 ● Fresh ground water

Figure 17. Selected noble-gas concentrations in water from selected wells in the East Bay Plain, Alameda County, California, 1999–2000.

The ground-water recharge temperatures calculated for samples collected from wells yielding freshwater (chloride concentrations less than 250 mg/L) were between 10.6 and 18.3°C, with a median recharge temperature of 14.4 °C. Excess-air values for these samples were between 2.9 and 4.9 cm³/kg (table 1). Depending on the thickness of the unsaturated zone, the recharge rate, and the seasonal distribution of precipitation, the recharge temperature at the water table is usually between 0.4 and 1.4°C warmer than the average annual air temperature (Stute and Schlosser, 2000). Given an average annual air temperature of about 13.2 °C, the median recharge temperature and recharge temperatures calculated for water from wells 2S/3W-25B3 and 3S/2W-8M3, 14.4 and 15.7 °C respectively (table 1), agree with values expected for recharge temperature from diffuse recharge sources such as areal recharge from infiltrating precipitation, irrigation return, or septic tank discharges. In contrast, lower recharge

temperatures calculated for water from wells 3S/3W-14K10 and 3S/3W-13A5 (10.6, and 11 °C respectively) (table 1), may represent water from wells having a higher percentage of water recharged as focused infiltration of streamflow through thinner unsaturated zones during the winter months when temperatures are cooler. The average temperature during the winter months is about 9°C, and this lower temperature may be preserved if the quantity of water infiltrated into the aquifer is large and the unsaturated zone is thin. Water-level contour maps show evidence of focused recharge from San Lorenzo Creek and, to a lesser extent, from San Leandro Creek (fig. 5). The recharge temperature calculated for water from well 2S/4W-3E1, 18.3 °C (table 1), was higher than expected given the mean annual temperature in the study area. Water from this well had a chloride concentration of 210 mg/L, and recharge temperatures may have been affected by mixing with water having high salinity.

Samples from wells yielding water having chloride concentrations greater than 250 mg/L have estimated recharge temperatures between 15.6 and 26.2°C and excess-air values as high as 9.3 cm³/kg. The highest estimated recharge temperatures were from water from wells 2S/3W-16R1 and 17K1, which are believed to be intruded by seawater. These data suggest that estimates of recharge temperature calculated using noble-gas data do not produce reasonable results for samples that are complex mixtures of water from different sources that differ greatly in salinity. Samples of water from wells affected by seawater intrusion also may contain high concentrations of dissolved gases due to strongly reducing conditions and subsequent geochemical reactions within aquifers, and may exolve gas during sample collection (Appello and Willemssen, 1987). Unreasonable recharge temperatures may be the result of partitioning of dissolved noble gases into bubbles formed during sample collection. In a similar problem, the water level in well 2S/3W-19Q3 was lowered below the screened interval during sample collection. The noble gases may have equilibrated with the atmosphere and temperature in the well at depth during sample collection, affecting calculated recharge temperature and excess-air values. The recharge temperatures for water from the wells having the highest salinity, 2S/3W-17K2 and 3S/3W-14K11, are reasonable and within the range of values obtained from wells yielding freshwater—even though samples from these wells have chloride concentrations as high as 42,000 mg/L. Water from these wells originated primarily from San Francisco Bay, and the recharge temperature may accurately represent the temperature of the water at the time it was isolated from the Bay.

Excess Nitrogen And Denitrification

Some samples have an excess of nitrogen gas in comparison with nitrogen-gas concentrations estimated from the noble-gas recharge temperatures and the presence of excess air (table 1). This result suggests that denitrification may be occurring within the aquifer.

The highest excess-nitrogen concentrations of 5.7 cm³/kg (corresponding to 7.2 mg/L nitrogen gas as N) are in water from well 3S/3W-8M3. This shallow well also has the highest nitrate concentration of any well sampled on the East Bay Plain during this study, 25 mg/L as N. The original nitrate concentration may have been as high as 32 mg/L as N and was reduced to the measured concentration by denitrification within the aquifer. The calculated recharge temperature for water from this well is consistent with recharge from a diffuse source such as septic tank recharge, rather than a focused source such as infiltration of winter streamflow. Further denitrification may eventually reduce nitrate concentrations to below the U.S. Environmental Protection Agency MCL for nitrate of 10 mg/L as N.

Other wells having high excess nitrogen, 2S/4W-3E1 and 3S/3W-13A5, have nitrate concentrations at, or below, the detection limit of 0.02 mg/L as N. Both wells are completed in the lower aquifer system more than 2 mi downgradient from recharge areas near the mountain front and, presumably, almost complete denitrification has occurred as ground water moved through the aquifer. However, the initial nitrate concentrations in water from these wells probably did not exceed the MCL for nitrate. In contrast, almost no excess nitrogen was present, in water from well 2S/3W-25B3 indicating that almost no denitrification has occurred in this water. This well has a nitrate concentration of 5.3 mg/L as N and is completed near the water table in the upper aquifer system near recharge areas along the mountain front.

ISOTOPIC COMPOSITION OF GROUND WATER

Isotopes are atoms of the same element, in which the nuclei of the atoms have the same number of protons but different numbers of neutrons. In this study, stable, naturally occurring isotopes of oxygen (oxygen-18) and hydrogen (deuterium) were used to determine the source of ground water to wells and trace its movement through aquifers underlying the East Bay Plain. Naturally occurring radioactive isotopes of hydrogen (tritium) and carbon (carbon-14) were used to determine the age (time since recharge) of the ground water. Tritium and its decay product helium-3 were used to estimate the age of younger ground water (water recharged after 1952). Carbon-14, the stable isotope carbon-13, and other chemical and mineralogic data were used to estimate the age of older ground water that did not contain tritium.

Oxygen-18 and Deuterium

Atoms of oxygen-18 (^{18}O) and deuterium (^2H) have more neutrons and a greater atomic mass than do atoms of the more common isotopes, oxygen-16 and hydrogen. The difference in weight results in differences in the physical and chemical behavior of the heavier, less abundant isotopes. Oxygen-18 and deuterium abundances are expressed as ratios of the heavy isotope to the light isotope, in delta notation (δ), as per mil (parts per thousand) differences, relative to Vienna Standard Mean Ocean Water (VSMOW) (Gonfiantini, 1978). By convention, the value of VSMOW is 0 per mil. Oxygen-18 ($\delta^{18}\text{O}$) and deuterium (δD) ratios relative to VSMOW can be measured more precisely than absolute abundance, and these ratios are useful in hydrologic studies (International Atomic Energy Agency, 1981). Based on duplicate analyses of samples collected as part of other studies, analytical precision is generally within ± 0.05 per mil for $\delta^{18}\text{O}$ and within ± 1.5 per mil for δD (Coplen, 1994; Izbicki, 1996).

The $\delta^{18}\text{O}$ and δD composition of a water sample can provide a record of the source and evaporative history of water. The differences in isotopic composition can be used as a tracer of the movement of the water. Most precipitation throughout the world

originates from the evaporation of seawater. As a result, the $\delta^{18}\text{O}$ and δD composition of precipitation throughout the world is linearly correlated (fig. 18) and plots along a line known as the meteoric water line (Craig, 1961). Differences in the isotopic composition of precipitation occur along this line if water vapor originated from evaporation of cooler or warmer seawater, and as moist air masses move across continents and heavier isotopes are preferentially removed by precipitation. At a given location, the isotopic composition of water vapor in different storms trends to an average value over time, and the isotopic composition of precipitation is determined by local differences in the temperature of condensation of water vapor. Water that condensed at cooler temperatures (associated with higher altitudes, cooler climatic regimes, or higher latitudes) is lighter (more negative δ values) than water that condensed at warmer temperatures (associated with lower altitudes, warmer climatic regimes, or lower latitudes.) Water that has been partly evaporated is enriched in the heavier isotopes, relative to its original composition; these values plot to the right of the meteoric water line along a line known as the evaporative-trend line.

The $\delta^{18}\text{O}$ and δD composition of water from sampled wells in the East Bay Plain ranged from -2.7 to -11.2 per mil and -23 to -82 per mil, respectively. The lightest (most negative) value was from well 3S/3W-14K9. At the time the sample was collected, water from well 14K9 was primarily imported water injected into the aquifer at a nearby well. The δD composition of imported water from the Sierra Nevada measured as part of this study is about -80 per mil. The sample from well 14K7 likely contained some water imported from the Sierra Nevada as well. The heaviest (least negative) values were from well 3S/3W-14K11. Well 14K11 is completed in estuarine deposits near San Francisco Bay and has chloride concentrations as high as 42,000 mg/L. The $\delta^{18}\text{O}$ and δD composition of water from this well does not approach the expected $\delta^{18}\text{O}$ and δD composition for seawater of 0 per mil, despite chloride concentrations more than twice that of seawater. These results suggest that much of the water from this well is meteoric in origin even though the dissolved salts probably have accumulated from the complete evaporation of seawater or of discharging ground water.

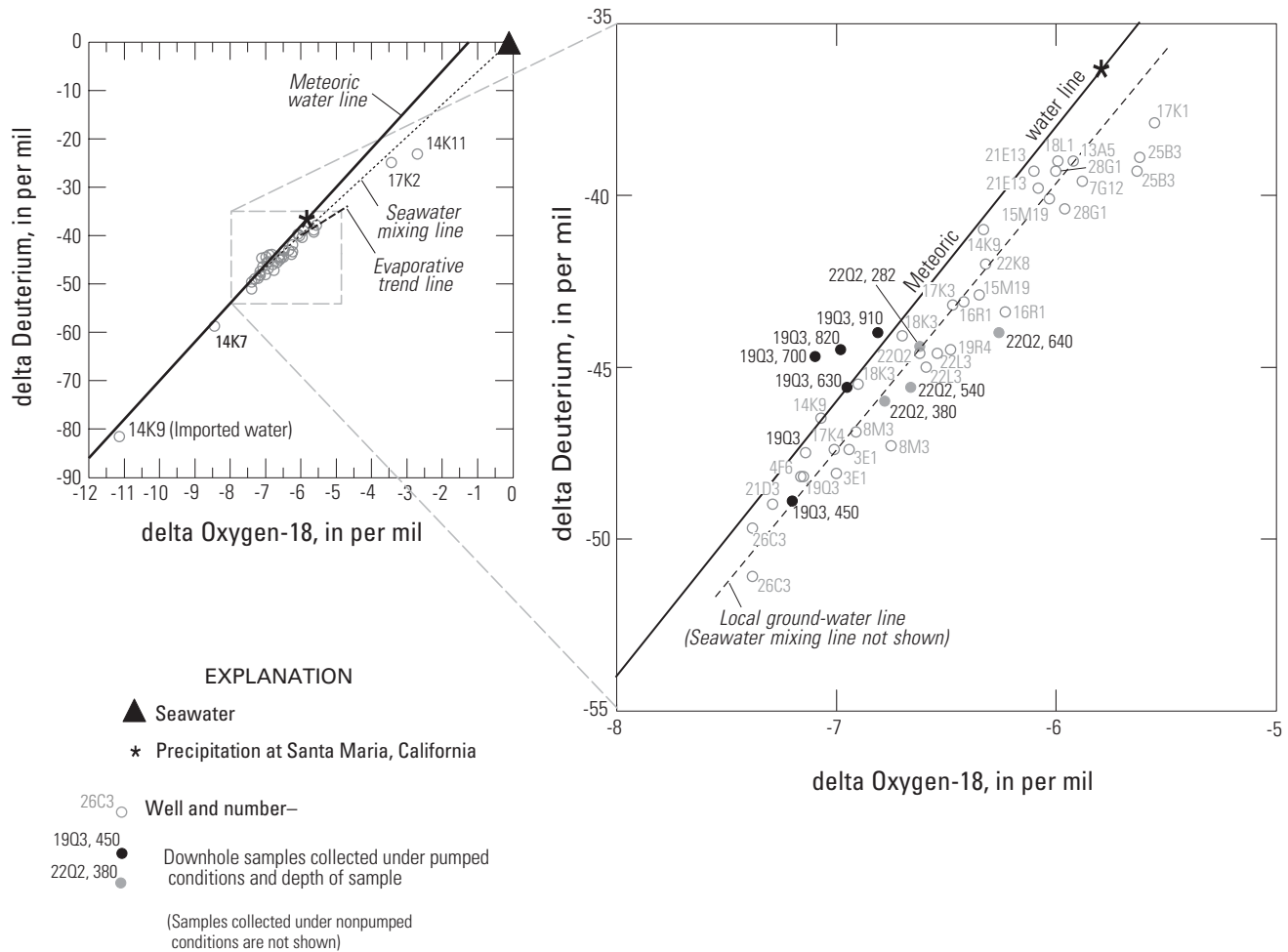


Figure 18. Delta oxygen-18 ($\delta^{18}\text{O}$) as a function of delta deuterium (δD) in water from wells, East Bay Plain, Alameda County, California, 1997–2000.

Neglecting well 14K9 and water from wells having chloride concentrations greater than 250 mg/L, the $\delta^{18}\text{O}$ and δD composition of water from most wells sampled in the East Bay Plain ranged from -5.6 to -7.4 per mil and -39 to -51 per mil, and had a median composition of -6.6 and -44 per mil, respectively. These values are slightly lighter than the median volume-weighted $\delta^{18}\text{O}$ and δD composition of precipitation of -5.8 and -36 per mil, measured at Santa Maria, California, between 1962 and 1976 by the International Atomic Energy Agency (1981). The difference is slightly greater than the 2 per mil per degree of latitude decrease in deuterium expected with increasing latitude for sea-level precipitation in western North America (Williams and Rodoni, 1997) and may

result from orographic uplift of condensing precipitation caused by coastal mountains in the San Francisco Bay area.

With the exception of water from well 3S/3W-14K9, large amounts of isotopically light water, similar in composition to imported water from the Sierra Nevada, were not observed in the study area. The absence of imported water in shallow wells completed in water-table aquifers underlying the East Bay Plain suggests that large amounts of recharge are not due to leaky pipes or irrigation return from lawn watering with imported water. This result was not expected. Water budget calculations done by Muir (1996a) suggested that leaking pipes are a large source of ground-water recharge to aquifers underlying the East

Bay Plain. Although some isotopically light water from shallow wells such as 2S/3W-26C3 and 3S/2W-21D3 may be due to mixing of native water and isotopically light imported water, it is possible that most recharge from leaking pipes is concentrated in the older urban areas and is not uniformly distributed across the study area. This result contrasts sharply with recent results by Metzger (2002) that show that isotopically light imported water from the Sierra Nevada recharges the shallow aquifers near Palo Alto, California, across the Bay.

As a group, most samples plot slightly below the meteoric water line along the local ground-water line. However, samples from wells 2S/3W-25B3 and 17K1 plot to the right of the local ground water line (fig. 18). Well 25B3 is shallow and recharge to this well may occur as irrigation return from lawn watering or partial evaporation of septic tank recharge. The recharge temperature calculated from noble-gas data for water from well 25B3 is consistent with recharge from a diffuse source such as irrigation return from lawn watering. Water from well 2S/3W-17K1 plots to the right of the meteoric water line due to mixing with seawater or water from estuarine deposits along San Francisco Bay.

The isotopic compositions of depth-dependent samples collected from well 2S/3W-22Q2 (fig. 11) collected under pumped conditions plot slightly to the right of the meteoric water line near the local ground-water line. The sample that plots farthest to the right was collected at a depth of 282 ft and had the highest chloride concentration. These data are consistent with seawater intrusion or high-chloride water mobilized from fine-grained deposits. The chloride concentrations and subsequent shifts in isotopic concentration are too small to distinguish between these sources (Izbicki,

1996). Borehole geophysical data discussed previously suggest that under nonpumped conditions this water flows downward through the well, entering deeper deposits (fig. 11A).

The isotopic compositions of depth-dependent samples collected from well 2S/3W-19Q3 (fig. 12) are different from those of most other sampled wells. Samples collected below the pump intake, 460 ft below land surface, plot above the meteoric water line (fig. 18). These samples have high chloride concentrations and would be expected to plot to the right of the meteoric water line if they were a simple mixture of native water and seawater. The sample collected above the pump intake is isotopically lighter and plots below the meteoric water line—even though chloride concentrations at this depth are lower (fig. 12). Samples collected from the surface discharge, which are a mixture of water from above and below the intake, plot between the two values. This result suggests that depth-dependent water samples collected from well 19Q3 may have a different hydrologic history than that of water from most sampled wells. Carbon-14 data presented later in this report will show that water from well 19Q3 is older than most other ground waters sampled and was recharged at a time when the climate was presumably different from the present-day climate. Comparison of the $\delta^{18}\text{O}$, δD , and chloride data shows that water from the well is meteoric in origin and has more chloride than expected on the basis of its isotopic composition, assuming only simple mixing with seawater. This result suggests dissolution of chloride from aquifer material at depth or incomplete removal of seasalts from the deposits—even though the water present at the time of deposition has been largely flushed from the deposits.

Tritium and Helium-3

Tritium (^3H) is a naturally occurring radioactive isotope of hydrogen that has a half-life of 12.43 years. In this study, tritium was measured in tritium units (TU); 1 tritium unit is equivalent to 1 tritium atom in 10^{18} atoms of hydrogen (Taylor and Roether, 1982). Prior to 1952, the tritium concentration in coastal California was about 2 TU (fig. 19). About 800 kg of tritium was released to the atmosphere as a result of the atmospheric testing of nuclear weapons during 1952-62 (Michel, 1976), and the tritium concentration of precipitation increased to a maximum of about 1,200 TU. After the cessation of atmospheric testing of nuclear weapons in 1962, the tritium concentration of precipitation decreased and present-day tritium levels in precipitation are near the pre-1952 levels. Because tritium is part of the water molecule, tritium is not affected by reactions other than radioactive decay, and—neglecting the effects of dispersion—tritium is an excellent tracer of the movement of ground water recharged less than 50 years before present.

Background

Tritium decays to the stable isotope of helium, helium-3 (^3He). If the tritium concentration of a water sample and the concentration of helium-3 produced by the radioactive decay of tritium in that sample are known, then the tritium concentration at the time the water was isolated from the atmosphere and the age (time since recharge) of the water can be estimated. As with many isotopes, the ratio of helium-3 to the more abundant isotope helium-4 (^4He) can be measured more precisely than can the absolute abundance of a single isotope, and helium-3 data are reported as delta helium-3 ($\delta^3\text{He}$):

$$\delta^3\text{He} = \left[\frac{(^3\text{He}/^4\text{He})_{\text{sample}}}{(^3\text{He}/^4\text{He})_{\text{atmo}}} - 1 \right] \times 100 \quad (6)$$

where

$(^3\text{He}/^4\text{He})_{\text{sample}}$ is the measured helium-3 to helium-4 ratio in the sample, and

$(^3\text{He}/^4\text{He})_{\text{atmo}}$ is the helium-3 to helium-4 ratio in the atmosphere.

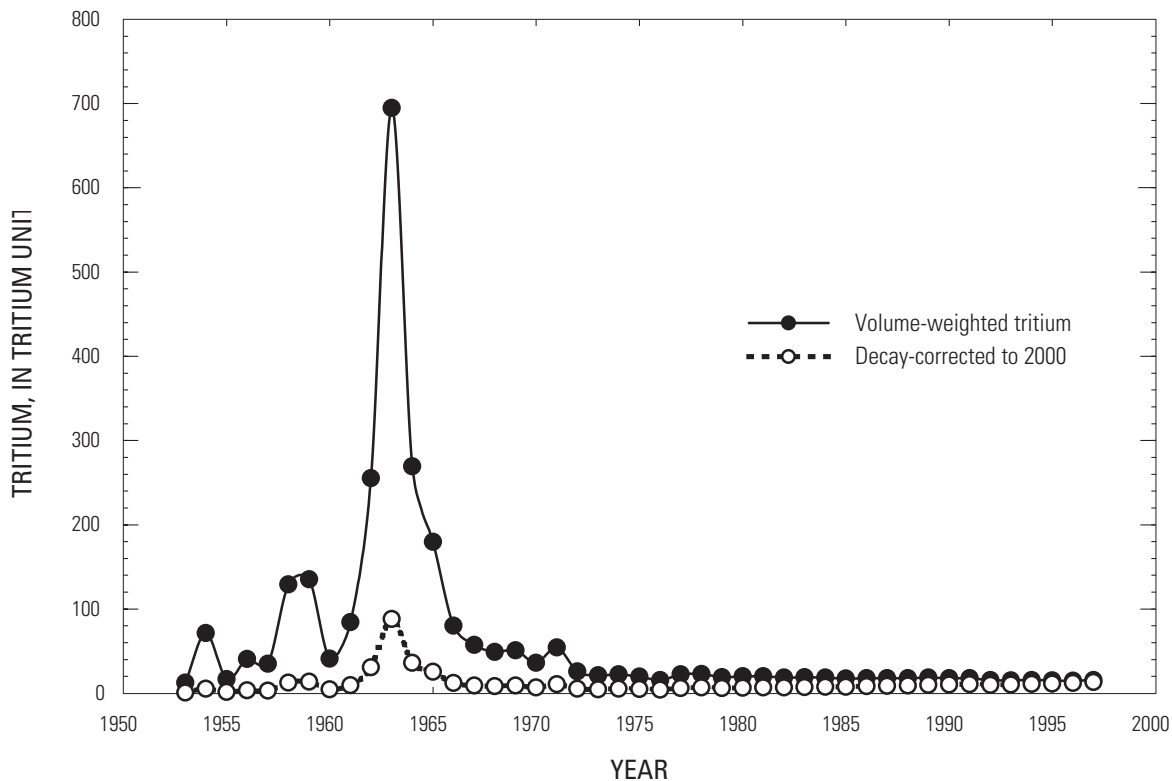


Figure 19. Volume-weighted tritium concentrations in p precipitation at Santa Maria, California, 1952–1997. Data were estimated from data collected at Ottawa during 1953–61 and 1977–97.

The helium-3 concentration can be calculated from the $\delta^3\text{He}$ value, assuming an atmospheric helium-3 to helium-4 ratio of 1.384×10^{-6} (Clarke and others, 1976). The concentration of helium-3 produced by the radioactive decay of tritium is calculated as a residual from the helium-3 mass-balance equation according to the following:

$${}^3\text{He}^* = {}^3\text{He}_{\text{total}} - {}^3\text{He}_{\text{atmo}} - {}^3\text{He}_{\text{rad}} - {}^3\text{He}_{\text{man}}, \quad (7)$$

where

- ${}^3\text{He}^*$ is the helium-3 produced by the radioactive decay of tritium (tritogenic helium-3),
- ${}^3\text{He}_{\text{total}}$ is the total helium-3 (calculated from the measured $\delta^3\text{He}$),
- ${}^3\text{He}_{\text{atmo}}$ is the helium-3 from the atmosphere (including excess air),
- ${}^3\text{He}_{\text{rad}}$ is the helium-3 from radioactive decay of elements other than tritium, and
- ${}^3\text{He}_{\text{man}}$ is the helium-3 from mantle degassing.

Given that 1 TU of tritium will decay to produce only a small amount of helium-3, about 2.487 cubic picocentimeters (pcm^3) of helium-3 per kilogram (kg) of water at STP (Standard Temperature and Pressure) (Solomon and Cook, 2000), it is necessary to estimate other components of the helium-3 mass balance precisely to obtain an accurate tritium/helium-3 age. For example, helium-3 is naturally present in the atmosphere, and water at 10 °C in equilibrium with the atmosphere will have a helium-3 concentration of 63.7 pcm^3/kg at 10 °C (Solomon and Cook, 2000). Excess air trapped during ground-water recharge will increase the helium-3 contribution from atmospheric sources. Because these values are large in comparison with helium-3 from the decay of tritium, errors in the recharge temperature and excess-air values will produce large errors in the tritium/helium-3 age determination. This is especially true for excess air. Cook and Solomon (1997) estimated that the sensitivity of tritium/helium-3 ages to excess air ranges from -5.0 years per cm^3/kg of excess air for very young ground water to -0.25 year per cm^3/kg of excess air for ground water recharged 25 years before present.

Helium-3 produced in the subsurface through the decay of lithium-6 is small and does not effect the tritium/helium-3 age in most ground-water systems (Solomon and Cook, 2000). Helium-3 from radioactive decay is combined with helium-3 from mantle degassing for the purposes of calculating a ground-water age. Helium-3 from mantle degassing is estimated from the helium-4 mass-balance equation according to the following :

$${}^4\text{He}_{\text{man}} = {}^4\text{He}_{\text{total}} - {}^4\text{He}_{\text{atmo}} - {}^4\text{He}_{\text{rad}}, \quad (8)$$

where the subscripts (man, total, atmo, and rad) have the same meaning as in the helium-3 mass balance.

The ratio of Helium-3 to helium-4 in mantle gases is between 1×10^{-5} and 1.4×10^{-5} (Torgerson and Clarke, 1987). Helium-4 is produced from the α decay of elements in the uranium-thorium radioactive decay series, other than ${}^6\text{Li}$. As in the helium-3 mass balance, the helium-4 from radioactive decay is usually small for young ground water and this term is combined with helium-4 from mantle degassing. Estimates of helium-4 are subject to the same uncertainty associated with recharge temperature and excess air as are estimates of helium-3.

Solomon and Cook (2000) published a simultaneous solution to the helium-3 and helium-4 mass-balance equations that uses measured helium-4 concentrations, $\delta^3\text{He}$ values, and neon concentrations (to constrain recharge temperatures and excess-air values) to calculate helium-3 from the radioactive decay of tritium (tritogenic helium-3, ${}^3\text{He}^*$). Ground-water ages are then calculated on the basis of the radioactive decay of tritium:

$$t = \lambda^{-1} \ln \left[\left(\frac{{}^3\text{He}^*}{{}^3\text{H}} \right) + 1 \right], \quad (9)$$

where

- t is the ground-water age in years before present,
- λ is the half-life of tritium (12.43 years), and
- ${}^3\text{H}$ is the measured tritium value.

For the purposes of this report, Solomon and Cook's solution to the mass-balance equations was modified to incorporate recharge temperatures and excess-air values calculated from neon and argon ([table 1](#)). Recharge temperatures and excess-air values calculated on the basis of three noble gases are presumably more accurate than values calculated on the basis of helium and neon data.

The tritium/helium-3 age dating method is applicable for ground water that contains tritium. If the helium-3 concentration is not known, or the contributions of helium-3 from other sources cannot be quantified, ground water having measurable tritium is considered water recharged after 1952, and water without detectable tritium is considered water recharged before 1952. In some cases, water from wells may be a mixture of younger water and older water that does not contain tritium—complicating the interpretation of tritium/helium-3 age determinations. As a result of radioactive decay and mantle degassing, helium-4 and helium-3 concentrations increase with ground-water residence time—providing a means to date ground water recharged thousands of years before present (Solomon, 2000).

Tritium and Helium-3 Ages

Tritium in water from wells in the study area ranged from less than the detection limit of 0.2 to 6.5 TU. The highest tritium values were in shallow wells near the mountain front. Tritium was present throughout the upper aquifer system at low concentrations as far downgradient as well 2S/3W-17K2 near San Francisco Bay. Water from this well has a chloride concentration of 17,000 mg/L, and tritium in water from this well may result from seawater intrusion (Michel and others, 1996). Tritium values were less than the detection limit in water from most deep wells completed in the lower aquifer system. However, tritium was detected in well 2S/3W-22L3. As previously discussed, this well is 809 ft deep and screened entirely within the lower aquifer system.

However, the well is located about 150 ft from well 2S/3W-22Q2, and physical measurements and water chemistry and isotopic data show that well 22Q2 allows water to move from the upper aquifer system into the lower aquifer system.

Helium-4 concentrations ranged from 63.1 to 1,285 $\mu\text{cm}^3/\text{kg}$ STP. The lowest concentration was in a sample collected from well 3S/3W-1K11. Water from this well has a chloride concentration of 42,000 mg/L, and noble-gas solubilities are less as a result of high salinity. Low helium-4 concentrations also were present in water from upper aquifer system wells near recharge areas along the mountain front. The highest helium-4 concentration was in water from well 3S/3W-14K7. The $\delta^3\text{He}$ values ranged from -33.9 to 218 percent. All samples that were depleted in ^3He relative to the atmospheric composition (had negative $\delta^3\text{He}$ values) were high-chloride waters. Recharge temperature and excess-air values for some of these samples may not have been accurately estimated due to mixing and salinity effects on the solubility of noble gases and possibly outgassing or other problems during sample collection.

Tritium/helium-3 ages calculated from the data in [table 1](#) ranged from 14 years before present to more than 50 years before present. Water within the tritium/helium-3 dating range was present only in the upper aquifer system and extended about 3 mi downgradient from recharge areas near the mountain front. Tritium/helium-3 ages are shown for water from wells along sections A-A' and B-B' in [figure 20](#). Samples containing low tritium concentrations near the detection limit were not included in [figure 20](#). Tritium/helium-3 ages are usually interpreted to be accurate to within ± 2 years and accurate to within ± 5 years where large concentrations of excess air are present (Solomon and Cook, 2000). Samples collected as part of this study where tritium concentrations are near the detection limit or where there are known to be problems associated with the calculation of recharge temperatures and excess-air values are probably less accurate.

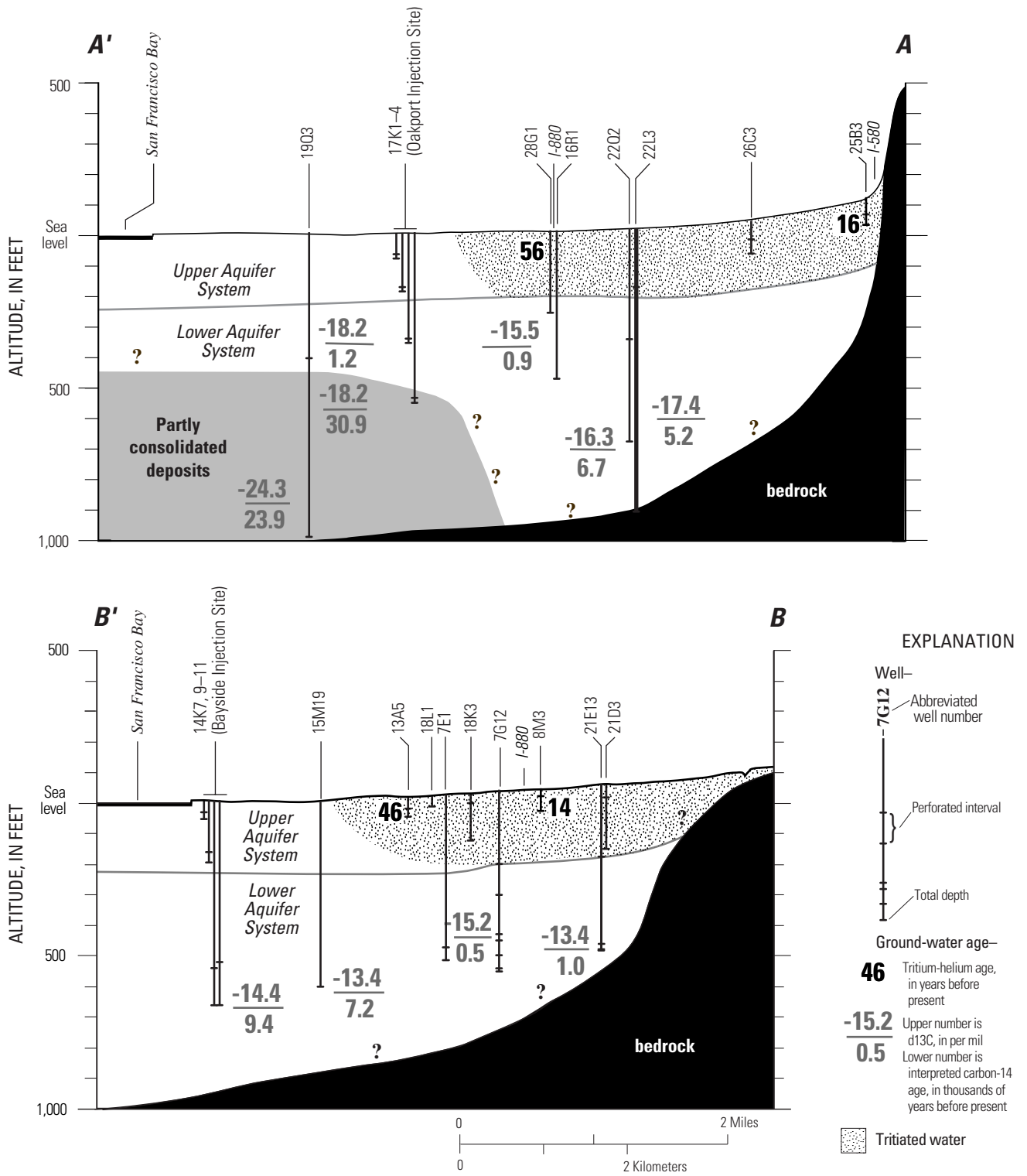


Figure 20. Ground-water ages (time since recharge) along hydrogeologic sections A-A' and B-B', East Bay Plain, Alameda County, California.

Carbon-14 and Carbon-13

Background

Carbon-14 (^{14}C) is a naturally occurring radioactive isotope of carbon having a half-life of about 5,730 years (Mook, 1980). Carbon-14 data are expressed as percent modern carbon (pmc) by comparing ^{14}C activities to the specific activity of National Bureau of Standards oxalic acid; 12.88 disintegrations per minute per gram of carbon in the year 1950 equals 100 percent modern carbon. Carbon-14 was produced, as was tritium, by the atmospheric testing of nuclear weapons (Mook, 1980), and carbon-14 activities may exceed 100 percent in areas where ground water contains tritium. Carbon-14 activities are used to determine the age (time since recharge) of ground water on scales ranging from recent to more than 20,000 years before present. Interpreted carbon-14 ages were used in this study to test hypotheses about the isolation of deeper aquifers from overlying aquifers and possible contamination associated with industrial, commercial, and residential land use in the study area.

Carbon-14 is not part of the water molecule, and carbon-14 activities are affected by chemical reactions that occur between dissolved constituents and the solid material that composes the aquifer. Interpretation of carbon-14 data requires data on the chemical and isotopic composition of the water and aquifer deposits, knowledge of reactions that occur within an aquifer, and an estimate of the initial carbon-14 activity of recharge water.

Carbon-13 (^{13}C), a naturally occurring stable isotope of carbon, was used in conjunction with chemical (Appendixes B and C) and mineralogic data (Appendix E) to evaluate chemical reactions that occur within the aquifer. These reactions may add inorganic carbon that does not contain carbon-14 to the dissolved phase or remove carbon that may contain carbon-14

from the dissolved phase. Carbon-13 data are expressed as ratios in delta notation (δ) as per mil (parts per thousand) differences relative the ratio of ^{13}C to ^{12}C in the standard Peedee Belemnite (PDB) (Gonfiantini, 1978).

Carbon-14 Activity and Carbon-13 Composition of Dissolved Inorganic Carbon

Inorganic carbon-14 activities for water from 12 wells in the study area ranged from 0.4 to 86.7 percent modern carbon (table 2). In general, carbon-14 activities were higher in the upper aquifer system near recharge areas. Carbon-14 activities decreased with increasing depth and were lower in deep wells at the downgradient end of long flow paths through the lower aquifer system and in the underlying partly consolidated rocks. The lowest carbon-14 activities were in samples from wells 2S/3W-19Q3 and 2S/3W-17K4 completed in partly consolidated deposits underlying section A-A' (fig. 20). These low-porosity deposits yield only small amounts of water to wells and are isolated from surface sources of recharge.

Measured $\delta^{13}\text{C}$ compositions of water from 13 wells in the study area ranged from -13.4 to -24.3 per mil (table 2). Delta carbon-13 values were lighter (more negative) in water from shallow wells near recharge areas along the front of the mountains and were heavier (less negative) in deep wells near the mountain front along section B-B'. Delta carbon-13 values became more negative as water flowed through the deep aquifers, and the most negative values were in water from well 2S/3W-19Q3 in the partly consolidated deposits underlying section A-A' (fig. 20). Such highly negative carbon-13 values typically occur in reducing aquifers where methane is utilized as a carbon source for sulfate reduction (Izbicki and others, 1992). As previously discussed, methane was detected in water from this well.

Table 2. Carbon-13 and carbon-14 data and time since recharge for water from selected wells, East Bay Plain, Alameda County, California, 1997–2000

[<, less than value shown; —, no data]

State well No.	Date	Delta carbon-13 (per mil)	Carbon-14 (percent modern carbon)	Uncorrected carbon-14 age (thousands of years before present)	Interpreted carbon-14 age (thousands of years before present)
2S/3W-17K3	03/23/99	-18.2	54.9	4,957	1,222
2S/3W-17K4	03/23/99	-18.2	.4	45,645	30,930
2S/3W-19Q3	12/08/98	-24.3	.9	38,940	23,860
2S/3W-22L3	12/11/98	-17.4	38.7	7,847	5,225
2S/3W-22Q2	12/07/99	-16.3	22.7	11,901	6,683
2S/3W-25B3	03/27/99	-19.1	86.7	1,179	< 50
2S/3W-28G1	08/25/99	-15.5	32.5	9,291	921
2S/4W-3E1	08/26/99	-16.1	12.6	17,124	15,283
3S/2W-7G12	11/15/99	-15.2	58.1	4,488	548
2S/3W-8M3	03/27/99	-17.2	—	—	—
3S/2W-21E13	08/25/99	-13.4	54.9	4,957	1,022
3S/3W-14K9	11/13/97	-14.4	18.9	13,772	9,366
3S/3W-15M19	08/25/99	-13.4	25.5	11,296	7,181

Interpretation of Carbon-14 Data

The computer program NETPATH (Plummer and others, 1991) was used to estimate the transfer of carbon and other constituents between the dissolved and solid phases for deep wells along flow paths through sections *A–A'* and *B–B'* in the lower aquifer system and to calculate carbon-14 ages of water from those wells. Inputs to the program include the chemical and isotopic composition of water from wells, chemical equations that describe reactions that occur within the aquifer (these equations also can describe the mixing of water from different sources), and the mineralogic composition of aquifer deposits. After accounting for the mass-transfer of carbon and other constituents between the dissolved and solid phases, carbon-14 ages between wells are then calculated from the equation for radioactive decay.

Changes in water chemistry with distance from recharge areas for water from deep wells along flow paths through sections *A–A'* and *B–B'* are shown in [figure 21](#). Cumulative changes were determined at each well along the flow path as differences from the initial water compositions. Water from well 2S/3W-25B3 was used as the initial water along section *A–A'* and water from well 3S/2W-8M3 was used as the initial water along section *B–B'*. In general, sodium and chloride concentrations increase, bicarbonate concentrations increase then decrease, and calcium, magnesium, and sulfate concentrations decrease, with increasing distance from recharge areas.

Aluminum, necessary to calculate thermodynamic data for aluminosilicate minerals, was not measured as part of this study. Instead, aluminum concentrations were estimated using the computer program PHREEQC (Parkhurst, 1995) assuming equilibrium with the mineral gibbsite.

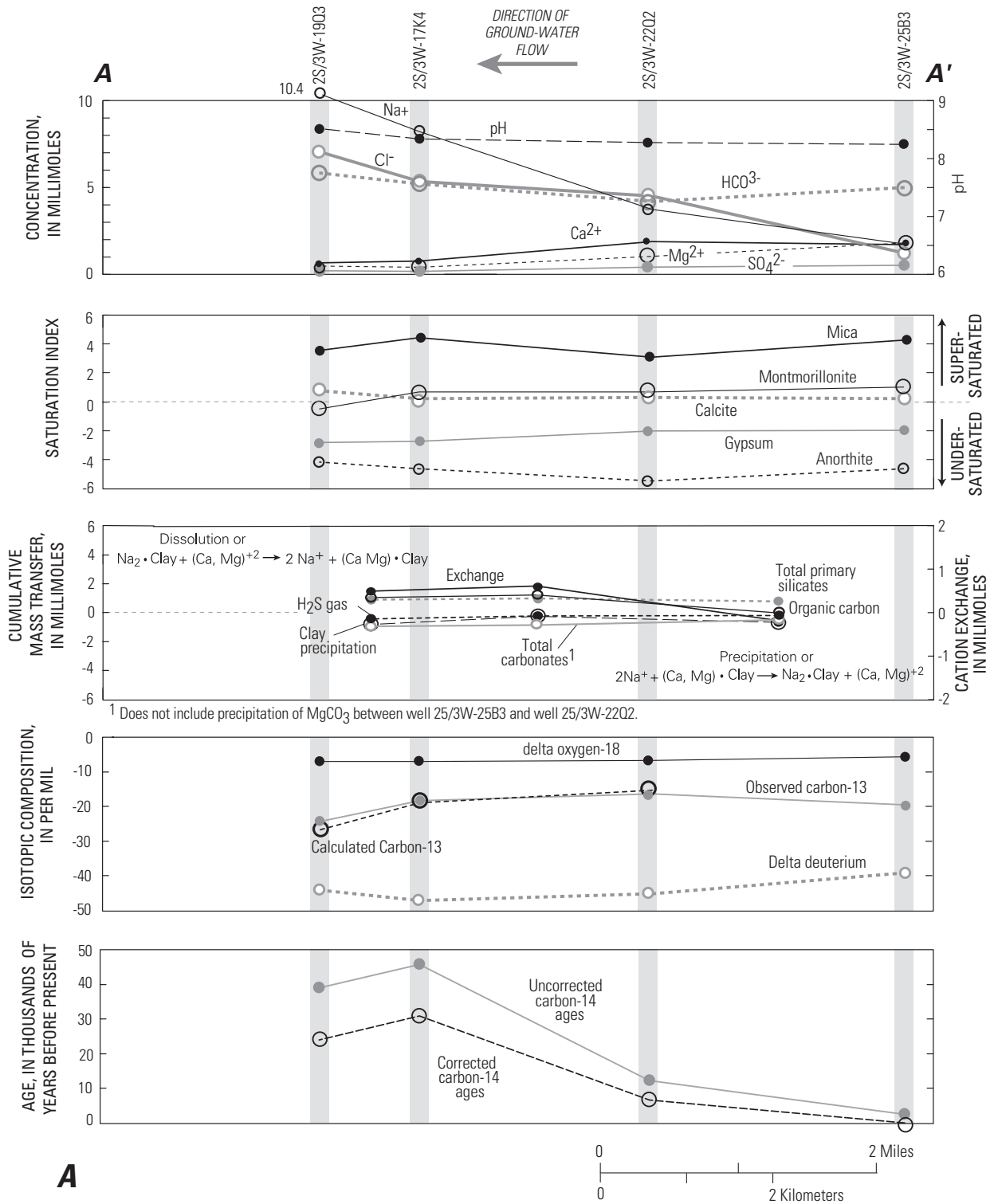


Figure 21. Selected changes in chemical and isotopic composition of water from wells used to interpret carbon-14 data along sections A–A' (**A**) and B–B' (**B**), East Bay Plain, Alameda County, California, 1998–2000.

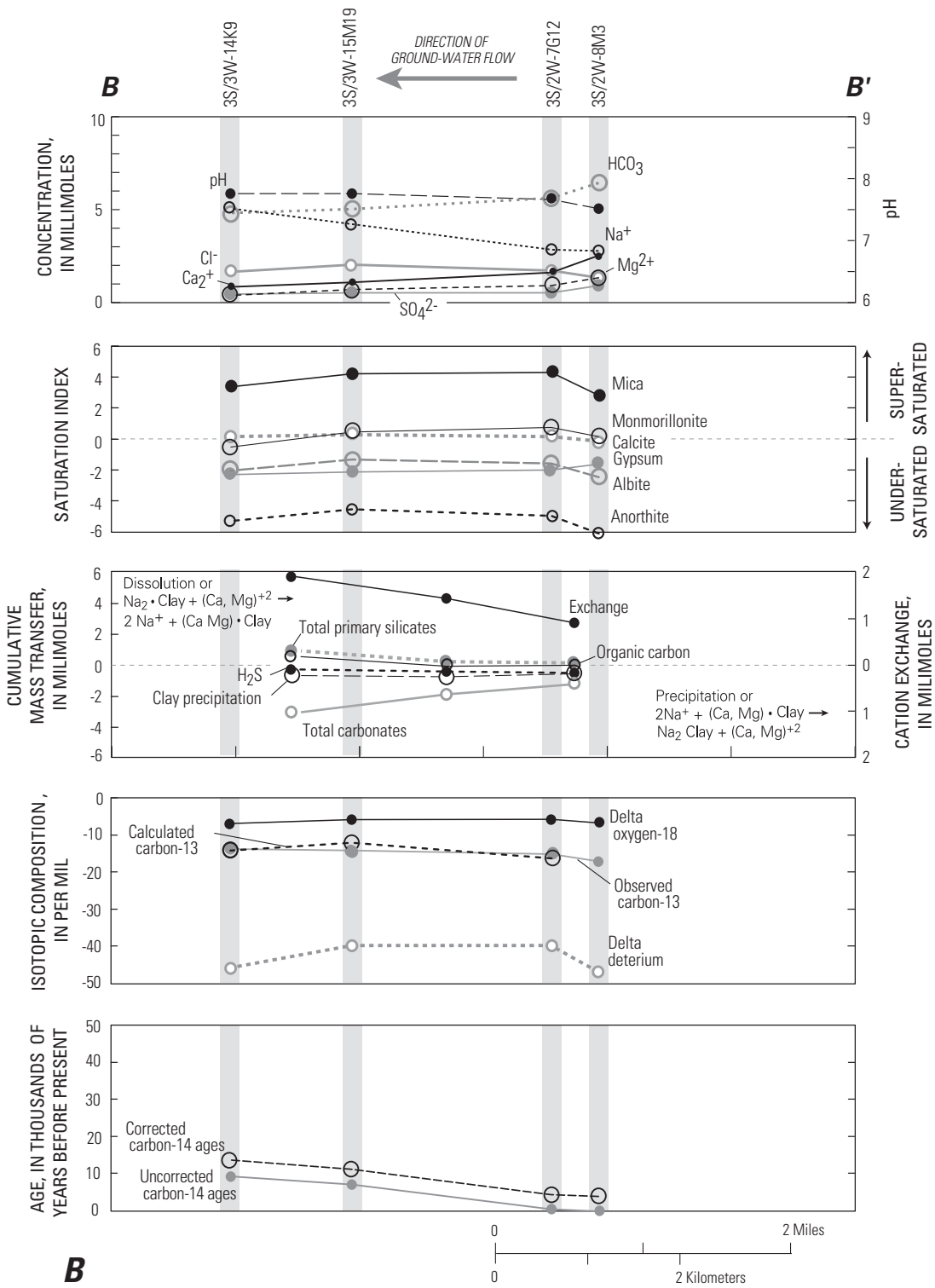


Figure 21.—Continued.

Thermodynamic data show that along both sections water is slightly oversaturated with respect to calcite and secondary silicate minerals such as montmorillonite. These minerals may tend to precipitate within the aquifer. Thermodynamic data also show that water is greatly undersaturated with respect to gypsum and most primary silicate minerals such as anorthite. Ground water also is undersaturated with respect to other primary silicate minerals such as albite, potassium feldspar, and chlorite even though these minerals are not shown in [figure 21](#). Where present, these minerals will tend to dissolve, although rates of silicate dissolution are slow in low-temperature ground-water systems. Water from all wells is supersaturated with respect to mica, indicating that this primary silicate mineral cannot dissolve within the aquifer system.

X-ray diffraction data (Appendix E) show that the aquifer is composed primarily of quartz mineral grains, although other silicate minerals also are present. Scanning electron photomicrographs (Appendix E) of mineral grains from core material show evidence of precipitation of calcite, but evidence of clay-mineral precipitation was not observed. Scanning electron photomicrographs (Appendix E) also show little evidence of dissolution of primary silicate minerals within the aquifer, confirming that these minerals are relatively nonreactive and that the rates of dissolution for these minerals are slow.

Changes in ground-water chemistry were simulated in NETPATH using the reactions listed in [table 3](#). These solutions are not unique and other possible combinations of reactions may explain observed changes in ground-water chemistry. However, the modeled reactions provide a reasonable match between observed and computed $\delta^{13}\text{C}$ values without violating thermodynamic constraints on dissolution or precipitation of mineral phases. Consistent with thermodynamic and mineralogic data, minerals such as calcite, which are near saturation, have much greater mass transfers between the solid and dissolved phases than do minerals such as primary silicates, which are greatly undersaturated with respect to the solution chemistry and are resistant to weathering.

Based on mass-transfer data shown in [figure 21](#), the changes in ground-water chemistry are controlled by exchange of sodium for calcium and magnesium on clay-mineral exchange sites and by precipitation of calcite. It was necessary to include small amounts of primary silicate weathering, and clay-mineral

precipitation, to obtain a reasonable match between observed $\delta^{13}\text{C}$ values and $\delta^{13}\text{C}$ values computed by NETPATH. Modeled data also indicate that even though water from most wells contains low concentrations of dissolved oxygen, reducing conditions must be present and a small amount of sulfate reduction may occur within microenvironments in the aquifer. Reducing conditions also are indicated by increasing iron and manganese concentrations in water from deeper wells. Sulfate reduction driven by organic material within aquifer deposits becomes increasingly important in water from deep wells at the downgradient ends of long flow paths through the aquifer and within the partly consolidated deposits underlying section A–A'. Methane was detected at a concentration of 8 cm³/L STP, and extremely reducing conditions must be present within parts of well 2S/3W-19Q3, which is completed in the partly consolidated deposits underlying section A–A'. It was not possible to match the very light $\delta^{13}\text{C}$ values obtained in water from this well unless methane having very light $\delta^{13}\text{C}$ composition is available as a carbon source for sulfate reduction. Similar reactions were observed in deep coastal aquifers underlying the Oxnard Plain of southern California. Methane in aquifers underlying the Oxnard Plain had $\delta^{13}\text{C}$ values between -55 and -91 per mil (Izbicki and others, 1992). For calculations presented in this report a value of -55 was used.

Interpreted carbon-14 ages ranged from recent in shallow wells in the upper aquifer system at the upgradient ends of each section to more than 20,000 years before present in water from wells 2S/3W-19Q3 and 17K4 completed in the partly consolidated deposits along section A–A' ([fig. 20](#)). Interpreted carbon-14 ages were as great as 9,400 years before present in well 3S/3W-14K9 in the lower aquifer system near San Francisco Bay along section B–B'. In general, water from wells along section A–A' was older, reflecting a combination of deeper wells available for sample collection, the presence of partly consolidated deposits at depth, and possibly less recharge to deeper deposits along this flow path. Water from shallower wells along section A–A' do not have great age and are similar in age to water from wells at similar depths along section B–B'.

Table 3. Chemical reactions used to interpret carbon-14 data

Process	Representative chemical equation	Comments
Cation exchange	$(\text{Ca, Mg})^{+2} + \text{Na}_2 \bullet \text{clay} \leftrightarrow 2\text{Na}^+ + (\text{Ca, Mg}) \bullet \text{clay}$	Simulated as exchange of equal parts dissolved Ca^{+2} and Mg^{+2} for each part Na^+ on the clay-exchange sites.
Carbonate precipitation	$\text{HCO}_3^- + \text{Ca}^{+2} \leftrightarrow \text{CaCO}_3 + \text{H}^+$ and $\text{HCO}_3^- + \text{Mg}^{+2} \leftrightarrow \text{MgCO}_3 + \text{H}^+$	Simulated as separate phases. Precipitation of only small amounts of MgCO_3 was needed to balance the mass-balance model. In the environment, Mg^{+2} probably substitutes for Ca^{+2} in variable amounts within carbonate minerals.
Silicate weathering	$\text{CaAl}_2\text{Si}_2\text{O}_8 + 8\text{H}^+ \Rightarrow \text{Ca}^{+2} + 2\text{Al}^{+3} + 2\text{H}_4\text{SiO}_4^0$ and $\text{NaAlSi}_3\text{O}_8 + 4\text{H}_2\text{O} + 4\text{H}^+ \Rightarrow \text{Al}^{+3} + 3\text{H}_4\text{SiO}_4^0 + \text{Na}^+$ and $\text{KAlSi}_3\text{O}_8 + 4\text{H}_2\text{O} + 4\text{H}^+ \Rightarrow \text{Al}^{+3} + 3\text{H}_4\text{SiO}_4^0 + \text{K}^+$	Simulated as dissolution of anorthite with smaller amounts of albite and potassium feldspar included to satisfy mass-balance constraints. In some settings dissolution of chlorite or sepiolite also may occur. Although other primary silicates also may dissolve, thermodynamic data show that the system is supersaturated with respect to biotite (mica) and that dissolution of this mineral will not occur.
Sulfate reduction	$2\text{CH}_2\text{O} + \text{SO}_4^{-2} \Rightarrow \text{HS}^- + 2\text{HCO}_3^- + \text{H}^+$ or $\text{CH}_4 + \text{SO}_4^{-2} \Rightarrow \text{HS}^- + \text{HCO}_3^- + \text{H}_2\text{O}$	Simulated as oxidation of organic matter having a $\delta^{13}\text{C}$ of -21 per mil. Simulated as oxidation of methane having a $\delta^{13}\text{C}$ of -55 per mil at the downgradient end of flow path A-A'.
Clay precipitation	$0.33\text{Na}^+ + 2.33\text{Al}(\text{OH})_3 + 3.67\text{H}_4\text{SiO}_4^0 + 2\text{H}^+ \Rightarrow \text{Na}_{0.33}\text{Al}_{2.33}\text{Si}_{3.67}\text{O}_{10}(\text{OH})_2 + 12\text{H}_2\text{O}$ or $2\text{Al}^{+3} + \text{H}_2\text{O} + 2\text{H}_4\text{SiO}_4^0 \Rightarrow \text{Al}_2\text{Si}_2\text{O}_5(\text{OH})_4 + 6\text{H}^+$	Only small differences in mass transfer result from simulation of clay precipitation as montmorillonite or as kaolinite. Both minerals detected by x-ray diffraction.

Limitations on Carbon-14 Interpretations

Carbon-14 ages calculated for ground water are interpretive and subject to considerable uncertainty. Davis and Bentley (1982) estimated that for aquifers for which the chemistry is well understood, interpreted carbon-14 ages are within ± 20 percent of the correct value. For areas where the chemistry is less well understood, Davis and Bentley (1982) estimated that errors may be as great as ± 100 percent of the correct value. In this study the greatest source of uncertainty in interpreting carbon-14 data is in determining the initial chemistry, ^{14}C activity, and $\delta^{13}\text{C}$ composition of the recharge water. This is a common problem in areas where present-day recharge may not reflect the composition of recharge for older ground water.

In aquifers underlying the East Bay Plain, the chemical and isotopic composition of recharge water may have been altered by partial evaporation prior to recharge and by mixing with septic discharges or irrigation return from lawn-watering with imported water. Although wells used to characterize recharge-water composition were selected to minimize these influences, their presence can not be completely eliminated. The problem is especially obvious along section A–A' (fig. 20) where water from well 2S/3W-25B3 has nitrate concentrations as high as 25 mg/L as N, possibly from septic discharges, and $\delta^{18}\text{O}$ and δD data that suggest that water from this well has been partly evaporated. This may result in errors in the initial mass-transfer calculations but probably results in only a small error in the absolute age of the ground water.

Water from well 2S/3W-25B3 along section A–A' and well 3S/2W-8M3 along section B–B' both contain tritium from the atmospheric testing of nuclear weapons. Atmospheric testing of nuclear weapons also increased the carbon-14 activity of water recharge during that time. To minimize this problem, the carbon-14 activity of recharging ground water and its carbon-13 composition were assumed to be in equilibrium with soil gasses, primarily carbon dioxide, and not greatly affected by isotopic exchange with carbonate minerals in the unsaturated zone. Given this assumption, the initial carbon-14 activity for well 2S/3W-25B3 along section A–A' was 74 pmc, and the initial carbon-14 activity for well 3S/2W-8M3 along section B–B' was 62 pmc. Because water from these wells contains tritium and increased carbon-14 activity

from the atmospheric testing of nuclear weapons, these estimates are lower than the measured activities (table 2). Although this assumption may affect the absolute age estimated for the ground water, the change in age calculated between wells farther downgradient are not affected by errors associated with estimating the isotopic composition or chemistry of the initial recharge water.

SUMMARY AND CONCLUSIONS

Ground-water management plans relying on the injection, storage, and recovery of imported water have been proposed for the Deep aquifer within the lower aquifer system underlying the San Lorenzo and San Leandro areas of the East Bay Plain, on the eastern shore of San Francisco Bay. Injection and recovery of imported water within the Deep aquifer has been successfully demonstrated in the San Lorenzo area by Fugro West, Inc., at the Bayside injection/recovery site. However, their hydrogeologic data show that injection and recovery of imported water into the Deep aquifer in the San Leandro area at the Oakport injection/recovery site is not feasible. There is concern that overlying land uses may contaminate high-quality imported water injected into aquifers during storage within the aquifer or during recovery.

Results of this study show that recharge occurs as infiltration of streamflow during winter months, as direct infiltration of precipitation. Large amounts of recharge from imported water leaking from water-supply pipes was not supported by the $\delta^{18}\text{O}$ and δD data. Most recent recharge is restricted to the upper aquifer system in areas near the mountain front. Recently recharged water was not present in the lower aquifer system—probably due to the presence of clay layers that separate the upper and lower aquifer systems. The carbon-14 ages (time since recharge) of deep ground water ranged from 500 to greater than 20,000 years before present; older ground water ages suggest that the lower aquifer system is isolated from surface sources of recharge. The younger ages were in water from wells near recharge areas along the mountain front, and the older ages were in partly consolidated deposits underlying the Oakport Injection site.

Water from wells in the lower aquifer system at the Bayside injection/recovery site has a carbon-14 age of 9,400 years before present. Given the small amount of natural recharge and the site's location at the downgradient end of a long flow path through the lower aquifer system, older ground water at the Bayside injection/recovery site is not unexpected. However, it is possible that the aquifers are hydraulically connected through discontinuities in the intervening clay layers or that the aquifers are connected through the failed casings of abandoned or unused wells.

Flow through one abandoned well, 2S/3W-22Q2, was studied along a hydrologic section through the San Leandro area. Results of data collected as part of this study show that a small amount of water, as much as 0.13 acre-ft/yr, may move downward into the lower aquifer system through this well, partly as a result of gradients induced by pumping in a nearby industrial well. Data collected at well 3S/3W-14K2 and nearby observation wells in the San Lorenzo area near the Bayside injection/recovery site show that downward flow into the lower aquifer system is likely during pumping and nonpumping conditions at the Bayside site. Even given the potentially large number of abandoned wells in the study area, the total quantity of flow through abandoned wells and subsequent recharge to the lower aquifer system is probably small on a regional basis. However, where this water contains contaminants from overlying land uses, flow through abandoned wells may be a potential source of low-level contamination, degrading the quality of imported water stored in the lower aquifer system. Although this does not preclude the injection of imported water into the Deep aquifer within the lower aquifer system, it suggests that care should be exercised in the siting, operation, and management of injection and recovery operations.

In addition to sources of contamination in overlying aquifers, freshwater aquifers underlying the San Leandro area, and perhaps the San Lorenzo area, of the East Bay Plain are underlain by partly consolidated deposits that yield poor-quality, high-chloride water. Depth-dependent samples collected from well, 2S/3W-19Q3, along cross section A-A' through the San Leandro area show that chloride concentrations in water from the underlying deposits may be as high as 700 mg/L. The presence of poor-quality water at depth may limit extended pumping of deeper aquifers in excess of injection—

especially near faults where partly consolidated deposits may have been uplifted and are adjacent to freshwater aquifers.

REFERENCES CITED

- Appelo, C.A., and Willemsen, A., 1987, Geochemical calculations and observations on salt water intrusion: I. A combined geochemical/mixing cell model: *Journal of Hydrology*, v. 94, p. 313–330.
- Atwater, B.F., Hedel, C.W., Helley, E.J., 1977, Late Quaternary depositional history, Holocene sea-level changes, and vertical crustal movement, southern San Francisco Bay, California: U.S. Geological Survey Professional Paper 1014, 15 p.
- Atwater, B.G., Ross, B.E., Wehmiller, J.F., 1981, Stratigraphy of the late Quaternary estuarine deposits and amino acid stereochemistry of oyster shells beneath San Francisco Bay, California: *Quaternary Research*, v. 16, p. 181–200.
- Benson, B.B., and Krause, Daniel, Jr., 1976, Empirical laws for dilute aqueous solutions of nonpolar gases: *Journal of Chemical Physics*, v. 64, no. 2, p. 689–709.
- Brown and Caldwell, Inc., 1986, Evaluation of groundwater resources and proposed design for emergency water supply wells: Pleasant Hill, California, [variously paged].
- California Department of Water Resources, 1960, Intrusion of salt water into groundwater basins of southern Alameda County: *Bulletin 81*, 44 p.
- _____, 1963, Alameda County Investigation: *Bulletin 13*, 196 p.
- CH₂M-Hill, Inc., 2000, Regional hydrogeologic investigation of the south East Bay Plain, Oakland, Calif., [variously paged].
- Clarke, W.B., Jenkins, W.J., and Top, Z., 1976, Determination of tritium by mass spectrometric measurements of ³He: *International Journal of Applied Radioactive Isotopes*, v. 27, p. 515–522.
- Cook, P. G., and Solomon, D.K., 1997, Recent advances in dating young groundwater: chlorofluorocarbons, ³H/³He and ⁸⁵Kr: *Journal of Hydrology*, v. 191, p. 245–265.
- Coplen, T.B., 1994, Reporting of the stable hydrogen, carbon and oxygen isotopic abundances. *Pure and Applied Chemistry*, v. 66, p. 273–276.
- Craig, Harmon, 1961, Isotopic variation in meteoric waters: *Science*, v. 133, p. 1702–1703.

- Davis, S.N., and Bentley, H.W., 1982, Dating groundwater, a short review, *in*: Currie, L.A., ed., Nuclear and chemical dating techniques—Interpreting the environmental record: American Chemical Society Symposium Series, v. 176, p. 187–222.
- Davis, S.N., Whittemore, D.O., Fabryka-Martin, June, 1998, Uses of chloride/bromide ratios in studies of potable water, *Ground Water*, v. 36, no., 2, p. 338–350.
- Driscoll, F.G., 1986, *Groundwater and wells*: Saint Paul, Minn., Johnson Filtration Systems, Inc., 1,089 p.
- Farrar, J.W., 2000, Results of the U.S. Geological Survey's analytical evaluation program for standard reference samples distributed in October 1999: U.S. Geological Survey Open-File Report 00-227, 107 p.
- Feth, J.H., 1981, Chloride in natural continental water—A review: U.S. Geological Survey Water-Supply Paper 2176, 30 p.
- Figuers, Sandy, 1998, *Groundwater study and water supply history of the East Bay Plain, Alameda and Contra Costa Counties, California*: Livermore, California, Norfleet Consultants, 90 p.
- Fugro West, Inc., 1998, *East Bay injection/extraction groundwater pilot project well construction and performance testing Oro Loma Phase III injection/extraction demonstration well—summary of operations report*: Ventura, Calif., Fugro West, Inc., [variously paged].
- _____, 1999a, *Oakport groundwater storage pilot project: Volume 1—Technical memorandum number 3, phase 2 field investigation*, Fugro West, Inc., Ventura, Calif., [variously paged].
- _____, 1999b, *East Bay injection/extraction pilot project, demonstration test operations report*, [variously paged].
- Galloway, D. L., and Rojstaczer, S., 1988, Analysis of the frequency response of water levels in wells to earth tides and atmospheric loading, p. 100-113. *in*: Hitchon, B., and Bachu, S., eds., *Proceedings of the Fourth Canadian/American Conference on Hydrogeology: Fluid flow, heat transfer and mass transport in rocks*, June 21–24, 1988, Banff, Alberta, Canada.
- Gonfiantini, R., 1978, Standards for stable isotope measurements in natural compounds: *Nature*, v. 271, p. 534–536.
- Hem, J.D., 1970, *Study and interpretation of the chemical characteristics of natural water* (2nd ed.). U.S. Geological Survey Water Supply Paper 1473, p. 363.
- Hickenbotton, Kelvin, and Muir, K.S., 1988, *Geohydrology and groundwater-quality overview, of the East Bay Plain area, Alameda County, California*: Alameda County Flood Control and Water Conservation District, 62 p.
- International Atomic Energy Agency, 1981, *Statistical treatment of environmental isotope data in precipitation*, Technical Report Series No. 206, 255 p.
- Izbicki, J.A., 1991, Chloride sources in a California coastal aquifer. *in*: Peters, Helen, ed., *Ground water in the Pacific rim countries: American Society of Civil Engineers, IR Div/ASCE Proceedings*, p. 71–77.
- _____, 1996, *Seawater intrusion in a California coastal aquifer*: U.S. Geological Survey Fact Sheet, FS-125-96, 4 p.
- Izbicki, J.A., Christensen, A.H., Hanson, R.T., 1999, U.S. Geological Survey combined well-bore flow and depth-dependent water sampler: U.S. Geological Survey Fact-Sheet, FS 196–99.
- Izbicki, J.A., Martin Peter, Densmore, J.N., and Clark, D.A., 1995, *Water-quality data for the Santa Clara-Calleguas Hydrologic Unit, Ventura County, California, October 1989 through December 1993*, U.S. Geological Survey Open-File Report 95-315, 124 p.
- Izbicki, J.A., Michel, R.L., and Martin, Peter, 1992, ³H and ¹⁴C as tracers of ground water recharge. *In*: Engman, Ted, *Saving a threatened resource—In search of solutions: American Society of Civil Engineers, IR Div/ASCE*, p. 122–127.
- Jones, B.F., Vengosh, A., Rosenthal, E., and Yechiele, Y., 1999, *Geochemical Investigations (Chapter 3)*, *in*: Bear, J., Cheng, A.H., Sorek, S., Ouazar, D., and Herrera, I., eds., *Seawater intrusion in coastal aquifers—concepts, methods, and practices*: London, Kluwer Academic Publishers, p. 51–71.
- Koltermann, C.E., and Gorelick, S.M., 1992, Paleoclimatic signature in terrestrial flood deposits: *Science*, v. 256, p. 1775–1782.
- Land, Michael, and Crawford, S.M., in press, *Ground-water quality conditions in the Dominguez Gap area, Los Angeles County California: preliminary results*: U.S. Geological Survey Water-Resources Investigations Report, 03-xxxx.
- Lehmann, B.E., Davis, S.N., and Fabryka-Martin, J.T., 1993, *Atmospheric and subsurface sources of stable and radioactive nuclides used for groundwater dating*: *Water Resources Research*, v. 29, no. 7, p. 2027–2040.
- Marlow, M.S., Jachens, R.C., Hart, P.E., Carlson, P.R., Anima, R.J., and Childs, J.R., 1999, *Development of San Leandro synform and neotectonics of the San Francisco Bay block, California*: *Marine and Petroleum Geology*, v. 16, p. 431–442.
- Maslonkowski, D.P., 1988, *Hydrogeology of the San Leandro and San Lorenzo alluvial cones of the bay plain groundwater basin, Alameda County, California*, Master of Science Thesis: San Jose State University, 143 p.

- Metzger, L.F., 2002, Streamflow gains and losses along San Francisco Creek, estimated ground-water recharge, and source of ground-water to wells, southern San Mateo and northern Santa Clara Counties, California: U.S. Geological Survey Water-Resources Investigations Report, 02-4078.
- Michel, R.L., 1976, Tritium inventories of the world's oceans and their implications: *Nature*, v. 263, p. 103–106.
- Michel, R.L., Busenberg, E., Plummer, L.N., Izbicki, J.A., Martin, Peter, Densmore, J.N., 1996, Use of tritium and chlorofluorocarbons to determine the rate of seawater intrusion in a coastal aquifer. *in*: Barrocu, Giovanni, ed., Proceedings of the 13th Salt-Water Intrusion Meeting, Cagliari, Italy, 5–10 June, 1994, 377 p.
- Mook, W.G., 1980, Carbon-14 in hydrogeological studies, *in* Fritz, P., and Fontes, J. Ch., eds., Handbook of environmental isotope geochemistry, Volume 1, p. 49–74.
- Muir, K.S., 1993, Classification of groundwater recharge potential in the East Bay Plain area, Alameda County, California: Alameda County Flood Control and Water Conservation District, Hayward, Calif., C-92-320, 10 p.
- _____, 1996a, Groundwater recharge in the East Bay Plain area, Alameda County, California: Hayward, Calif., Alameda County Flood Control and Water Conservation District, 17 p.
- _____, 1996b, Groundwater discharge in the East Bay Plain area, Alameda County, California: Hayward, Calif., Alameda County Flood Control and Water Conservation District, 17 p.
- _____, 1997, Ground water quality in the East Bay Plain: Hayward, Calif., Alameda County Department of Public Works, 7 p.
- Neter, John, and Wasserman, William, 1974, Applied linear statistical models: Homewood, Illinois, Richard D. Irwin, Inc., 842 p.
- Parkhurst, D.L., 1995, Users guide to PHREEQC—A computer program for speciation, reaction-path, and advective-transport, and inverse geochemical calculations: U.S. Geological Survey Water-Resources Investigations Report 95-4227, 143 p.
- Piper, A.M., 1945, A graphic procedure in the geochemical interpretation of water analyses: American Geophysical Union Transactions, 25th Annual Meeting, p. 914–928.
- Piper, A.M., Garrett, A.A., and others, 1953, Native and contaminated ground waters in the Long Beach-Santa Ana areas, California: U.S. Geological Survey Water-Supply Paper, 1136, 320 p.
- Plummer, L.N., Prestemon, E.C., and Parkhurst, D.L., 1991, An interactive code (NETPATH) for modeling net geochemical reactions along a flowpath: U.S. Geological Survey Water-Resources Investigations Report 91-4078, 227 p.
- Rai, D., and Zachara, J.M., 1984, Chemical attenuation rates, coefficients, and constants in leachate migration, Volume 1: A critical review: U.S. Environmental Protection Agency EA-3356, Volume 1 [variously paged].
- Rogers, J.D., and Figuers, S.H., 1991, Engineering geologic site characterization of the greater Oakland-Alameda area, Alameda and San Francisco Counties, California: Pleasant Hill, Calif., Rogers/Pacific, Inc., 59 p.
- Ross, B.E., 1977, The Pleistocene history of San Francisco Bay along the southern crossing: Master of Science thesis, San Jose State University, 121 p.
- San Francisco Bay Regional Water Quality Control Board, 1999, East Bay Plain groundwater basin beneficial use evaluation report: Oakland, California [variously paged].
- Sedlock, R.L., 1995, Tectonic framework, origin, and evolution of the San Francisco Bay region, pp. 1–17, *in* Sangines, E.M., Andersen, D.W., and Buising, A.V., eds., Recent geologic studies in the San Francisco Bay area: Pacific Section of the Society of Economic Paleontologists and Mineralogists, Book 76, 278 p.
- Sloan, Doris, 1992, The Yerba Buena mud: Record of the last-interglacial predecessor of San Francisco Bay, California: Geological Society of America, v. 104, p. 716–727.
- Solomon, D.K., 2000, ³⁴He in groundwater (Chapter 14), p. 425–439, *in* Cook, P.G., and Herczeg, A.L., eds., Environmental tracers in subsurface hydrology: Boston, Kluwer Academic Publishers, 529 p.
- Solomon, D.K., and Cook, P.G., 2000, ³H and ³He (Chapter 13), p. 397–424, *in* Cook, P.G., and Herczeg, A.L., eds., Environmental tracers in subsurface hydrology: Boston, Kluwer Academic Publishers, 529 p.
- Stumm, Werner, and Morgan, J.J., 1996, Aquatic chemistry. New York, John Wiley & Sons, Inc., 1022 p.
- Stute, Martin, and Schlosser, Peter, 2000, Atmospheric noble gases (Chap. 11), p. 349–377, *in* Cook, Peter, and Herczeg, A.L., eds., Environmental tracers in subsurface hydrology: Boston, Kluwer Academic Publishers, 529 p.
- Taylor, C.B., and Roether, W., 1982, A uniform scale for reporting low-level tritium in water. Methods of low-level counting and spectrometry: Vienna, International Atomic Energy Agency, p. 303–323.

- Torgerson, T., and Clarke, W.B., 1987, Helium accumulation in groundwater. III. Limits on helium transfer across the mantle-crust boundary beneath Australia and the magnitude of mantle degassing: *Earth and Planetary Science Letters*, v. 84, p. 345–355.
- Trask, P.D., and Rolston, J.W., 1951, Engineering geology of San Francisco Bay, California: *Bulletin of the Geological Society of America*, v. 82, p. 1079–1110.
- Van der Kamp, G., 1972, Tidal fluctuations in a confined aquifer extending under the sea: *Proceedings of the 24th International Geological Congress, Section 11*, p. 102–106.
- Weiss, R.F., 1970, The solubility of nitrogen, oxygen, and argon in water and seawater: *Deep Sea Research*, v. 17, p. 721–735.
- _____, 1971, The solubility of helium and neon in water and seawater: *Journal of Chemical Engineering Data*, v. 16, p. 235–241.
- Williams, Alan E., and Rodoni, Daniel P., 1997, Regional isotope effects and application to hydrologic investigations in southwestern California: *Water Resources Research*, v. 33, no. 7, p. 1721–1729.

APPENDIXES